Models of few optical cycle solitons beyond the slowly varying envelope approximation

Hervé Leblond, Dumitru Mihalache

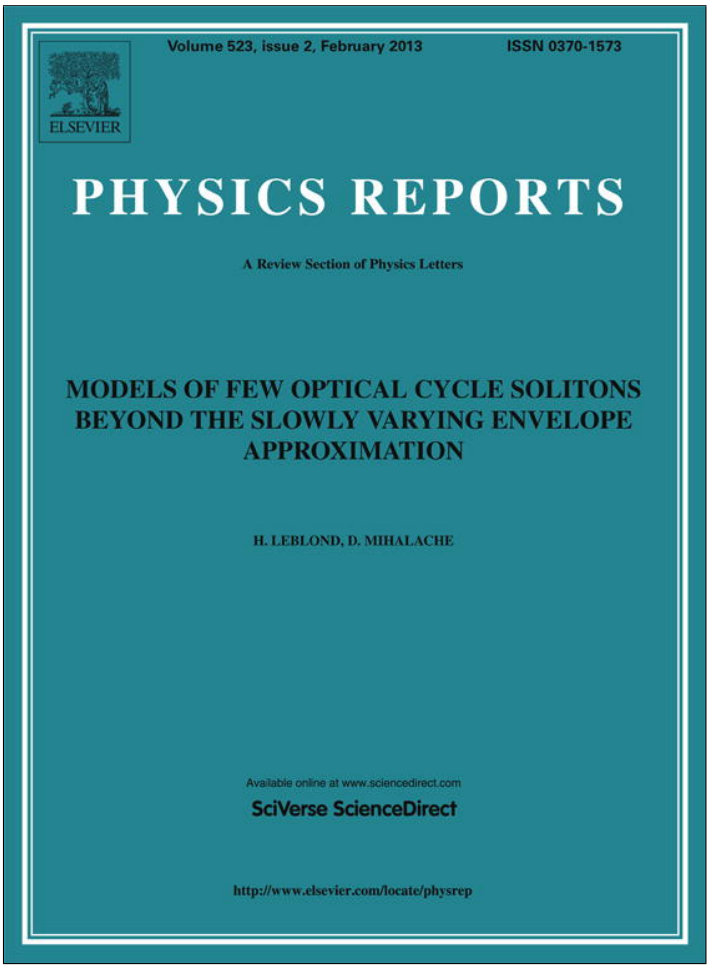

Physics Reports 523 (2013) 61–126

Contents lists available at SciVerse ScienceDirect

Physics Reports

journal homepage: www.elsevier.com/locate/physrep

Models of few optical cycle solitons beyond the slowly varying envelope approximation

H. Leblond [a,*], D. Mihalache [a,b,c]

[a] LUNAM University, Université d'Angers, Laboratoire de Photonique d'Angers, EA 4464, 2 Bd. Lavoisier, 49045 Angers Cedex 01, France

[b] Horia Hulubei National Institute for Physics and Nuclear Engineering, P.O.B. MG-6, 077125 Magurele, Romania

[c] Academy of Romanian Scientists, 54 Splaiul Independentei, 050094 Bucharest, Romania

ARTICLE INFO

Article history:
Accepted 12 October 2012
Available online 17 October 2012
editor: G.I. Stegeman

Keywords:
Few-cycle pulses
Few-optical-cycle solitons
Half-cycle optical solitons
Reductive perturbation method
Maxwell–Bloch equations
Density matrix
Two-level atoms
Long-wave approximation
Short-wave approximation
Modified Korteweg–de Vries equation
Sine–Gordon equation
Complex modified Korteweg–de Vries equation
Few-cycle dissipative solitons
Generalized Kadomtsev–Petviashvili equation
Few-cycle light bullets
Unipolar pulses
Linear polarization
Circular polarization

ABSTRACT

In the past years there was a huge interest in experimental and theoretical studies in the area of few-optical-cycle pulses and in the broader fast growing field of the so-called extreme nonlinear optics. This review concentrates on theoretical studies performed in the past decade concerning the description of few optical cycle solitons beyond the slowly varying envelope approximation (SVEA). Here we systematically use the powerful reductive expansion method (alias multiscale analysis) in order to derive simple integrable and nonintegrable evolution models describing both nonlinear wave propagation and interaction of ultrashort (femtosecond) pulses. To this aim we perform the multiple scale analysis on the Maxwell–Bloch equations and the corresponding Schrödinger–von Neumann equation for the density matrix of two-level atoms. We analyze in detail both long-wave and short-wave propagation models. The propagation of ultrashort few-optical-cycle solitons in quadratic and cubic nonlinear media are adequately described by generic integrable and nonintegrable nonlinear evolution equations such as the Korteweg–de Vries equation, the modified Korteweg–de Vries equation, the complex modified Korteweg–de Vries equation, the sine–Gordon equation, the cubic generalized Kadomtsev–Petviashvili equation, and the two-dimensional sine–Gordon equation. Moreover, we consider the propagation of few-cycle optical solitons in both $(1+1)$- and $(2+1)$-dimensional physical settings. A generalized modified Korteweg–de Vries equation is introduced in order to describe robust few-optical-cycle dissipative solitons. We investigate in detail the existence and robustness of both linearly polarized and circularly polarized few-cycle solitons, that is, we also take into account the effect of the vectorial nature of the electric field. Some of these results concerning the systematic use of the reductive expansion method beyond the SVEA can be relatively easily extended to few-cycle solitons in the general case of multilevel atoms. Prospects of the studies overviewed in this work are given in the conclusions.

Contents

* Corresponding author. Tel.: +33 2 41 73 54 31; fax: +33 2 41 73 52 16.
E-mail address: herve.leblond@univ-angers.fr (H. Leblond).

0370-1573/$ – see front matter © 2012 Elsevier B.V. All rights reserved.
doi:10.1016/j.physrep.2012.10.006

1. Introduction

Following a series of challenging works on experimental generation and characterization of two-cycle and even sub-two-cycle pulses from Kerr-lens mode-locked Ti: sapphire lasers [1–4], interest in intense ultrashort light pulses containing only a few optical cycles has grown steadily in recent years since their first experimental realization more than one decade ago. This mature research area has considerable potential for ultrafast optics applications in metrology of ultrafast phenomena, in systems performing laser ablation (micromachining, etching, microsurgery), etc. It still presents many exciting open problems from both a fundamental and an applied point of view. Notably, the ultrashort pulses possess extensive applications to the field of light–matter interactions, high-order harmonic generation, extreme [5] and single-cycle [6] nonlinear optics, and attosecond physics [7,8]; see Ref. [9] for a review of earlier works in this area.

We should point out that such ultrashort laser pulses with duration of only a few optical cycles are of much importance because they are brief enough to resolve temporal dynamics on an atomic level. They are currently used to study chemical reactions, molecular vibrations, electron motion in atoms and molecules, etc. Moreover, since few-cycle pulses are very broadband and can become extremely intense, they became a useful tool for coherently exciting and controlling matter on a

microscopic scale. The availability of ultrashort and ultraintense laser pulses generated by the powerful technique of chirped pulse amplification along with the development of high-fluence laser materials has opened up the field of optics in the relativistic regime [10]. Thus the ultrahigh electromagnetic field intensities produced by these techniques ($I > 10^{18}$ W/cm^2), lead to relativistic effects generated by the motion of electrons in such laser fields [10]. We also note an overview by Mourou and Tajima [11] on recent activity in the area of realization of future large laser facilities, namely exawatt-class lasers. Such huge powers will be obtained by releasing a few kilojoules of energy into an ultrashort pulse with a duration of only 10 fs.

The possibility to increase the laser peak powers relies on three revolutionary experimental achievements. The first laser amplification technique, namely the chirped pulse amplification which had a great influence on applications, was introduced in 1985 by Strickland and Mourou [12]. The second important advance in this area has been the optical parametric chirped pulse amplification introduced in 1992 by Dubietis et al.; see Ref. [13]. It is conceptually similar to the chirped pulsed amplification, however, it relies on the parametric amplification of light. This second revolutionary amplification technique is currently used for broadband, few-optical-cycle pulse amplification. The third important amplification technique, which was introduced in 1999 by Malkin et al. [14], is a new compression technique based on backwards Raman scattering and has the advantage of avoiding diffraction gratings. Very recently, Mourou et al. [15] have introduced a new amplification technique, the so-called cascaded conversion compression, which has the capability to compress with good efficiency nanosecond laser pulses with energy of about 10 kJ into femtosecond pulses having the same energy; exawatt peak powers being therefore reachable.

From the fundamental point of view, other physical phenomena involving ultrashort optical pulses (with very broad spectra) are of much interest at present. We mention here the supercontinuum generation (the spectral width exceeds two octaves) in microstructured photonic crystal fibers, which is seeded by femtosecond pulses in the anomalous group velocity dispersion regime of such fibers. Unique physical processes such as soliton fission, stimulated Raman scattering, and dispersive wave generation were studied in detail; see, e.g., Refs. [16–18] and two comprehensive recent reviews [19,20]. Also, it is worthy to mention here a recent experimental work demonstrating the synthesis of a single cycle of light by using compact erbium-doped fiber technology [21]; the obtained pulse duration of only 4.3 fs was close to the shortest possible value for a data bit of information transmitted in the near-infrared spectrum of light, at a wavelength of 1300 nm; see Ref. [21].

In the following we survey other recent relevant experimental and theoretical results in the area of few-cycle and strong field optical physics. First we mention a recent review paper [22] on few-optical-cycle light pulses with passive carrier-envelope phase (CEP) stabilization. One notices that the control of CEP of light pulses enables the generation of optical waveforms with reproducible electric field profiles. The passive approach allows the generation of CEP-controlled few-optical-cycle pulses covering a very broad range of parameters in terms of carrier frequency (from visible to mid-infrared), energy (up to several millijoules) and repetition rate (up to hundreds of kHz); see Ref. [22] for more details. A light source, using coherent wavelength multiplexing, that enables sub-cycle waveform shaping with a two-octave-spanning spectrum and a pulse energy of 15 microjoules was recently developed in Ref. [23]. This optical source offers full phase control and allows generation of any optical waveform supported by the amplified spectrum; see Ref. [23]. Extensive numerical simulations of ultrafast noncritical cascaded second-harmonic generation in lithium niobate, which were performed in a recent work [24], showed that few-cycle solitons can be formed that shed near- to mid-IR optical Cherenkov radiation in the 2.2–4.5 micrometer range with few-cycle duration, excellent pulse quality, and a high conversion efficiency (up to 25%). Note that alternative methods for generating energetic few-cycle mid-IR pulses, like optical rectification [25] or noncollinear optical parametric amplification [26] proved to be either inefficient or very complex techniques. Thus it was clearly proved in Ref. [24] by performing extensive numerical computations that cascaded second-harmonic generation might provide an efficient bridge between near-IR femtosecond laser technology and ultrashort energetic mid-IR pulses. In a subsequent experimental work performed by Wise's group [27] it was shown the few-cycle soliton compression with noncritical cascaded second-harmonic generation; energetic 47 fs infrared pulses were compressed in a just 1-mm long bulk lithium niobate crystal to 17 fs (under four optical cycles) with high efficiency (about 80%). The experimental results reported in Ref. [27] indicate that short semiconductor crystals can be used to compress multi-cycle mid-infrared pulses towards few-cycle duration, thereby facilitating a mid-infrared front-end for high-harmonic generation.

As concerning the creation of CEP-stabilized intense pulses we also mention the generation of 1.5 cycle pulses at 1.75 μm [28] and the generation of multi-μJ, CEP-stabilized, two-cycle pulses from an optical parametric chirped pulse amplification system with up to 500 kHz repetition rate [29].

Other recent works on few-cycle pulses (FCPs) deal with few-cycle light bullets created by femtosecond filaments [30], the study of ultrashort spatiotemporal optical solitons in quadratic nonlinear media [31], the ultrashort spatiotemporal optical pulse propagation in cubic (Kerr-like) media without the use of the slowly varying envelope approximation (SVEA) [32,33], single-cycle gap solitons generated in resonant two-level dense media with a subwavelength structure [34], observation of few-cycle propagating surface plasmon polariton wavepackets [35], and the possibility of generating few-cycle dissipative optical solitons [36–38]. In a recent work by Kozlov et al. [37] it was numerically demonstrated how to use the coherent mode locking technique for the generation of single-cycle pulses directly from a laser. We also mention recent studies of ultrafast pulse propagation in mode-locked laser cavities in the few femtosecond pulse regime and the derivation of a master mode-locking equation for ultrashort pulses [39]. Another relevant recent theoretical work presents a class of

few-cycle elliptically polarized solitary waves in isotropic Kerr media, propose a method of producing multisolitons with different polarization states, and study their binary-collision dynamics [40].

We also mention the experimental study of intrinsic chirp of single-cycle pulses [41], the proposal of a method to generate extremely short unipolar half-cycle pulses based on resonant propagation of a few-cycle pulse through asymmetrical media with periodic subwavelength structure [42], the demonstration of high quality sub-two-cycle pulses (with duration of about 5 fs) from compression of broadband supercontinuum generated in all-normal dispersion photonic crystal fibers [43], the realization of essentially dispersion-free and diffraction-limited focusing of few-cycle pulses (with duration of about 6 fs) through all-reflective microscope objectives [44], generation of unipolar pulses from nonunipolar optical pulses in a quadratic nonlinear medium [45], and the existence of guided optical solitons of femtosecond duration and nanoscopic mode area, that is, femtosecond nanometer-sized optical solitons [46]. In recent comprehensive numerical simulations performed by Li et al. [47] it was put forward an efficient and realizable scheme for the generation of ultrashort isolated attosecond (as) pulses by the optimization of three-color laser fields. As a result, an isolated 23 as pulse can be obtained directly by superimposing the supercontinuum harmonics near the cutoff region [47]. Note that this very short attosecond pulse (23 as) is less than one atomic unit of time (the time scale of electron motion in atoms), which is about 24 as.

The continuing experimental progress in the study of the wave dynamics of FCPs in nonlinear optical media has paved the way for the development of new theoretical approaches to model their propagation in physical systems. Three classes of main dynamical models for FCPs have been put forward: (i) the quantum approach [48–52], (ii) the refinements within the framework of SVEA of the nonlinear Schrödinger-type envelope equations [53–63], and the non-SVEA models [64–70, 70–82]. Extremely short pulses can be described by solving directly the Maxwell–Bloch equations for a two-level system. Sech-type solutions have been derived [83]. The propagation of FCPs in Kerr media can be described beyond the SVEA by using the modified Korteweg–de Vries (mKdV) [70–72], sine–Gordon (sG) [73–75], or mKdV–sG equations [76–80]. Note also a reduced Maxwell–Duffing model, very close to the mKdV equation, for the description of extremely short pulses in nonresonant media [84]. The mKdV and sG equations are completely integrable by means of the inverse scattering transform method [85,86], whereas the mKdV–sG equation is completely integrable only if some condition between its coefficients is satisfied [87,88].

The traditional SVEA is no longer valid for ultrashort optical pulses with duration of only a few femtoseconds. Although several generalizations of the SVEA have been proposed and have proven their efficiency (see the detailed discussion in Ref. [89]. These generalizations are referred to as higher-order nonlinear Schrödinger equation (NLS) models, see e.g. Refs. [53–56]), a completely different approach to the study of few-cycle pulses, which completely abandons the SVEA was put forward in a series of published works during the past two decades. First, we mention that first-order nonlinear evolution equations can be obtained under the so-called unidirectional approximation [90,91]. Non-SVEA models were proposed within the framework of the unidirectional approximation; see, e.g., Refs. [18] and [56]. Second, to the best of our knowledge, the necessity of using the non-SVEA approach for the adequate description of FCPs was put forward in the early seminal work by Akhmediev, Mel'nikov and Nazarkin published in 1989 [92]. In a subsequent paper, Belenov and Nazarkin [64] obtained exact solutions of nonlinear optics equations outside the approximation of slowly varying amplitudes and phases for light pulses a few wavelengths long and with power densities of the order of 10^9–10^{18} W/cm^2, clearly stating that traditional SVEA methods "*are becoming ineffective in describing wave processes at such small spatial and temporal scales and at such high fields*". We also mention that in a recent study of ultrafast pulse propagation in a mode-locked laser cavity in the few femtosecond pulse it was clearly stated that the standard NLS-based approach of ultrafast pulse propagation, though has been shown "*to work quantitatively beyond its expected breakdown, into the tens of femtoseconds regime, and has been used extensively for modeling supercontinuum generation . . . when pushed to the extreme of a few femtosecond pulses, the NLS description becomes suspect . . .*" [39].

This review is organized as follows. In Section 2 we briefly present the basic notions of the reductive perturbation method (multiscale expansion) and its applications to the general soliton theory. As a typical example of the application of the multiscale analysis, we give a direct derivation of a macroscopic nonlinear Schrödinger equation from Maxwell–Bloch equations for two-level atoms. One-dimensional approximate models for few-cycle optical solitons in two-level media are introduced in Section 3. First, two-cycle optical solitons in the long-wave approximation regime and the corresponding derivation of a modified Korteweg–de Vries equation are presented. Then, we also consider two-cycle optical solitons in the short-wave approximation regime, which are adequately described by a sine–Gordon equation. Ultrashort pulses in quadratically nonlinear media in the form of half-cycle optical solitons (with a definite polarity of the electric field) are also introduced in Section 3. In Section 4 we derive a general model for few-cycle optical soliton propagation, namely a modified Korteweg–de Vries–sine–Gordon equation, which describes two-cycle optical pulses propagating in two-component nonlinear media. We also make a detailed comparison between the most general modified Korteweg–de Vries–sine–Gordon model and other non slowly varying envelope approximation models introduced in the study of ultrashort solitons, such as the short-pulse equation, the modified Korteweg–de Vries equation, and the sine–Gordon equation. Moreover, the salient features of interactions of few-optical-cycle solitons are discussed in Section 5. Section 6 is devoted to the study of circularly polarized few-optical-cycle solitons in nonlinear media in both long wave and short wave approximation regimes. The unique features of few-optical-cycle dissipative solitons are discussed in Section 7. Section 8 deals with the generalization of these studies to $(2 + 1)$-dimensional physical settings, that is, to the description of spatiotemporal few-optical-cycle solitons beyond the slowly varying envelope approximation. Finally, in Section 9 we present our conclusions and we give some prospects of the studies overviewed in this paper.

2. The reductive perturbation method

2.1. Basic notions of the method and its applications

The *reductive expansion method* or *multiscale analysis* is a very powerful way of deriving simplified models describing both nonlinear wave propagation and interaction; see e.g., a tutorial review of this topic [93]. Here we only describe the basic notions of this mathematical method which is widespread in the modern soliton theory. We give a few examples concerning $(1+1)$-dimensional problems: (a) the envelope equations described by the universal nonlinear Schrödinger equation, (b) the Korteweg–de Vries and modified Korteweg–de Vries equations which adequately describe the long-wave-approximation regime, for quadratic and cubic nonlinearities respectively, and (c) the sine–Gordon equation describing the short-wave-approximation regime. A simple definition of the multiscale expansion is as follows: it is a perturbative approach, whose first order is a linear approximation, that allows us to write, not only small corrections valid for the same evolution time as in the linear approximation regime, but also their cumulative effect for a very long evolution time. Note that the reductive perturbation method is intimately related to soliton theory and it is frequently used in works devoted to the mathematical aspects of solitons.

We next give two generic examples of multiple scales by analyzing the NLS equation describing envelope solitons in optical fibers and the universal KdV equation arising, e.g., in hydrodynamics and in the study of ultrashort pulse propagation in quadratically nonlinear optical media beyond the SVEA (see Section 3.3). First, regarding envelope solitons, let us consider optical solitons in fibers. The wavelength, the pulse length, and the propagation distance, are three lengths measured along the fiber axis, that are first distinguished by their different orders of magnitude. Experimental setups may rather measure some of the corresponding durations: optical period, pulse duration, and propagation time, which simply deduce from lengths by multiplying by the light velocity. Considering a quantity either as a length or as a time does not induce any change to the analysis. The formation of a soliton occurs only if some relationships are satisfied between these orders of magnitude, and between them and that of the wave amplitude. Thus, multiple scales exist in the physics itself. Second, in the case of the KdV equation in hydrodynamics the formation of a KdV soliton assumes relations to be satisfied between the amplitude of the solitary wave, its length, the canal depth, and the propagation distance. All these quantities are lengths, whose orders of magnitude differ, but are in no way arbitrary. From the physical nature of the phenomenon itself, we again have multiple scales.

The mathematical formalism of the multiple scale analysis involves the introduction of some small perturbation parameter ε, so that the orders of magnitude of the various effects are determined by means of their order in an expansion in a series of powers of ε. This induces homogeneity properties of the considered mathematical expressions. Therefore, the model equations which are derived this way must satisfy these homogeneity properties. Due to this constraint the number of possible nonlinear evolution equations is hence rather small. Only a few generic equations are shown to account for analogous phenomena in very different physical settings. Such nonlinear evolution equations are called universal. Generally, in $(1+1)$ dimensions and for conservative systems, only one degree of freedom is involved in the dynamics and the universal evolution equation is completely integrable. However, the integrability property is very rare, and the model equations obtained as asymptotics fail to be integrable in most cases, as soon as the dimensionality of either the dependent or the independent variables increases. Then, the complete integrability may still be ensured if and only if some relationships between the coefficients of the nonlinear evolution equation are fulfilled.

To the best of our knowledge, the reductive perturbation method, or multiscale analysis, was first introduced by Gardner and Morikawa in 1960 in an unpublished report on hydromagnetic waves in a cold plasma (New York University Report NYU-9082, Courant Institute of Mathematical Sciences). This method has been applied in 1966 by Washimi and Taniuti [94] to the study of ion-acoustic solitary waves of small amplitudes. Later on, Taniuti and Wei [95] provided a general method of the derivation of the Korteweg–de Vries equation by using the reductive perturbation technique. Su and Gardner [96] derived both the Korteweg–de Vries and Burgers' equations. Taniuti and his co-workers initiated the perturbation method for 'a nonlinear wave modulation', leading to the generic nonlinear Schrödinger equation. Thus the NLS equation was derived by Taniuti using a multiscale method, in two fundamental works [97,98].

2.1.1. Length scales for envelope solitons

The nonlinear evolution of dispersive wave packets, e.g., those propagating through optical fibers, involves several length scales, the phase velocity of the wave being a constant in this specific case [85]. The first length scale is the wavelength λ of the carrier, that will be the reference length (zero order). The length L of the wave packet must be large with regard to the wavelength, so that an approximation of slowly varying envelope type can be envisaged. A third scale length is the propagation distance D; see Fig. 1. We require that the effect of dispersion appears on propagation distances of the order of D, which is much larger than the pulse length L. We are briefly discussing here the formation of *envelope solitons*, that is, an equilibrium between the dispersion effect and the nonlinear effect should occur. The propagation distances D will thus typically have the same order of magnitude as the dispersion length (temporal Fresnel length) $L_f = (\Delta t)^2/(2\pi k_2)$. Here $k_2 = d^2\omega/dk^2$ measures the dispersion, and Δt is the initial pulse duration (in the picosecond range for envelope solitons in fibers). We mention that in the seminal experiment of Mollenauer et al. [99] on envelope solitons in optical fibers the wavelength was $\lambda = 1.55\ \mu$m, the propagation distance, i.e. the length of the fiber was $D = 700$ m, and the

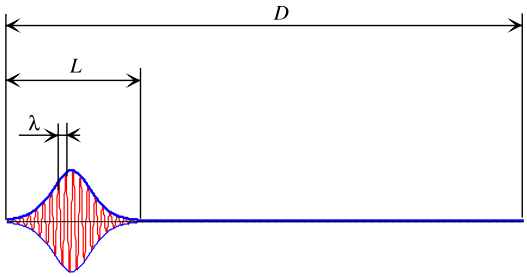

Fig. 1. (Color online) The various length scales for envelope solitons. Here λ is the wavelength, L is the pulse length, which is large with respect to λ, and D is the propagation distance, which is large with respect to L.

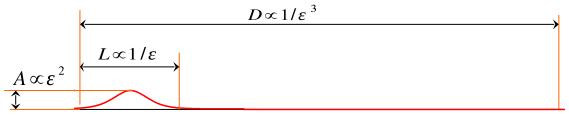

Fig. 2. (Color online) The different length scales of the KdV soliton: A is the small amplitude, L is the long wavelength, and D is the much longer propagation distance.

pulse duration was $\Delta t = 7$ ps, which corresponds to a pulse length $L = 1.4$ mm. With the above notations, $\Delta t = nL/c$, and $k_2 = (2n' + \omega n'')/c$, where n' and n'' are the first and second derivatives of the refractive index n with regard to the pulsation $\omega = 2\pi c/\lambda$. Hence, we get $D = L_f = [n^2/(2n'\omega + n''\omega^2)](L^2/\lambda)$. It is easily seen that the ratio $n^2/(2n'\omega + n''\omega^2)$ is dimensionless. The most simple procedure is to treat it as a number of order ε^0. From this, it is deduced that $\varepsilon \sim \lambda/L \sim L/D$. Thus we have the following length scales: $\lambda \sim \varepsilon L \sim \varepsilon^2 D$. In this way we have identified the small perturbation parameter ε for this physical situation. The temporal and spatial slow variables τ, respectively ζ, are then given by: $\tau = \varepsilon(t - z/V)$ and $\zeta = \varepsilon^2 z$. The generic NLS equation describing envelope solitons will be derived by using the quantum formalism in Section 2.2. Note that it is obtained at the order ε^3 of the perturbative scheme.

2.1.2. *Length scales for long-wave and short-wave expansions*

We briefly consider here some typical examples of long-wave expansions in the study of solitons. One of the first works devoted to this issue was that of Su and Gardner [96]. In that paper were derived both Burgers' equation and the KdV equation for the description of shallow water waves. (Let us mention that the KdV equation and the KdV soliton were derived for the first time by Boussinesq in 1872 [100], 23 years before Korteweg and de Vries.) We note that the Burgers' equation describes an equilibrium between nonlinearity and dissipation, and the formation of smooth shock profiles, whereas the KdV equation describes an equilibrium between nonlinearity and dispersion and the formation of localized waveforms propagating and interacting with each other without shape deformation; such robust localized waves were called *solitons*. The nonlinearity of the KdV equation is quadratic. However, these localized structures described by these two universal nonlinear partial differential equations exist in several physical settings; we only mention here that there exists an electromagnetic wave mode in ferromagnetic media which obeys either the Burgers' equation [101] or the KdV one [102], depending on the values of the wave amplitude and the damping constant.

We consider a solitary wave with a long wavelength L, a weak amplitude A, propagating on a distance D. The propagation distance D is much longer than the wavelength L; see Fig. 2. The orders of magnitude of A, D, and L are not independent. They can be expressed by means of a single small parameter ε, through $A \propto \varepsilon^2$, $L \propto 1/\varepsilon$, and $D \propto 1/\varepsilon^3$, as it is shown in Fig. 2. The relative size of the various terms can be determined as follows. The generic KdV equation is $\partial_\tau g + Pg\partial_\xi g + Q\partial_\xi^3 g = 0$. It involves a third-order derivative $\partial_\xi^3 g$, which accounts for dispersion to be counteracted by nonlinearity. If the length of the solitary wave is large, $L \sim 1/\varepsilon$ with $\varepsilon \ll 1$, then the dispersion term is about $\partial_\xi^3 g \sim \varepsilon^3 g$. It must arise at the propagation distance D, accounted for in the equation by the term $\partial_\tau g \sim g/D$. Hence $D \sim \varepsilon^{-3}$. Regarding the nonlinear term, which has the form $g\partial_\xi g$, it has an order of magnitude $g^2/L \sim \varepsilon g^2$. The formation of the soliton requires that the nonlinear effect exactly balances the dispersion effect. Therefore the nonlinear and dispersion terms should have the same order of magnitude, that is, $\varepsilon^3 g = \varepsilon g^2$. Hence we get the order of magnitude of $g \sim \varepsilon^2$, and correspondingly, the order of magnitude of the wave amplitude $A \sim \varepsilon^2$; see Fig. 2. For this physical situation the temporal and spatial slow variables τ, respectively ζ, are then given by $\tau = \varepsilon(t - z/V)$ and $\zeta = \varepsilon^3 z$.

Note that the generic KdV equation describing half-cycle optical solitons in quadratic nonlinear media will be derived by using the quantum formalism in Section 3.3. We will see that it is obtained at the order ε^6 of the perturbative scheme applied to the Maxwell wave equation. In Section 3.1 we will derive a generic modified KdV equation describing two-cycle optical solitons in cubic (Kerr) nonlinear media by using the quantum formalism based on the density matrix. The temporal and spatial slow variables are the same as in the case of the KdV equation because we are dealing with a long-wave expansion, however in the case of modified KdV solitons the nonlinearity is cubic, in contrast with KdV which involves a quadratic nonlinearity. Consequently, the wave amplitude scales differently: $A \sim \varepsilon^1$. The generic evolution equation for the case of

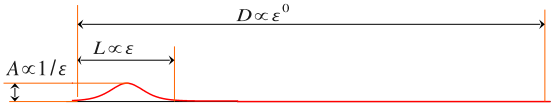

Fig. 3. (Color online) The length scales of the short-wave solitons: A is the large amplitude, L is the short wavelength and D is the relatively long propagation distance.

short-wave approximation is the sine–Gordon partial differential equation. It will be derived in Section 3.2 by using the quantum formalism. In this case we have the following scalings: $L \sim \varepsilon$ and $D \sim \varepsilon^0$, and we introduce the following rescaled variables $\tau = (1/\varepsilon)(t - z/V)$ and $\zeta = \varepsilon^0 z = z$; hence τ is no more a slow variable but becomes a fast one, whereas ζ, being still slow with respect to τ, becomes a zero order variable. The amplitude scales very differently here, it is indeed formally a large amplitude, $A \sim 1/\varepsilon$; see Fig. 3.

2.2. Direct derivation of a macroscopic nonlinear Schrödinger equation from Maxwell–Bloch equations

In this section we show that by using the *multiscale expansion technique* and the quantum mechanical matrix density formalism, it is possible to derive in a rigorous way the NLS equation, which is a macroscopic nonlinear evolution equation for a light pulse in a nonlinear medium; see Ref. [103] for a comprehensive study of this issue. In the following we only consider the simple case of a monochromatic plane wave, interacting with independent two-level atoms. We will show that for the linear part of this particular, though relevant case, the obtained results agree with those of the linear dispersion theory. However, the expression of the nonlinear (Kerr-type) coefficient in the NLS equation appreciably differs from that derived from the computation of the so-called nonlinear susceptibilities, see e.g. the standard book [104], except in the simple case of a linearly polarized transverse wave, i.e., when the atomic dipoles are oriented perpendicular to the propagation direction, see Ref. [103].

Notice that in the field of nonlinear optics the so-called 'nonlinear susceptibilities' expansion formalism is commonly used; it is an expansion of a phenomenological response function in a power series of the electric field. This technique has been proved to be a very useful theoretical framework for the physical interpretation of many nonlinear optical phenomena, and for the analysis of quantitative measurements of the nonlinear properties of optical materials, though this approach is not completely satisfactory for both theoreticians and experimenters; for a fresh look at these subtle issues see the recent comprehensive textbook on nonlinear optics (phenomena, materials and devices) [105]. However, in other areas, such as hydrodynamics or wave propagation in ferromagnetic media, the use of nonlinear-susceptibilities-like techniques has been avoided. Instead, in these two fields the standard framework is the *multiscale analysis* which allows us to get in a systematic and rigorous way the wave-packets evolution equations directly from the basic equations, such as the Navier–Stokes in hydrodynamics, or the Maxwell–Landau ones in ferromagnetism. Thus the traditional framework for studying water waves was the multiscale expansion, which also allowed us the treatment of multidimensional problems, e.g., the study of wave packets [106], and of solitary waves [107]. Notice that electromagnetic waves in magnetic media have also been studied using multiscale analysis [108–110].

Following the work [103] we will see that using the quantum mechanical density matrix formalism, and the multiscale analysis, allows a direct derivation of a macroscopic nonlinear evolution equation of the NLS-type for the propagation of light pulses in nonlinear media. For the sake of simplicity, we restrict ourselves to the problem of the interaction between a plane wave and a set of independent identical two-level atoms.

2.2.1. The Maxwell–Bloch equations and the multiscale analysis.

In this section we write down the basic Maxwell–Bloch equations for a collection of two-level atoms and we briefly discuss the essential points of the multiscale expansion technique, which allow us a rigorous derivation of the macroscopic NLS equation from the microscopic quantum theory; see Ref. [103] for a detailed first study of this issue. We consider a homogeneous medium, in which the dynamics of each atom is described by a two-level Hamiltonian

$$H_0 = \hbar \begin{pmatrix} \omega_a & 0 \\ 0 & \omega_b \end{pmatrix}. \tag{2.1}$$

The atomic dipolar electric momentum is described by the operator $\vec{\mu}$, with

$$\mu_s = \begin{pmatrix} 0 & \mu_s \\ \mu_s^* & 0 \end{pmatrix}, \quad (s = x,\ y,\ z). \tag{2.2}$$

The electric field $\vec{E}$ is governed by the Maxwell equations; in the absence of magnetic effects they reduce to

$$\vec{\nabla}(\vec{\nabla} \cdot \vec{E}) - \Delta \vec{E} = -c^{-2} \partial_t^2 (\vec{E} + 4\pi \vec{P}). \tag{2.3}$$

Here $\vec{P}$ is the polarization density, c is the light velocity in vacuum. Throughout this review paper we denote by ∂_t the derivative operator $\frac{\partial}{\partial t}$ with regard to the time variable t, and $\vec{\nabla}$ is the three-dimensional gradient operator. The coupling

between the atoms and the electric field is taken into account by a coupling energy term $-\vec{\mu}\cdot\vec{E}$ in the total Hamiltonian H, that reads as

$$H = H_0 - \vec{\mu}\cdot\vec{E}, \tag{2.4}$$

and by the expression of the polarization density $\vec{P}$,

$$\vec{P} = N\mathrm{Tr}(\rho\vec{\mu}), \tag{2.5}$$

where N is the number of atoms per volume unit.

The time evolution of the density matrix is given by the so-called Schrödinger–von Neumann equation:

$$i\hbar\partial_t\rho = [H, \rho], \tag{2.6}$$

where ρ is the density matrix. Notice that the set of Eqs. (2.3)–(2.6) is sometimes called the Maxwell–Bloch equations, although this name usually denotes a reduction of this set of equations; see, e.g., [104].

The electric field can thus be written as

$$\vec{E} = \sum_{n\geq 1, p\in Z} \varepsilon^n e^{ip\varphi}\vec{E}_n^p, \tag{2.7}$$

where the quantities $\vec{E}_n^p$ are functions of the slow variables τ and ζ, as

$$\begin{cases} \tau = \varepsilon\left(t - \dfrac{z}{V}\right), \\ \zeta = \varepsilon^2 z. \end{cases} \tag{2.8}$$

Thus the electric field describes a quasi-monochromatic plane wave, slowly modulated along its propagation direction, so that it yields a wave packet that propagates over distances which are very large with respect to the length of the 'temporal' wavepacket itself. In the above relationships defining the slow temporal and spatial variables, ε is a small reductive parameter in the multiscale analysis, V is the group velocity of the wave to be determined in a consistent way in the process of multiscale expansion, and $\varphi = kz - \omega t$ is the phase of the fundamental harmonic frequency (i.e., we take $p = 1$ in the expansion of $\vec{E}$ in order to get the fundamental harmonic). Thus, for the sake of simplicity, the propagation direction is chosen to be the z axis, and the problem is a purely one-dimensional one.

We assume that the dominant term in the series expansion (2.7) is of order ε^1:

$$\vec{E} = \varepsilon\left(\vec{E}_1^1 e^{i\varphi} + cc\right) \tag{2.9}$$

(here cc denotes the complex conjugate), so that the incident wave contains only the frequency $\omega/2\pi$ and its sidebands due to the finite pulse length. The scaling given by Eqs. (2.7)–(2.9) is the one that is commonly used for the derivation of the NLS equation in different physical settings; see e.g., Ref. [85].

At this point a few comments are necessary on the order of magnitude of different physical quantities involved in the description of radiation–matter interaction. Notice that the electric field is of order ε, thus it is a 'small' quantity. However, when using phenomenological response functions, it is rather difficult to give a reference point for this smallness. From another point of view, the typical values of the laser wave fields needed for usual experiments in nonlinear optics are large, at least with regard to the optical fields attainable without using laser sources. In the present context, the wave field compares to the intra-atomic electric field, or more precisely, the electrostatic energy of the atomic dipole in the presence of the electric field compares to the difference $\hbar\Omega = \hbar(\omega_b - \omega_a)$ between the energies of the atomic levels. Thus the zero-th order in the spatial variable is that of the optical wavelength, which may seem a bit strange for a theory valid at the atomic scale, where the spatial scale is less than a nanometer, even though it concerns optical wavelengths (about one micrometer). However, from the energetic point of view, we must compare the energy $\hbar\omega$ of the incident photon to the energy difference between the atomic levels $\hbar\Omega$. It is a well-known fact that only the transitions corresponding to frequencies of the same order of magnitude as the wave frequency ω affect appreciably the wave propagation. Summarizing these comments on different scales involved in the reductive perturbation approach we should stress that in this specific physical situation the energy scale fixes the frequency scale; then the time scale is that of the corresponding wave oscillation period, and the length scale can be simply deduced by using the numerical value of the light velocity c.

The polarization density $\vec{P}$ and the density matrix ρ are expanded in the same way as in (2.7), except that ρ has a ε^0 order term ρ_0 that gives account for the initial state of the atoms: $\rho = \rho_0 + \varepsilon\rho_1 + \cdots$, and we assume that all atoms are initially in their fundamental state 'a', so that: $\rho_0 = \begin{pmatrix} 1 & 0 \\ 0 & 0 \end{pmatrix}$. Notice that the fact that the photon wavelength is very large with regard to the atomic scale also allows the use of the electric dipolar approximation, which justifies the use of expressions (2.4) and (2.5) for the total Hamiltonian H and the polarization density $\vec{P}$.

2.2.2. The resolution of the perturbative expansion and the obtaining of a NLS equation.

We next give only the main line of the argument; for a detailed account of the derivation of the macroscopic NLS equation from the quantum theory, by using a suitable multiscale expansion; see Ref. [103]. Thus the expansion (2.7) is imported into

Eq. (2.3) to Eq. (2.6), and the coefficients of each power of ε are equated. We denote the components of ρ by

$$\rho_n^p = \begin{pmatrix} \rho_{na}^p & \rho_{nt}^p \\ \rho_{nu}^p & \rho_{nb}^p \end{pmatrix}. \tag{2.10}$$

Here the subscripts a and b stand for the 'populations', whereas the subscripts t and u stand for the 'coherences'. Notice that ρ is a Hermitian matrix; hence $\left(\rho_{nt}^p\right)^* = \rho_{nu}^{-p}$. However, there is no simple relation between ρ_{nt}^p and ρ_{nu}^p. Then expression (2.5) for $\vec{P}$ simply yields

$$P_n^{ps} = N\left(\rho_{nu}^p \mu^s + \rho_{nt}^p \mu^{*s}\right), \tag{2.11}$$

for all n, p, and $s = x, y, z$.

At order 1 in the perturbation expansion in ε, the term of interest is that with $p = 1$. The Maxwell equation (2.3) at order ε^1 gives

$$E_1^{1s} = -\frac{4\pi}{\beta} P_1^{1s} \quad \text{for } s = x, y, \qquad E_1^{1z} = -4\pi P_1^{1z}, \tag{2.12}$$

with $\beta = 1 - \frac{k^2 c^2}{\omega^2}$. The Schrödinger–von Neumann equation (2.6) shows that the corrections to the populations at this order, ρ_{1a}^1 and ρ_{1b}^1, are zero and the coherences ρ_{1t}^1 and ρ_{1u}^1 are coupled with the electric field through

$$\hbar\omega\rho_{1t}^1 = -\hbar\omega\rho_{1u}^1 + \sum_{s=x,y,z} \mu_s E_1^{1s}. \tag{2.13}$$

Making use of Eq. (2.12) in (2.13) and the similar equations for the coherences ρ_{1u}^1, we are left with a linear system of equations for the unknowns ρ_{1t}^1 and ρ_{1u}^1, of the form

$$\mathcal{L}\begin{pmatrix} \rho_{1t}^1 \\ \rho_{1u}^1 \end{pmatrix} = \begin{pmatrix} 0 \\ 0 \end{pmatrix}, \tag{2.14}$$

where $\mathcal{L}$ is a 2×2 matrix. Then by imposing the condition that the two coherences ρ_{1t}^1 and ρ_{1u}^1 are not both equal to zero, i.e., considering the relevant case when the wave field excites the atomic dipoles we get the corresponding implicit dispersion relation $\det(\mathcal{L}) = 0$, which is

$$\hbar^2\omega^2 = (\hbar\Omega + NQ)^2 - N^2 K K^*, \tag{2.15}$$

where

$$K = 4\pi\left(\frac{1}{\beta}\left(\mu_x^2 + \mu_y^2\right) + \mu_z^2\right), \tag{2.16}$$

$$Q = 4\pi\left(\frac{1}{\beta}\left(|\mu_x|^2 + |\mu_y|^2\right) + |\mu_z|^2\right). \tag{2.17}$$

From the implicit dispersion relation (2.15) we can derive the explicit dispersion relation $k = k(\omega)$ by assuming that the polarization operator $\vec{\mu}$, in the two-level model, describes oscillations of the molecular dipole along some direction, making an angle α with the propagation direction z, as

$$\vec{\mu} = \begin{pmatrix} \cos\alpha \\ 0 \\ \sin\alpha \end{pmatrix} \mu. \tag{2.18}$$

Note that the two-level model is most relevant if the molecular dipole under consideration is aligned with the electric field ($\alpha = 0$); however the general case $\alpha \neq 0$ yields a simplified model of an anisotropic medium. It gives some insight into the validity of the susceptibility approach to the analysis of propagation in anisotropic media.

Thus the explicit dispersion relation $k = k(\omega)$ is given by

$$k = k(\omega) = \frac{\omega}{c}\left(\frac{\omega^2 - \omega_2^2}{\omega^2 - \omega_1^2}\right)^{1/2}, \tag{2.19}$$

where

$$\omega_1^2 = \Omega\left(\Omega + \frac{8\pi N|\mu|^2}{\hbar}\sin^2\alpha\right), \tag{2.20}$$

$$\omega_2^2 = \Omega\left(\Omega + \frac{8\pi N|\mu|^2}{\hbar}\right). \tag{2.21}$$

In other words, the refractive index n is given by

$$n^2 = \frac{\omega^2 - \omega_2^2}{\omega^2 - \omega_1^2}. \tag{2.22}$$

It is seen from this dispersion relation that the wave cannot propagate if $\omega_1 \leq \omega \leq \omega_2$.

Then the solution at order ε^1 can be written as

$$\rho_1^1 = f \begin{pmatrix} 0 & -NK \\ \hbar(\Omega + \omega) + NQ & 0 \end{pmatrix}, \tag{2.23}$$

$$\vec{E}_1^1 = \vec{e}_1^1 f \quad \text{with } \vec{e}_1^1 = -N \begin{pmatrix} \theta_x/\beta \\ \theta_y/\beta \\ \theta_z \end{pmatrix}, \tag{2.24}$$

where, for $s = x, y, z$,

$$\theta_s = 4\pi \left[\mu_s(\hbar(\Omega + \omega) + NQ) - \mu_s^* NK \right]. \tag{2.25}$$

Next, following the procedure given in detail in Ref. [103], it is easily seen that at order 2 in the perturbation expansion in ε, nonlinear terms appear at this order in the Schrödinger equation (2.6). The term with $p = 1$ (the fundamental harmonic), at order ε^2, is treated as follows. The Maxwell equation (2.3) gives a relation between $\vec{E}_2^1$ and $\vec{P}_2^1$ analogous to (2.12) but involving the previous order, i.e., ε^1:

$$E_2^{1s} = -\frac{4\pi}{\beta} P_1^{1s} + i\hbar N \Lambda \theta_s \partial_\tau f \quad \text{for } s = x, y, \qquad E_2^{1z} = -4\pi P_2^{1z}, \tag{2.26}$$

where

$$\Lambda = \frac{(-2c)}{\hbar\omega\beta^2 V} \left[\frac{V}{c}(\beta - 1) + \frac{kc}{\omega} \right]. \tag{2.27}$$

Then, from the solvability condition of a corresponding linear system of equations for the coherences ρ_{2t}^1 and ρ_{2u}^1, we get the value of the group velocity V. It is checked by direct computation that $V = \frac{d\omega}{dk}$, where $k = k(\omega)$ is the dispersion relation. By making the necessary computations we get the complete solution ρ_2^1 and $\vec{E}_2^1$ at order 2; see Ref. [103]. Finally, at order 3 in the perturbation expansion in ε, from the Maxwell equations for the fundamental harmonic ($p = 1$), we get the value of $\vec{E}_3^1$. In addition, from the Schrödinger equation (2.6), which involves only one nonlinear term in this order, we get a linear system of equations for the two coherences ρ_{3t}^1 and ρ_{3u}^1. The solvability condition of this linear system can be written as

$$iA\partial_\zeta f + B\partial_\tau^2 f + Cf|f|^2 = 0, \tag{2.28}$$

i.e., we get the NLS equation for the amplitude f of the wave electric field, which was defined as $\vec{E}_1^1 = \vec{e}_1^1 f$. Here the coefficients A, B, and C are real constants. We recast the above NLS equation into the standard form, see e.g., Ref. [85]:

$$i\partial_\zeta \mathcal{E} - \frac{1}{2} k_2 \partial_\tau^2 \mathcal{E} + \gamma \mathcal{E} |\mathcal{E}|^2 = 0, \tag{2.29}$$

where $\vec{E}_1^1 = \mathcal{E}\vec{u}$, denoting by $\vec{u}$ a unitary polarization vector. The linear dispersion coefficient $(-\frac{1}{2}k_2)$ and the nonlinear coefficient γ are thus identified as

$$-\frac{1}{2}k_2 = \frac{B}{A}, \qquad \gamma = \frac{C}{A\left|\left|\vec{e}_1^1\right|\right|^2}. \tag{2.30}$$

In the following we will compare the values of the coefficients of the NLS equation k_2 and γ obtained here to those given in standard textbooks; see e.g., Ref. [104]. We will see that all linear properties, i.e., the dispersion relation, the values of the group velocity and of the dispersion coefficient in the NLS equation obtained by using the multiscale expansion [103] are in complete accordance with those given in the literature. However, we will see that the nonlinear coefficient γ in the NLS equation does not agree with the result given in standard textbooks even in the simple case of a linearly polarized transverse wave, i.e., when the atomic dipoles are excited perpendicular to the propagation direction.

Notice first that the dispersion relation (2.15) exactly coincides with that found from the linear susceptibility $\overleftrightarrow{\chi}^{(1)}(\omega)$ computed, e.g., in Ref. [104], in the case of density matrix description of a two-level model, as was discussed here. For a two-level Hamiltonian in our notations, we write down the expression of $\overleftrightarrow{\chi}^{(1)}(\omega)$:

$$\chi_{ij}^{(1)}(\omega) = \left(\frac{\mu_i \mu_j^*}{\Omega - \omega} + \frac{\mu_i^* \mu_j}{\Omega + \omega} \right). \tag{2.31}$$

Seeking for a monochromatic plane wave solution of the Maxwell equation (2.3) with:

$$\vec{P} = \overleftrightarrow{\chi}^{(1)}(\omega) \cdot \vec{E} \tag{2.32}$$

a corresponding linear dispersion relation is obtained, that exactly coincides with (2.15). From this dispersion relation we then calculate the derivative $\frac{d\omega}{dk}$, and we arrive at the conclusion that this quantity coincides with the expression of the group velocity V obtained in a consistent way in the process of the multiscale expansion technique.

As concerning the nonlinear coefficient γ we restrict ourselves to a specific physical situation by assuming that the polarization operator $\vec{\mu}$, in the two-level model, describes oscillations of the molecular dipole along some direction, making an angle α with the propagation direction z (Eq. (2.18)). After rather straightforward but tedious calculations the following formula for the nonlinear coefficient was obtained in Ref. [103]:

$$\gamma(\omega) = \frac{(-8\pi)N|\mu|^4\omega\Omega\left(\omega^2-\Omega^2\right)^2\cos^4\alpha}{\hbar^3 c\sqrt{\left(\omega^2-\omega_1^2\right)^3\left(\omega^2-\omega_2^2\right)}\left[\left(\omega^2-\omega_1^2\right)^2-\left(\Omega^2-\omega_1^2\right)\left(\omega_2^2-\omega_1^2\right)\right]}. \tag{2.33}$$

We see that the nonlinear coefficient γ presents not only resonance terms for the linear resonance frequency ω_1, but also a weaker divergence for the frequency ω_2 at which the wave vector k is zero. From Eq. (2.20) we see that the resonance frequency ω_1 depends on the propagation direction. In the particular physical situation when it is assumed that the atomic dipoles are excited perpendicular to the propagation direction (i.e., for $\alpha = 0$), then $\omega_1 = \Omega$; therefore in this case ω_1 is exactly the frequency Ω corresponding to the difference between the atomic levels, and the nonlinear coefficient reduces to

$$\gamma(\omega) = \frac{-8\pi N|\mu|^4\omega\Omega}{nc\hbar^3\left(\omega^2-\Omega^2\right)^2}, \tag{2.34}$$

in which the refractive index $n = n(\omega)$ is given by (2.22).

In order to compare the above expression of the nonlinear coefficient γ to previous calculations performed by means of the technique of nonlinear susceptibilities, we see that according to Ref. [104] the nonlinear coefficient γ is related to the nonlinear susceptibility $\chi^{(3)}(\omega) = \chi^{(3)}(\omega;\omega,\omega,-\omega)$ through the relationship:

$$\gamma(\omega) = \frac{2\omega\pi}{nc}\chi^{(3)}(\omega). \tag{2.35}$$

The susceptibility $\chi^{(3)}$ can be computed from a rather complicated formula; see Refs. [104,103] for more details.

We next consider a particular situation when the polarization operator $\vec{\mu} = (\mu, 0, 0)$ is parallel to the x-axis (i.e., we take the angle $\alpha = 0$). This means that the transition considered in the two-level model corresponds to oscillations of the charge along the x-axis, and can be excited by light, which is linearly polarized along the x direction. For this specific situation the only component of $\chi^{(3)}$ to be considered is $\chi^{(3)}_{xxxx}$. Computation yields

$$\chi^{(3)}_{xxxx}(\omega;\omega,\omega,-\omega) = \frac{4N|\mu|^4}{3\hbar^3}\frac{\Omega\left(\omega^2+3\Omega^2\right)}{\left(\omega^2-\Omega^2\right)^3}. \tag{2.36}$$

(Note that Eqs. (78)–(79) in Ref. [103] are erroneous). Then making use of (2.35), we find the value of the nonlinear coefficient γ as computed with the help of the susceptibilities. It is seen that it appreciably differs from the value computed from the multiple scale expansion theory, given by (2.34). Therefore as a final conclusion of this section we state that the multiple scale expansion theory agrees only qualitatively with previous calculations performed by using the susceptibility series expansion, even in the simpler case of a linearly polarized transverse wave.

3. One-dimensional approximate models for two-level media

3.1. Two-cycle optical solitons in the long-wave approximation: a modified Korteweg–de Vries equation

3.1.1. The multiple scales method and the derivation of the modified KdV equation from quantum equations

In this section we derive a modified Korteweg–de Vries equation for optical pulse propagation in a medium described by a two-level Hamiltonian, without the use of the slowly varying envelope approximation. The presentation of the material in this section, closely follows the previous work [73]. We assume that the resonance frequency of the two-level atoms is well above the inverse of the characteristic duration of the pulse (long-wave regime). We will see that the two-soliton solution of the mKdV equation is very close to the experimentally observed two-cycle pulses as reported, e.g., in Ref. [111].

Before describing the multiple scales method adapted to this specific problem, a few comments on the long-wave hypothesis is in order. It may seem strange that we use a long-wave approximation to describe propagation of ultrashort pulses in nonlinear media. Recall however that the word ‘long’ is here relative to some reference value of the wavelength.

The latter is the characteristic wavelength $\lambda_r = ct_r = 2\pi c/\Omega$ of the transition, which is assumed to belong to the ultraviolet spectral range, i.e., which is much smaller than the characteristic wavelength λ_w of the ultrashort pulse belonging to the visible spectral range, which can therefore be considered as being comparatively 'long' ($\lambda_r \ll \lambda_w$). The main application of the long-wave approximation is the hydrodynamic KdV soliton, which is a solitary wave in the sense that it contains only a single oscillation. More generally, such a formalism is well suited to the investigation of the exact wave profile, when the wave packet contains few oscillations and the use of wave envelope is not adequate. This is the specific case we study here in what follows.

The nonlinear medium is treated using the density-matrix formalism and the electromagnetic field is described using the Maxwell equations. For simplicity we consider a homogeneous medium, in which the dynamics of each atom is described by a two-level Hamiltonian H_0; see Eq. (2.1).

The atomic dipolar electric momentum is assumed to be along the x-axis. It is thus described by the operator $\vec{\mu} = \mu\vec{e}_x$, where $\vec{e}_x$ is the unitary vector along the x-axis and μ is the 2×2 matrix

$$\mu = \begin{pmatrix} 0 & \mu \\ \mu^* & 0 \end{pmatrix}. \tag{3.1}$$

The polarization density $\vec{P}$ is related to the density matrix ρ through $\vec{P} = N\mathrm{Tr}(\rho\vec{\mu})$, where N is the number of atoms per volume unit; thus $\vec{P}$ reduces to $P\vec{e}_x$ in our case.

The electric field $\vec{E}$ is governed by the Maxwell equations, which in the absence of magnetic effects, and assuming that we consider a plane wave propagating along the z-axis (polarized along the x-axis, $\vec{E} = E\vec{e}_x$), reduce to

$$\partial_z^2 E - c^{-2}\partial_t^2(E + 4\pi P) = 0, \tag{3.2}$$

where c is the light velocity in vacuum, t and z are the time and space variables, respectively. The coupling between the atoms and the electric field is taken into account by a coupling energy term in the total Hamiltonian H, that reads as $H = H_0 - \mu E$.

The density matrix evolution equation (i.e., the Schrödinger–von Neumann equation) writes

$$i\hbar\partial_t\rho = [H, \rho]. \tag{3.3}$$

Relaxation can be taken into account using some phenomenological term

$$\mathcal{R} = i\hbar \begin{pmatrix} \rho_b/\tau_b & -\rho_t/\tau_t \\ -\rho_t^*/\tau_t & -\rho_b/\tau_b \end{pmatrix}, \tag{3.4}$$

where τ_b and τ_t are the relaxation times for the populations and for the coherences, respectively, so that the Schrödinger equation (3.3) becomes

$$i\hbar\partial_t\rho = [H, \rho] + \mathcal{R}. \tag{3.5}$$

However, the numerical values of the relaxation times τ_b and τ_t are in the picosecond range, or even in the nanosecond domain; thus they are very large with regard to the pulse duration t_w, which is in the femtosecond range. Hence relaxation occurs very slowly with regard to optical oscillations, and consequently relaxation is negligible [73]. Therefore, the relaxation term $\mathcal{R}$ is omitted in what follows.

The set of Eqs. (3.2)–(3.3) is sometimes called the Maxwell–Bloch equations, although this name denotes more often a reduction of these equations.

We denote the components of matrix ρ by

$$\rho = \begin{pmatrix} \rho_a & \rho_t \\ \rho_t^* & \rho_b \end{pmatrix}, \tag{3.6}$$

and we denote by $\Omega = \omega_b - \omega_a$ the resonance frequency of the atom.

In the following we derive the modified Korteweg–de Vries equation as the generic equation describing FCPs in the long-wave approximation regime. We consider the situation where the pulse duration $t_w = 2\pi/\omega$ is long with regard to the period $t_r = 2\pi/\Omega$ that corresponds to the resonance frequency of the two-level atoms. We assume that t_w is about one optical period, i.e., is of the order of a few femtoseconds. Thus we assume that the resonance frequency Ω is large with regard to optical frequency ω: $\omega \ll \Omega$. In order to obtain soliton-type propagation, nonlinearity must balance dispersion, thus the two effects must arise simultaneously in the propagation. This involves a small amplitude approximation. Further, one can speak of soliton-type propagation only if the pulse shape is kept unchanged on a large propagation distance. Therefore we next use the powerful *reductive perturbation method* as elaborated by Taniuti and Wei [95] in the early days of the development of rigorous mathematical methods of solitons in various physical settings. We expand the electric field E, the polarization density P and the density matrix ρ as power series of a small parameter ε as

$$E = \sum_{n\geqslant 1} \varepsilon^n E_n, \qquad P = \sum_{n\geqslant 1} \varepsilon^n P_n, \qquad \rho = \sum_{n\geqslant 0} \varepsilon^n \rho_n, \tag{3.7}$$

and introduce the slow variables $\tau = \varepsilon\left(t - \frac{z}{V}\right)$ and $\zeta = \varepsilon^3 z$.

A few comments on the above series expansions and on the slow temporal and spatial variables are necessary at this point. Here the retarded time variable τ describes the pulse shape, which propagates at speed V in a first approximation. Its

order of magnitude ε gives an account for the *long-wave approximation*. In this propagation regime the pulse duration t_w has the same order of magnitude as t_r/ε. The propagation distance D is assumed to be very long with regard to the pulse length $L = ct_w \sim ct_r/\varepsilon$; therefore it will have the same order of magnitude as ct_r/ε^n, with $n \geqslant 2$. The value of n is determined by the distance at which dispersion effects occur. According to the general theory of the derivation of KdV-type equations [95], it is $n = 3$, i.e., the propagation distance D is proportional to $1/\varepsilon^3$. Therefore the ζ variable of order ε^3 describes a long-distance propagation. Thus we have the following length scales: $A \propto \varepsilon$, $L \propto 1/\varepsilon$, and $D \propto 1/\varepsilon^3$, where A is the small pulse amplitude, L is the long pulse length, and D is the much longer propagation distance.

We next proceed with the multiple scale expansion technique in order to derive the governing evolution equation. Notice that the Schrödinger–von Neumann equation (3.3) at order ε^0 is satisfied by the following value of ρ_0, which represents a steady state in which all atoms are in their fundamental state 'a': $\rho_0 = \begin{pmatrix} 1 & 0 \\ 0 & 0 \end{pmatrix}$. Then the Schrödinger–von Neumann equation (3.3) at order ε^1 yields $\rho_{1t} = \frac{\mu E_1}{\hbar\Omega}$, so that $P_1 = \frac{2N|\mu|^2}{\hbar\Omega}E_1$. The Maxwell equation (3.2) at order ε^3 gives the value of the velocity V and correspondingly, the value of the refractive index n of the medium:

$$n = \frac{c}{V} = \left(1 + \frac{8\pi N|\mu|^2}{\hbar\Omega}\right)^{\frac{1}{2}}, \tag{3.8}$$

which coincides with the refractive index derived above (Eq. (2.22)), taking into account the fact that the polarization is here perpendicular to the propagation direction ($\alpha = 0$), and that we are considering a long-wave approximation ($\omega = 0$).

Then the Schrödinger–von Neumann equation (3.3) at order ε^2 yields $\rho_{1a} = \rho_{1b} = 0$ and $\rho_{2t} = \frac{\mu E_2}{\hbar\Omega} - \frac{i\hbar\mu}{(\hbar\Omega)^2}\partial_\tau E_1$. Notice that the second term in the previous equation is an imaginary number and has no contribution to the polarization P_2, which is given by $P_2 = \frac{2N|\mu|^2}{\hbar\Omega}E_2$. It is easily seen that the Maxwell equation (3.2) at order ε^4 is automatically satisfied.

The Schrödinger–von Neumann equation (3.3) at order ε^3 gives

$$\rho_{2b} = -\rho_{2a} = \frac{|\mu|^2}{(\hbar\Omega)^2}E_1^2, \tag{3.9}$$

and

$$\rho_{3t} = \frac{\mu E_3}{\hbar\Omega} - \frac{i\hbar\mu}{(\hbar\Omega)^2}\partial_\tau E_2 - \frac{\hbar^2\mu}{(\hbar\Omega)^3}\partial_\tau^2 E_1 - \frac{2\mu|\mu|^2}{(\hbar\Omega)^3}E_1^3. \tag{3.10}$$

Notice that the second term in the above expression of ρ_{3t} is imaginary and therefore does not contribute to the polarization P_3, and as we said before the terms containing the relaxations were neglected. Next by calculating the polarization density P_3 we get an expression containing a nonlinear term:

$$P_3 = \frac{2N|\mu|^2}{\hbar\Omega}E_3 - \frac{2N\hbar^2|\mu|^2}{(\hbar\Omega)^3}\partial_\tau^2 E_1 - \frac{4N|\mu|^4}{(\hbar\Omega)^3}E_1^3. \tag{3.11}$$

Finally, the Maxwell equation at order ε^5 yields the following mKdV evolution equation for the main electric field amplitude E_1 (order 1 in the series expansion of the electric field E):

$$\partial_\zeta E_1 = \frac{4\pi N\hbar^2|\mu|^2}{cn(\hbar\Omega)^3}\partial_\tau^3 E_1 + \frac{8\pi N|\mu|^4}{cn(\hbar\Omega)^3}\partial_\tau E_1^3. \tag{3.12}$$

At this point a few comments about the coefficients of the mKdV equation (3.12) are necessary. From the standard procedure of obtaining KdV-type evolution equations we expect that the coefficient of the dispersive term $\partial_\tau^3 E_1$ in this equation must be $(1/6)d^3k/d\omega^3$, which can be crosschecked in the present case by a direct computation of the dispersion relation. Moreover, the value of the nonlinear coefficient of Eq. (3.12) can be related to the third order nonlinear susceptibility $\chi^{(3)}$, by using the NLS equation describing the evolution of a short pulse envelope in the same nonlinear medium: $i\partial_\zeta \mathcal{E} - \frac{1}{2}k_2\partial_\tau^2\mathcal{E} + \gamma\mathcal{E}|\mathcal{E}|^2 = 0$, where $\mathcal{E}$ is the envelope amplitude of the wave electric field ($E_1 = \mathcal{E}\exp[i(k\zeta - \omega\tau)] + cc$, with k and ω large), k_2 is the group velocity dispersion, and γ is related to $\chi^{(3)}$ through relation (2.35); see Section 2.2. The relevant component of the third order nonlinear susceptibility tensor $\chi^{(3)}_{xxxx}(\omega;\omega,\omega,-\omega)$ is given by expression (2.36), i.e., in the long-wave limit $\omega \to 0$ (let us recall that we are working in the long-wave regime, i.e., for $\omega \ll \Omega$),

$$\chi^{(3)}_{xxxx}(\omega;\omega,\omega,-\omega)\big|_{\omega=0} = \frac{-4N|\mu|^4}{\hbar^3\omega^3}. \tag{3.13}$$

(Note that Eq. (27) in [73], for $\omega = 0$, yields the same expression as in Eq. (3.13) but divided by 3, and consequently a coefficient 6 instead of 2 in the nonlinear coefficient of Eq. (3.14) below). We check that the expression of the nonlinear coefficient obtained from the associated NLS equation, is consistent with that obtained from the mKdV equation (3.12). Thus we can rewrite the generic evolution equation (3.12) as

$$\partial_\zeta E_1 = \frac{1}{6}\frac{d^3k}{d\omega^3}\bigg|_{\omega=0}\partial_\tau^3 E_1 - \frac{2\pi}{nc}\chi^{(3)}_{xxxx}(\omega;\omega,\omega,-\omega)\bigg|_{\omega=0}\partial_\tau E_1^3\,. \tag{3.14}$$

The dispersion coefficient can be written in terms of the refractive index $n(\omega)$ as

$$\frac{1}{6}\frac{d^3k}{d\omega^3}\bigg|_{\omega=0} = \frac{n''(0)}{2c}, \tag{3.15}$$

where the prime denotes derivative. Hence this coefficient involves the second derivative of the refractive index n and not the third one. Thus the dispersion term in Eq. (3.12) or (3.14) should be considered as a second-order dispersion term rather than as a third one, insofar such concepts make sense beyond SVEA.

If we consider a general Hamiltonian with an arbitrary number of atomic levels (non degenerated), and assume that the inverse of the characteristic pulse duration is much smaller than any of the transition frequencies of the atoms, and that the medium is centrosymmetric, we can derive, by means of the reductive perturbation method in the long-wave approximation, the same mKdV equation (3.14) [112]. This shows that Eq. (3.14) holds in a very general frame, and that the relations between its coefficients and the dispersion relation on one hand, the nonlinear susceptibility on the other, are valid in a general frame.

3.1.2. The breather soliton of the modified KdV equation: a prototype of few-cycle solitons

The mKdV equation (3.14) is completely integrable by means of the inverse scattering transform; see e.g., [113]. The general N-soliton solution has been given by Hirota [114]. The mKdV equation (3.14) can be written into its dimensionless form as

$$\partial_Z u + 2\partial_T u^3 + \sigma\partial_T^3 u = 0, \tag{3.16}$$

where $\sigma = \pm 1$, u is a dimensionless electric field, and Z and T are dimensionless space and time variables defined relative to the laboratory variables as

$$u = \frac{E}{E_0}, \qquad Z = \frac{z}{L}, \qquad T = \frac{t - z/V}{t_w}. \tag{3.17}$$

The reference time is thus chosen to be the pulse length t_w (in physical units). Recall that the atomic resonance frequencies Ω_{nm} have been chosen above as zero order quantities in the perturbative scheme, while t_w is assumed to be formally large, of order $1/\varepsilon$, with respect to the zero order times $1/\Omega_{nm}$. The characteristic electric field and propagation distance are

$$E_0 = \frac{1}{t_w}\sqrt{\frac{-2\sigma n_0 n_0''}{\chi^{(3)}}}, \qquad L = \frac{2ct_w^3}{(-\sigma n_0'')}, \tag{3.18}$$

where we have set

$$n_0'' = \frac{d^2 n_0}{d\omega^2}\bigg|_{\omega=0}, \qquad \chi^{(3)} = \chi^{(3)}_{xxxx}(\omega;\omega,\omega,-\omega)\big|_{\omega=0}. \tag{3.19}$$

In the present case of the Maxwell–Bloch equations, $\chi^{(3)} < 0$ (see Eq. (3.13)), and dispersion is normal ($n_0'' > 0$), consequently $\sigma = +1$, and the mKdV equation (3.12) is a focusing one. This occurs in general if $\chi^{(3)}$ and n_0'' have opposite sign, which happens most frequently for $\chi^{(3)} > 0$ and anomalous dispersion. Else, typically for $\chi^{(3)} > 0$ and normal dispersion, $\sigma = -1$, Eq. (3.12) is a defocusing one and describes nonlinear dispersion (see Ref. [78] and Section 3.1.3).

In the focusing case, the mKdV equation admits real single-soliton solutions, and N-soliton and breather solutions.

The *single soliton solution* u_{one} of the mKdV equation (3.16) is written as $u_{\text{one}} = p\ \text{sech}\,(\eta)$, with $\eta = pT - p^3Z - \gamma$, where p and γ are arbitrary parameters of the solution. The two-soliton solution u_{two} of the mKdV equation (3.16) is then given by

$$u_{\text{two}} = \frac{e^{\eta_1} + e^{\eta_2} + \left(\frac{p_1-p_2}{p_1+p_2}\right)^2\left(\frac{e^{\eta_1}}{4p_1^2} + \frac{e^{\eta_2}}{4p_2^2}\right)e^{\eta_1+\eta_2}}{1 + \frac{e^{2\eta_1}}{4p_1^2} + \frac{2}{(p_1+p_2)^2}e^{\eta_1+\eta_2} + \frac{e^{2\eta_2}}{4p_2^2} + \left(\frac{p_1-p_2}{p_1+p_2}\right)^4\frac{e^{2\eta_1+2\eta_2}}{16p_1^2p_2^2}}, \tag{3.20}$$

with $\eta_j = p_jT - p_j^3Z - \gamma_j$, for $j = 1, 2$. The parameters p_1, p_2, γ_1, and γ_2 are arbitrary. In the particular case when these parameters are real numbers, the explicit analytic solution (3.20) describes the interaction of two localized bell-shaped pulses, i.e., the interaction of two mKdV solitons, each of which would be described individually by u_{one}. The above expression (3.20) also describes the *breather soliton*, which can be considered as a pair of linked together identical mKdV solitons. This soliton is obtained when $p_2 = p_1^*$ and has a typical oscillatory behavior. An example of the breather soliton is given in Fig. 4. The values of soliton parameters are $p_1 = 1 + 4i$, $p_2 = 1 - 4i$, and $\gamma_1 = -\gamma_2 = i\pi/2$. The corresponding spectrum of this breather is also drawn in Fig. 4.

One notices that both pulse profile and spectrum are comparable to the corresponding results reported in experiments on FCPs; see e.g., [111]. Thus it can be thought that the two-cycle pulses produced in a series of essential experimental works on FCPs performed more than one decades ago [1–4,111] could propagate as true solitons in certain nonlinear media, according to the generic mKdV model. Concluding this section we stress that we have given a generic completely integrable

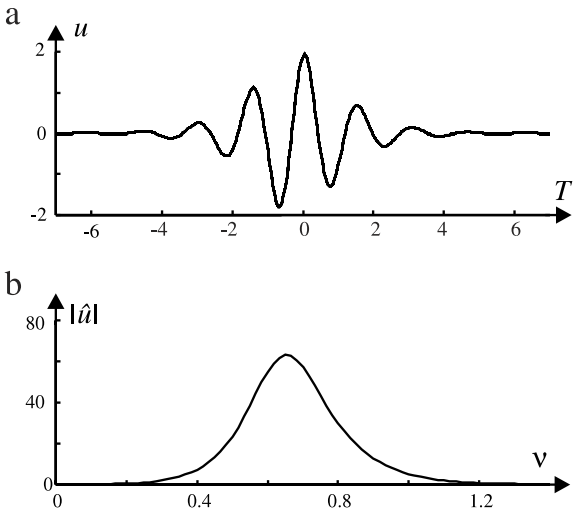

Fig. 4. (a) Pulse profile and (b) spectrum of the breather soliton solution of the dimensionless mKdV equation (3.16). After Ref. [73].

mKdV model that allows us the description of ultrashort optical pulse propagation in a medium described by a two-level Hamiltonian, when the slowly varying envelope approximation cannot be used. Thus when the resonance frequency is well above the inverse of the typical pulse width of about few femtoseconds, a long-wave approximation leads to a mKdV equation which adequately describes two-cycle optical solitons.

It is worth mentioning that we expect that this rigorous approach concerning the use of the reductive expansion method beyond the SVEA in the long-wave regime for the case of two-level atoms, is relatively easily extended to the more general case of multilevel atoms. Thus in the general physical setting involving multilevel atoms we get a similar mKdV evolution equation, assuming that the quadratic nonlinearity of the nonlinear medium is absent [112].

3.1.3. FCP soliton propagation for defocusing Kerr nonlinearities

For the two-level model, as considered in Ref. [73], the group-velocity dispersion is normal ($n'' > 0$) and the third-order nonlinear susceptibility $\chi^{(3)}$ is negative; hence the mKdV equation is of self-focusing type, and can be written in its dimensionless form as

$$\partial_z u + u^2 \partial_t u + \partial_t^3 u = 0, \tag{3.21}$$

where $u \propto E$, E being the electric field. This situation occurs also, and even more frequently, for anomalous dispersion and positive third-order nonlinear susceptibility $\chi^{(3)}$.

However a general situation of a defocusing optical nonlinearity may be considered [78], with either a normal dispersion ($n'' > 0$) and a positive cubic nonlinearity, or with an anomalous dispersion ($n'' < 0$) and a negative cubic nonlinearity. Therefore the obtained mKdV equation is of defocusing type and can be written in its normalized form as

$$\partial_z u - u^2 \partial_t u + \partial_t^3 u = 0. \tag{3.22}$$

It is well-known that Eq. (3.22) does not admit any soliton solution [86]. An incident wavepacket is spread out by the joint action of dispersion and cubic (Kerr) nonlinearity, as shown by numerical computation using the so-called "exponential time differencing method" [115] along with absorbing boundary conditions introduced to avoid numerical instability of the background; see Fig. 5. The results displayed in this figure clearly demonstrate that the nonlinear effect is stronger than the linear one and therefore no exact balance of the two concurring effects can occur.

3.2. Two-cycle optical solitons in the short-wave approximation: a sine–Gordon equation

3.2.1. The multiple scales method and the derivation of the sine–Gordon evolution equation from quantum equations

In this section we consider few-cycle optical solitons in the short-wave approximation regime [73], i.e., the situation in which the resonance frequency Ω of the atoms is well below the optical frequencies ω ($\Omega \ll \omega$), in the infrared if the FCP belongs to the visible range.

In this case the characteristic pulse duration t_w is very small with regard to $t_r = 2\pi/\Omega$. In order to perform the multiscale analysis we thus introduce a small perturbative parameter $\varepsilon \sim t_w/t_r$, such that the pulse duration $t_w = \hat{t}_w/\varepsilon$, where $\hat{t}_w$ has the same order of magnitude as the resonance period t_r. We next introduce a fast variable τ, which is the retarded time $\tau = \frac{1}{\varepsilon}\left(t - \frac{z}{V}\right)$, and a propagation variable which, being slow with respect to τ, in fact coincides with the original variable $\zeta = z$. We insist on the fact that the reduced time variable τ is not a slow variable but a fast one; we present here the computation using the same scaling as was applied to short-wave propagation in ferrites and in the study of surface wind

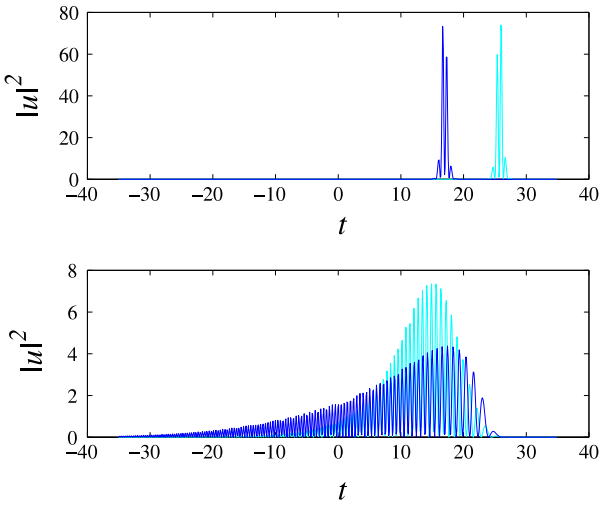

Fig. 5. (Color online) Top: the intensity $|u|^2$ of the input FCP [light blue (gray) curve] and its evolution at $z = 0.2$ according to the focusing mKdV equation (3.21) [dark blue (black) curve]. Bottom: the linear dispersion (the nonlinear term was omitted) of the same input at the same propagation distance [light blue (gray)], and its nonlinear dispersion according to the defocusing mKdV equation (3.22) [dark blue (black) curve]. The input is a breather of the focusing mKdV equation, with angular frequency $\omega = 4$ and inverse pulse duration $1/\tau_0 = 2$. After Ref. [78].

waves; see Refs. [116,117]. The sG model was originally derived in [73] using an alternative scaling, which is fully equivalent to the present one and in which the Hamiltonian H_0 of the atom was replaced in the Schrödinger–von Neumann equation (3.3) by $\varepsilon\hat{H}_0$. It is easily shown that the dispersion effects arise at distances z of the order of ct_w/ε, from which follows the choice of the slow propagation variable ζ.

Note that the pulse duration t_w is still assumed to be of the order of a few femtoseconds, corresponding to a pulse of only a few optical cycles. As in the case of the long-wave approximation regime the relaxation times τ_b, τ_t are very long with regard to t_w and their contributions can be neglected in the process of performing the reductive perturbation analysis. The electric field E, polarization P, and density matrix ρ are expanded as $E = \frac{1}{\varepsilon}(E_0 + \varepsilon E_1 + \cdots)$, $P = \frac{1}{\varepsilon}(P_0 + \varepsilon P_1 + \cdots)$, and $\rho = \rho_0 + \varepsilon\rho_1 + \cdots$. We use here a high-amplitude assumption, in contrast with the low amplitude assumption used in the long-wave approximation. In fact, the high amplitude assumption means here that the energy due to the interaction between the field and an atom is large with respect to the energy of the atomic transition $\hbar\Omega$. It is hence fully consistent with the assumption that the transition frequency Ω is small with respect to the wave frequency.

It is easily seen that the Schrödinger–von Neumann equation (3.3) of order ε^0 yields the following coupled system of differential equations:

$$i\hbar\partial_\tau\rho_{0a} = -E_0\left(\mu\rho_{0t}^* - \mu^*\rho_{0t}\right), \tag{3.23}$$

$$i\hbar\partial_\tau\rho_{0b} = E_0\left(\mu\rho_{0t}^* - \mu^*\rho_{0t}\right), \tag{3.24}$$

$$i\hbar\partial_\tau\rho_{0t} = -E_0\mu\left(\rho_{0b} - \rho_{0a}\right). \tag{3.25}$$

From Eqs. (3.23)–(3.24) we get the normalization condition of the density matrix $\rho_{0b} + \rho_{0a} = 1$. If we introduce the population difference $w = \rho_{0b} - \rho_{0a}$ we get the density matrix ρ_0 at order $1/\varepsilon$:

$$\rho_0 = \begin{pmatrix} \dfrac{1-w}{2} & \dfrac{i\mu}{\hbar}\displaystyle\int^\tau E_0 w \\ -\dfrac{i\mu^*}{\hbar}\displaystyle\int^\tau E_0 w & \dfrac{1+w}{2} \end{pmatrix}, \tag{3.26}$$

where $\int^\tau$ denotes an antiderivative operator with respect to the variable τ, the antiderivative being assumed to vanish as τ tends to $-\infty$.

Next we write down the integro-differential equation for the population difference w:

$$\partial_\tau w = -\frac{4E_0|\mu|^2}{\hbar^2}\int^\tau E_0 w. \tag{3.27}$$

Then from the expression of the polarization P we get $P_0 = 0$, and the Maxwell equation (3.2) at order $1/\varepsilon^3$ is satisfied if the velocity V is chosen as $V = c$.

The Schrödinger–von Neumann equation (3.3) at order ε is then written as $i\hbar\partial_\tau\rho_1 = [H_0, \rho_0] - [\mu E_0, \rho_1] - [\mu E_1, \rho_0]$, where we have left out the terms containing the relaxations. Defining $w_1 = \rho_{1b} - \rho_{1a}$, the off-diagonal components of the above equation for ρ_1 give

$$\rho_{1t} = i\Omega\int^\tau \rho_{0t} + i\frac{\mu}{\hbar}\int^\tau (E_0 w_1 + E_1 w), \tag{3.28}$$

so that the corresponding term $P_1 = \mu^* \rho_{1t} + \mu \rho_{1u}$ of the polarization is

$$P_1 = -\frac{2\Omega N\,|\mu|^2}{\hbar} \int^\tau \int^\tau E_0 w.$$

The Maxwell equation (3.2) at order $1/\varepsilon^2$ then reduces to

$$\partial_\zeta \partial_\tau E_0 = \frac{4\pi \Omega N |\mu|^2}{c\hbar} E_0 w. \tag{3.29}$$

Next if we set $p = -\frac{i|\mu|^2}{\hbar} \int^\tau E_0 w$, Eqs. (3.27) and (3.29) reduce to a nonlinear system of coupled differential equations

$$\partial_\zeta E_0 = \frac{4i\pi \Omega N}{c} p, \tag{3.30}$$

$$\partial_\tau p = -\frac{i|\mu|^2}{\hbar} E_0 w, \tag{3.31}$$

$$\partial_\tau w = -\frac{4i}{\hbar} E_0 p. \tag{3.32}$$

One notices that the above nonlinear system of coupled equations is similar to that describing the *self-induced transparency* [118,119] although the present physical situation is quite different. In our case the characteristic frequency $(2\pi)^{-1}\omega = 1/t_w$ of the pulse is far above the resonance frequency Ω, while the self-induced transparency occurs when the optical field with frequency ω oscillates at the resonance frequency Ω. The quantities E and w describe here the electric field and population difference themselves, and not amplitudes modulating a carrier with frequency Ω. Moreover one notices that E and w are here real quantities, and not complex ones as in the case of the self-induced transparency. Also, the quantity p is not the polarization density, but is proportional to its τ-derivative. At this point a brief comment should be made concerning the validity of the model equations (3.30)–(3.32). We should stress that the above described model assumes a high amplitude, or equivalently, a very strong nonlinearity. In [73], this assumption is expressed as a very large value of the atomic dipolar momentum μ. Thus in a more realistic situation, it can be expected that only the transition corresponding to the largest value of the dipolar momentum will have a significant contribution. If several transitions correspond to large values of the dipolar momentum with the same order of magnitude, one can expect that the short-wave approximation will yield a much more complicated asymptotic system of coupled differential equations involving the populations of each level concerned. However, the study of such a complicated model is outside the scope of this review paper.

In the following we write down the two-soliton solution of the sine–Gordon equation; from this solution we obtain for a specific choice of its free parameters the breather solution of the sine–Gordon equation which adequately describes optical solitons in the two-cycle regime. Next we use dimensionless variables defined by $\Theta = E_0/E_r$, $T = \tau/T_0$, and $Z = \zeta/L$ (w is already dimensionless). By setting $\eta = \int^Z W$, the system (3.30)–(3.32) reduces to

$$\partial_Z \partial_T \Theta = 2\Theta \partial_Z \eta, \tag{3.33}$$

$$\partial_Z \partial_T \eta = -2\Theta \partial_Z \Theta. \tag{3.34}$$

One notices that Eqs. (3.33)–(3.34) have been also found to describe short electromagnetic wave propagation in ferrites, using the same kind of short-wave approximation [116].

By making the following change of variables

$$\partial_Z \eta = A \cos u, \tag{3.35}$$

$$\partial_Z \Theta = A \sin u, \tag{3.36}$$

we transform Eqs. (3.33)–(3.34) into [116,86]

$$\partial_T A = 0, \tag{3.37}$$

$$\partial_Z \partial_T u = 2A \sin u. \tag{3.38}$$

Since, according to Eq. (3.37), A is a constant, Eq. (3.38) is the generic sine–Gordon equation. Now let us determine the physical meaning of the constant A in the present physical framework. Using relations (3.35)–(3.36) and the definition of η, we find that

$$A^2 = \lim_{T\to\infty} \left(w^2 + (\partial_Z \Theta)^2\right). \tag{3.39}$$

Since Θ is the dimensionless electric field, it vanishes at infinity. Thus we can have a non-vanishing solution only if the initial population difference w_i is not zero. The constant involved in Eq. (3.38) is then $A = w_i$. Using the new variable $\hat{Z} = 2w_i Z$,

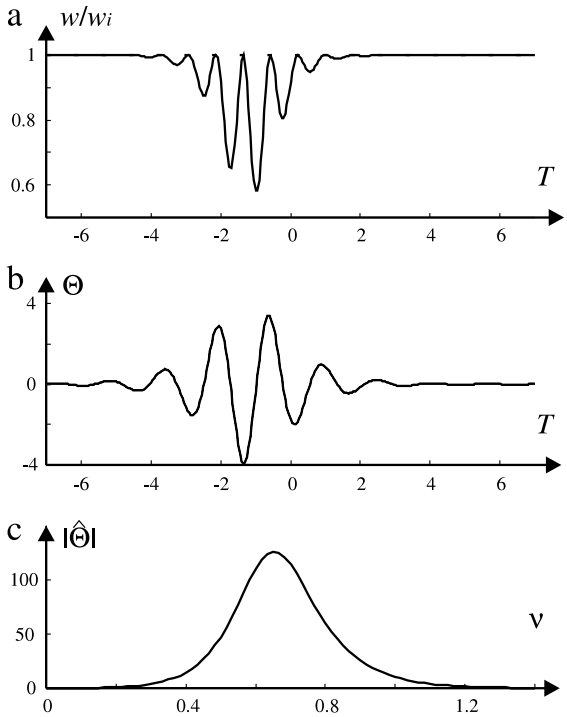

Fig. 6. (a) Population difference, (b) pulse profile, and (c) spectrum, of the breather solution of the sine–Gordon equation. After Ref. [73].

Eq. (3.38) reduces to the dimensionless sine–Gordon equation

$$\partial_{\hat{Z}}\partial_T u = \sin u. \tag{3.40}$$

The dimensionless quantities involved by Eq. (3.40) are related to the physical quantities through $\hat{Z} = z/\hat{L}$, $T = {t_w}^{-1}(t - z/c)$, $E = \frac{E_r}{2}\int^{\hat{Z}} \sin u$, and $w = w_i \cos u$.

The electric field and propagation length scaling parameters are $E_r = \hbar/(|\mu| t_w)$, $\hat{L} = (\hbar c)/(4\pi\Omega t_w N|\mu|^2 w_i)$, in which the initial population difference w_i and typical pulse duration t_w are explicitly involved. The small perturbative parameter ε can be identified with $\Omega t_w/(2\pi)$, expressing the fact that t_w is very small with regard to $1/\Omega$, i.e. we consider the short-wave approximation regime.

3.2.2. The breather soliton of the sine–Gordon equation: a few-cycle soliton

It is a well known fact that the sine–Gordon equation (3.40) is completely integrable [86]. A general N-soliton solution can be found using either the IST or the Hirota bilinear method. As in the case of long-wave approximation regime we will give here the explicit form of the two-soliton solution only, which can be written as [86]

$$u = 2i \ln\left(\frac{f^*}{f}\right), \tag{3.41}$$

with

$$f = 1 + ie^{\eta_1} + ie^{\eta_2} - \frac{(k_1 - k_2)^2}{(k_1 + k_2)^2} e^{\eta_1 + \eta_2}, \tag{3.42}$$

where

$$\eta_j = k_j T + \frac{Z}{k_j} + \gamma_j \quad \text{for } j = 1, 2. \tag{3.43}$$

Here k_1, k_2, γ_1, and γ_2 are free parameters describing the two-soliton solution. One notices that when these arbitrary parameters take real values, Eqs. (3.41)–(3.43) describe the interaction of two sine–Gordon solitons. As in the case of the long-wave approximation regime discussed in the preceding section, the two-soliton solution (3.41)–(3.43) is also able to describe soliton-type propagation of an ultrashort optical pulse in the two-cycle regime; the obtained analytical solution is very close in shape and spectrum to the ultrashort femtosecond-pulses of this type currently produced in experiments; see e.g., Ref. [111]. The corresponding analytic solution is a breather soliton of the sine–Gordon equation, which can be considered as two bounded sine–Gordon solitons. It is obtained when the soliton parameters k_1 and k_2 are complex conjugate numbers. A typical example is shown in Fig. 6; here the numerical values of the parameters are $k_1 = 1 + 4i$, $k_2 = 1 - 4i$, and $\gamma_1 = \gamma_2 = 0$.

One notices again that an initial population difference $w_i \neq 0$ is required. However, a properly speaking population inversion (i.e., when $w_i > 0$) is not necessary. Both nonlinear and dispersive effects vanish at the saturation of absorption, which corresponds to $w_i = 0$. Because the propagation reference length $\hat{L}$ is inversely proportional to the population difference parameter w_i, a relatively small value of the population difference increases the propagation distance at which nonlinear effects occur.

Concluding this section we stress that we have given a sine–Gordon model that allows us the description of ultrashort optical pulses which propagate in a medium described by a two-level Hamiltonian, when the slowly varying envelope approximation cannot be used. When the resonance frequency is well below the optical field frequency, a short-wave approximation leads to a model similar to that describing self-induced transparency, but in very different validity conditions. The model obtained in the short-wave approximation regime can be thus reduced to the generic completely integrable sine–Gordon equation.

3.3. Ultrashort pulses in quadratically nonlinear media: half-cycle optical solitons

In this section we show that few-cycle optical pulses launched in quadratically nonlinear optical media may result in robust half-cycle optical solitons, which exhibit a single hump, with no oscillating tails; for a detailed study of this issue, see Ref. [120]. We also mention here the important earlier works by Kazantseva et al. [121–123] on propagation and interaction of extremely short electromagnetic pulses in quadratic nonlinear media. In Ref. [123] the problem of propagation of extremely short unipolar electromagnetic pulses (the so-called 'videopulses') was considered in the framework of a model in which the material medium is represented by anharmonic oscillators (approximating bound electrons) with both quadratic and cubic nonlinearities. Two families of exact analytical solutions (with positive or negative polarity) were found for the moving solitary pulses. Those videopulses were very robust against perturbations. Moreover, it was found in Ref. [123] that two such unipolar pulses collide nearly elastically, while collisions between pulses with opposite polarities and a small relative velocity are inelastic, leading to the emission of radiation and generation of a small-amplitude additional pulse.

As in the case of cubic (Kerr-like) nonlinear media, the analysis to be given below is based on the reductive multiscale expansion and an adequate choice of the small parameter ε involved in this series expansion. In Ref. [120] it was derived a completely integrable Korteweg–de Vries equation from both a classical and a quantum mechanical simple model of matter–radiation interaction. The classical model was the same as in Ref. [121], the quantum one very close to the model considered above, but with additional quadratic nonlinearity. One notices the important result that the sign of the electric field in the half-cycle KdV soliton is fully determined by the properties of the optical medium and as a direct consequence of this feature, the mean value of the optical electric field is different from zero. It is well-known that the quadratic nonlinearity exists in media which break the central symmetry only. Due to this lack of symmetry the material has a preferential polarization direction, which determines the sign of the optical soliton.

An important issue is the phase invariance of a FCP; in some sense the FCP loses the phase invariance, and the importance of the so-called carrier-envelope phase has been emphasized in a series of works; see e.g., Ref. [7]. However, although different ways of stabilizing the carrier-envelope phase have been proposed [76,124], it remains a very difficult task. Further, even if a zero carrier-envelope phase is realized, the existing experimental setups cannot distinguish it from a phase equal to π; thus the polarity of the electric field of the FCP remains random, and its mean value is equal to zero. Notice that the studies of FCP solitons were mainly restricted to the case of a cubic (Kerr) optical nonlinearity; however a comprehensive study of FCPs in quadratic media was also reported [120]. In the following, for the sake of completeness, we will briefly summarize the main studies performed in the past years in the area of quadratic solitons for long pulse durations. One notices that for long pulse durations, when the slowly varying envelope approximation is valid, the study of optical solitons in quadratic nonlinear media has shown several unique features with respect to the cubic (Kerr) case [125,126]. First, the quadratic nonlinearity, in principle, allows one to observe nonlinear effects with much lower input powers than a cubic one. However, such an effect and the formation of *envelope solitons* in quadratically nonlinear media, involve at least two field components, a fundamental frequency and a second harmonic [127]. The interaction between the two optical components of frequency ω and 2ω is efficient if some phase-matching condition is satisfied; it can be achieved in experiments, e.g., by temperature adjustment [128]. Second, it has been shown that a result of the interaction between the two optical fields is the suppression of the collapse which occurs in a two-dimensional (2D) Kerr medium, leading to the formation of stable 2D quadratic solitons [129], and to the stabilization of other types of both spatial and spatiotemporal quadratic solitons [130]. Third, far from the phase-matching regime, the so-called *cascading* effect [131] leads to an effective cubic nonlinearity [132]. However, self-rectification and electro-optic effect remain, which are able to arrest the collapse [133], and can be also efficiently used to control the optical pulse by means of adequately matched microwaves [134]. As a brief conclusion of these comments on previous studies of quadratic solitons in the SVEA regime we stress that it is worth investigating the possibility to build a simple theory for FCP soliton propagation in quadratic media beyond the SVEA. We will show in this section that launching a FCP into a medium with an electronic quadratic nonlinearity allows one to produce half-cycle pulses, with no oscillating tail, a carrier-envelope phase equal to zero, a definite polarity of the electric field and a nonzero mean value of the optical field. It is expected that breather soliton solutions of integrable mKdV, sG, and mKdV–sG equations are good candidates for the description of FCPs [73,76]. However, these equations present cubic nonlinearities, while the completely integrable KdV equation itself is quadratic, and we show in the following, that FCP soliton propagation in a

quadratic medium can be adequately described by the latter [120]. One notices that the KdV equation does not present breather soliton solutions, and it will be shown in what follows that the KdV soliton itself, which is a half cycle pulse, will arise from the propagation of an arbitrary FCP input with mean value equal to zero. As mentioned above, all these unique features originate in the noncentrosymmetry of the medium exhibiting a quadratic optical nonlinearity.

3.3.1. Derivation of a KdV equation

As in the case of cubic nonlinear media [73] we consider a set of two-level atoms with the Hamiltonian H_0. The evolution of the electric field E (for the sake of simplicity we restrict to only one field component) is described by the Maxwell wave equations. The light propagation is coupled with the medium by means of a dipolar electric momentum μ directed along the same direction x as the electric field, and the corresponding Hamiltonian is $H = H_0 - \mu E$. The polarization density is therefore $P = N\mathrm{Tr}\,(\rho\mu)$, along the x direction, N being the volume density of atoms, and ρ the density matrix. The density matrix obeys the Schrödinger–von Neumann evolution equation $i\hbar\partial_t\rho = [H, \rho] + \mathcal{R}$, where as in the case of cubic optical nonlinearity [73], the phenomenological relaxation term $\mathcal{R}$ can be neglected.

The quadratic nonlinearity can be phenomenologically accounted for in the Maxwell–Bloch equations as follows. First, one notices that it corresponds to a deformation of the electronic cloud induced by the electric field E; hence it gives a dependence of the energy of the excited level 'b' on the electric field E, i.e., a Stark effect. Second, by definition, the optical nonlinearity is a quadratic one if this dependence is linear, i.e., $\hbar\omega_b \to \hbar\omega_b - \alpha E$. This dependence of the energy of the excited level on the electric field can be included phenomenologically in the Maxwell–Bloch equations by replacing the free Hamiltonian H_0 with

$$H_0 - \alpha E \begin{pmatrix} 0 & 0 \\ 0 & 1 \end{pmatrix}.$$

It is fully equivalent to assume that the excited state 'b' has some permanent dipolar momentum.

As in the case of cubic nonlinear media, one notices that transparency of the medium implies that the characteristic frequency ω_w of the considered radiation in the optical range of the spectrum strongly differs from the resonance frequency Ω of the atoms; hence it can be either much higher or much lower. We consider here the latter case, i.e. we assume that ω_w is much smaller than Ω, i.e., we consider the *long-wave propagation regime*. This assumption motivates the introduction of the slow temporal and spatial variables $\tau = \varepsilon\left(t - \frac{z}{V}\right)$ and $\zeta = \varepsilon^3 z$, and the use of a reductive perturbation expansion technique, where ε is the small parameter in the corresponding series expansions. The delayed time τ involves propagation at some group velocity V to be determined. The pulse shape described by the variable τ is expected to evolve slowly in time, the corresponding scale being that of the spatial propagation variable ζ. A weak amplitude assumption is needed in order that the nonlinear effects arise at the same propagation distance scale as the dispersion does: $E = \varepsilon^2 E_2 + \varepsilon^3 E_3 + \varepsilon^4 E_4 + \cdots$, as in standard reductive perturbation series expansions; see Ref. [93] for a comprehensive overview of different kinds of such expansions applied to several solitonic models of physical relevance. The polarization density is expanded in the same way $P = \varepsilon^2 P_2 + \varepsilon^3 P_3 + \varepsilon^4 P_4 + \cdots$, whereas the density matrix expansion has also the zero order term in the small parameter ε: $\rho = \rho_0 + \varepsilon^2\rho_2 + \varepsilon^3\rho_3 + \varepsilon^4\rho_4 + \cdots$. We assume that all atoms are initially in the fundamental state, i.e. $\rho_{0a} = 1$, $\rho_{0b} = 0$, and $\rho_{0t} = 0$.

The Schrödinger–von Neumann equation at order ε^2 gives $\rho_{2t} = \frac{\mu}{\hbar\Omega}E_2$, and we observe that $\rho_{2a,b}$ remain free. Then we deduce $P_2 = \frac{2N|\mu|^2}{\hbar\Omega}E_2$. If we insert the value of P_2 into the Maxwell equation at order ε^4 we are left with the value of the velocity V. We get the same expression of V and of the refractive index $n = c/V$ as in the case of cubic nonlinearity (Eq. (3.8) above) [73], since the linear parts of the two models are exactly the same. At order ε^3 the Schrödinger–von Neumann equation gives $\rho_{2a} = \rho_{2b} = 0$ and $\rho_{3t} = \frac{\mu}{\hbar\Omega}E_3 - \frac{i\hbar\mu}{(\hbar\Omega)^2}\partial_\tau E_2$, from which we deduce $P_3 = \frac{2N|\mu|^2}{\hbar\Omega}E_3$. Hence the Maxwell equation at order ε^5 does not give any further information.

The Schrödinger–von Neumann equation at order ε^4 gives

$$\rho_{4t} = \frac{\mu}{\hbar\Omega}E_4 - \frac{i\hbar\mu}{(\hbar\Omega)^2}\partial_\tau E_3 - \frac{\hbar^2\mu}{(\hbar\Omega)^3}\partial_\tau^2 E_2 + \frac{\alpha\mu}{(\hbar\Omega)^2}(E_2)^2, \tag{3.44}$$

from which we deduce the expression of P_4, as

$$P_4 = \frac{2N|\mu|^2}{\hbar\Omega}E_4 - \frac{2N\hbar^2|\mu|^2}{(\hbar\Omega)^3}\partial_\tau^2 E_2 + \frac{2N\alpha|\mu|^2}{(\hbar\Omega)^2}(E_2)^2. \tag{3.45}$$

If we insert the expression (3.45) into the Maxwell equation at order ε^6 we get a nonlinear evolution equation for the field E_2. After observing that all terms involving E_4 cancel out each other, and after performing one integration with respect to τ:

$$\partial_\zeta E_2 = \frac{4\pi NV\hbar^2|\mu|^2}{c^2(\hbar\Omega)^3}\partial_\tau^3 E_2 - \frac{4\pi NV\alpha|\mu|^2}{c^2(\hbar\Omega)^2}\partial_\tau(E_2)^2. \tag{3.46}$$

When performing the integration with respect to τ we have assumed that the electric field and its derivatives vanish at $\tau \to \pm\infty$. Eq. (3.46) is exactly the KdV equation,

$$\partial_\zeta E_2 = A\partial_\tau^3 E_2 + B\partial_\tau \left(E_2\right)^2, \tag{3.47}$$

with the linear dispersion coefficient A and nonlinear coefficient B given in physical units by the expressions

$$A = \frac{4\pi N \hbar^2 |\mu|^2}{nc(\hbar\Omega)^3}, \tag{3.48}$$

$$B = -\frac{4\pi N\alpha |\mu|^2}{nc(\hbar\Omega)^2}. \tag{3.49}$$

Since the dispersion relation is the same as in the Kerr case, see Ref. [73] and the preceding section on FCPs in the cubic (Kerr) case, the same expression of linear dispersion coefficient A still holds in the quadratic case discussed in the present section.

The second order susceptibility $\chi^{(2)}(2\omega;\omega,\omega)$ can be directly computed as follows: we consider a monochromatic electric field $E = \varepsilon\mathcal{E}\left(e^{i\omega t} + e^{-i\omega t}\right)$, and we calculate the corresponding polarization P by using the expressions of E into the Maxwell–Schrödinger–Von Neumann equations. The nonlinear susceptibility $\chi^{(2)}$ is defined by the relation $P = \varepsilon^2\chi^{(2)}(2\omega;\omega,\omega)\mathcal{E}^2 e^{2i\omega t}$.

Consequently, from the expression of P we deduce

$$\chi^{(2)}(2\omega;\omega,\omega) = \frac{N\alpha\,|\mu|^2}{\hbar^2}\left[\frac{1}{(\Omega+2\omega)\,(\Omega+\omega)} + \frac{1}{(\Omega-2\omega)\,(\Omega-\omega)}\right]. \tag{3.50}$$

Finally, comparing this expression with the formula (3.49) obtained by using the reductive perturbation analysis, we obtain the expression of nonlinear coefficient B of the above written KdV equation in terms of the second order susceptibility:

$$B = -\frac{2\pi}{nc}\,\chi^{(2)}(2\omega;\omega,\omega)\big|_{\omega=0}. \tag{3.51}$$

A brief comment is necessary at this point: here we have a pure quadratic nonlinearity for a single wave and no effective third order nonlinearity due to cascaded second-order ones is involved. This makes a sharp contrast with the nonlinear propagation of quadratic (parametric) solitons within the SVEA where phase matching is needed. One notices that in the present case no phase matching is required.

A brief comment is necessary at this point: here we have a pure quadratic nonlinearity for a single wave, and no phase matching is required, which makes a sharp contrast with the nonlinear propagation of quadratic (parametric) solitons within the SVEA where phase matching is needed. In addition, in contrast with the SVEA case for solitons in quadratic media far from phase-matching, no effective third order nonlinearity due to cascaded second-order ones is involved.

3.3.2. Half-cycle optical solitons

The fundamental soliton of the KdV equation expresses in the present case as

$$E_2 = \frac{k_3 ncp^2}{(-2\pi\chi^{(2)})}\operatorname{sech}^2\left(p\tau + \frac{2}{3}k_3 p^3\zeta\right), \tag{3.52}$$

where p is the soliton parameter, $k_3 = \frac{d^3k}{d\omega^3}\Big|_{\omega=0}$, and $\chi^{(2)} = \chi^{(2)}(2\omega;\omega,\omega)\big|_{\omega=0}$. The single-soliton solution of the KdV equation can be obtained (a) by direct integration [100], (b) by the Hirota method [135–138], or (c) by the inverse scattering transform [139,85]. At this point let us remind the reader a couple of well known properties of such localized solutions of completely integrable models. First, the stability and robustness of the fundamental soliton (3.52) is ensured from the inverse scattering transform for any positive value of the soliton parameter p. Second, the corresponding soliton solutions are proved to be the fundamental nonlinear modes of the KdV equation, in the sense that any input field distribution decomposes into a combination of a finite number of solitons and Fourier-type linear modes called 'radiation' which evolve separately, conserving their features during propagation.

For the sake of convenience, below we write down the standard dimensionless form of the KdV equation (3.47):

$$\partial_Z u + 6u\partial_\tau u + \partial_\tau^3 u = 0, \tag{3.53}$$

which is obtained by means of the change of variables $Z = -A\zeta$, $u = (B/6A)\,E_2$. Direct numerical simulations of this equation illustrates and confirms the rigorous mathematical result mentioned above: for a KdV equation, a FCP-type input decays into solitons, with a definite sign; see Fig. 7. For a short enough FCP, the number of emitted solitons is only one or two, see Fig. 7. One notices also that the number of emitted solitons depends on the carrier-envelope phase of the initial FCP at the entrance of the quadratic medium; see Fig. 7. When the value of the carrier-envelope phase is equal to zero, only one soliton is emitted from a short enough FCP input. By increasing the value of the carrier-envelope phase to, e.g., $\pi/2$ the

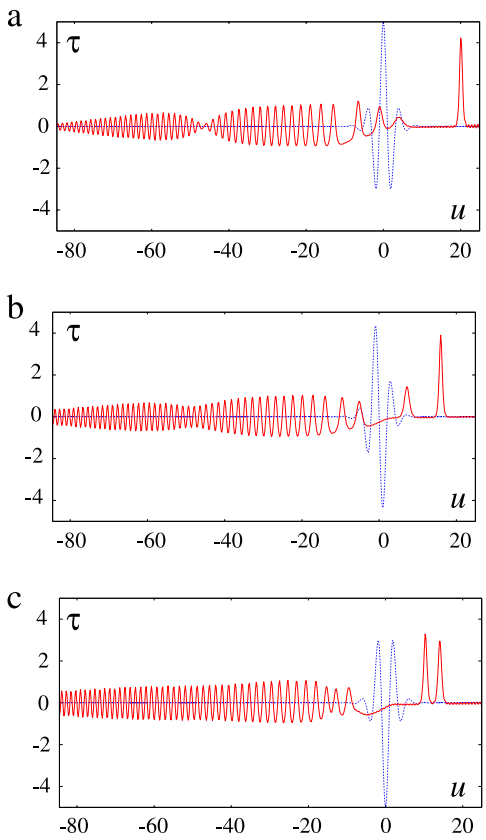

Fig. 7. (Color online) The input (dotted blue line) and output (solid red line) wave profiles for input carrier-envelope phase equal to 0 (a), $\pi/2$ (b), and π (c). It is seen that the number of emitted solitons (either one or two solitons) depends on the carrier-envelope phase of the input few-cycle pulse. After Ref. [120].

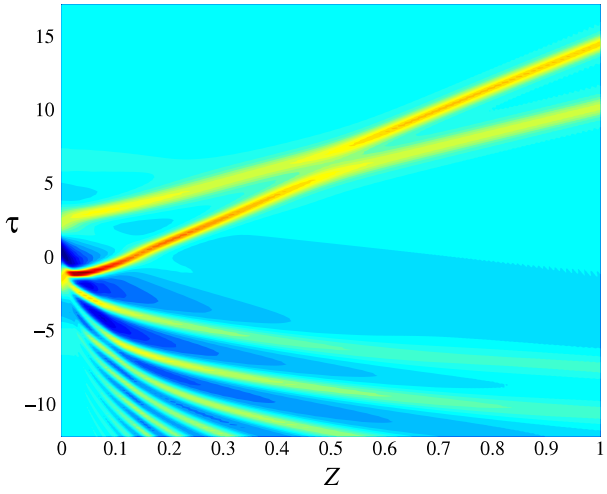

Fig. 8. (Color online) An input few-cycle pulse evolves into two half-cycle solitons and radiation for the input carrier-envelope phase is equal to 0.8π. The two half-cycle solitons have different velocities, higher than that of the radiation and they interact keeping their features. After Ref. [120].

number of emitted solitons is now equal to two. By further increasing the value of carrier-envelope phase the number of emitted solitons remains equal to two; see Fig. 7. The two emitted solitons have different velocities, and these velocities are conserved when the solitons interact with each other (elastic collision); see Fig. 8.

As a final comment of this section devoted to ultrashort solitons in quadratic media, we should stress that as a consequence of the non-existence of regular breathers to the KdV equation, in a medium with quadratic optical nonlinearity the fundamental soliton always occurs, i.e., half-cycle single-oscillation solitons will be produced from FCP inputs, and they have always the same field polarity. The obtained result is closely related to the non-centrosymmetry of media displaying quadratic optical nonlinearities.

4. A general model for few-cycle optical soliton propagation: the modified Korteweg–de Vries–sine–Gordon equation

4.1. Two-cycle optical pulses propagating in two-component nonlinear media: derivation of a governing nonlinear evolution equation

In this section by using Maxwell–Bloch equations, we analyze the response of a *two-component medium* of two-level atoms driven by a two-cycle optical pulse beyond the traditional approach of slowly varying amplitudes and phases; see Ref. [76] for a detailed study of this problem. We show that in the integrable case, a two-cycle analytical solution is available and enables us to generalize the notion of envelope and carrier to a FCP, without resorting to the SVEA, which is by no means valid in this case. Both group and phase velocities can be determined, and we show that the usual relation $v_g = \mathrm{d}\omega/\mathrm{d}k$ is not valid for a FCP. On the other hand, the envelope of the FCP soliton has the known sech shape of the envelope soliton of the NLS equation. In the integrable case there exist a family of two-cycle solitons with a *stable carrier-envelope phase*. The FCP soliton depends strongly on the dopant's matrix elements as well as on the relative population difference of the two components. In the general non-integrable case, the existence of two-cycle solitons and the stabilization of the carrier-envelope phase have been demonstrated by adequate numerical techniques; see Ref. [76]. The two-component approximation therefore provides a valuable starting point for the assessment of few-cycle optical pulses and the estimation of the carrier-envelope phase, which is a key issue in the area of ultrashort solitons.

In a seminal paper by Sazonov [68] it was derived a partial differential equation of the mKdV–sG type, governing the evolution of an optical FCP in a two-component medium. In some particular cases it reduces to either the mKdV equation or to the sG equation. Thus we consider the time-dependent propagation of a femtosecond pulse through a two-component medium. The response of the medium upon interaction with the femtosecond electromagnetic field $E(x, z, t)$ is described by the total macroscopic polarization P:

$$P = -2\,\mathrm{Im}\left(\sum_{j=1}^{2} N_j d_j R_j\right), \tag{4.1}$$

where d_j is the dipole transition matrix element and N_j is the atomic density of the jth component. The time dependence of the off-diagonal density-matrix elements $\rho_{21}^{(j)} \equiv R_j$ is given by the following coupled Maxwell–Bloch equations:

$$\left(\partial_z^2 - \frac{1}{c^2}\partial_t^2\right) E = \frac{4\pi}{c^2}\partial_t^2 P, \tag{4.2}$$

$$\partial_t R_j = -i\omega_j R_j - \frac{2d_j}{\hbar} E\, W_j, \tag{4.3}$$

$$\partial_t W_j = \frac{2d_j}{\hbar} E\,\mathrm{Re}\left(R_j\right). \tag{4.4}$$

Here W_j is the difference of transition populations of the jth component ($-1/2 \le W \le 1/2$) and ω_j is the atomic transition frequency of the jth component. We assume that the FCP duration τ_p is such that $\epsilon \sim \omega_1\tau_p \ll 1$ for the first component, and correspondingly $\epsilon^{-1} \sim \omega_2\tau_p \gg 1$, for the second component. In terms of the underlying physical situation, these two requirements can be met when a two-cycle pulse of a Ti: sapphire laser at 780 nm traverses, e.g., a Yb-doped $KGd(WO_4)_2$ crystal where the former condition is satisfied for the dopant and the latter condition is valid for the wolframate matrix. Notice that the two-component medium under the above two assumptions can be considered as a simplified model of a general transparent dielectric; see the discussion in Ref. [76].

Next it is convenient to rewrite the Bloch equations in terms of $U_j = \mathrm{Im}\left(R_j\right)$, then Eq. (4.3) involves

$$\mathrm{Re}\left(R_j\right) = \frac{1}{\omega_j}\partial_t U_j. \tag{4.5}$$

For the first component $W_1(t)$ the condition $\epsilon \sim \omega_1\tau_p \ll 1$ ensures a short-wave approximation, which yields the following solution of the Bloch equations:

$$W_1(t) = W_1(-\infty)\cos\theta, \qquad R_1 = -W_1(-\infty)\sin\theta, \qquad \theta = \frac{2d_1}{\hbar}\int_{-\infty}^{t} E dt', \tag{4.6}$$

where $W_1(-\infty)$ is the initial population difference, e.g., in the case of a medium in the ground state $W_1(-\infty) = -1/2$. For the second component the condition $\epsilon^{-1} \sim \omega_2\tau_p \gg 1$ implies that the FCP interaction with this component can be described within a long-wave approximation so that the level population renders almost intact; we then get the expressions for the quantities $U_2(t)$ and $W_2(t)$, as

$$U_2(t) = -\frac{2d_2E}{\hbar\omega_2}W_2(t) + \frac{2d_2W_2(-\infty)}{\hbar\omega_2^3}\partial_t^2 E, \tag{4.7}$$

$$W_2(t) = W_2(-\infty)\left[1 - 2\left(\frac{d_2 E}{\hbar\omega_2}\right)^2\right]. \tag{4.8}$$

Now eliminating the population differences W_j enables one to rewrite the Maxwell wave equation in terms of the pulse area θ. To this aim we then introduce a local time $\tau = t - zn_0/c$ and a 'slow' propagation variable $\zeta = \varepsilon z$. Then in the second order of the small parameter ε, and returning back to the physical propagation variable z, we arrive at the nonlinear propagation equation:

$$\partial_z\partial_\tau\theta + c_1\sin\theta + c_2\partial_\tau\left[(\partial_\tau\theta)^3\right] + c_3\partial_\tau^4\theta = 0, \tag{4.9}$$

where $c_1 = -8\pi d_1^2\omega_1 N_1 W_1(-\infty)/(n_0\hbar c)$, $c_2 = d_2^2 c_3/(2d_1^2)$,

$c_3 = 8\pi d_2^2 N_2 W_2(-\infty)/(n_0\hbar c\omega_2^3)$,

and $n_0 = \left[1 - 16\pi d_2^2 N_2 W_2(-\infty)/(\hbar\omega_2)\right]^{1/2}$. Here n_0 is the value of the linear refractive index when dispersion is neglected.

The refractive index is here

$$n^2 = 1 - 16\pi\sum_{j=1}^{2}\frac{d_j^2 N_j W_j(-\infty)\omega_j}{\hbar(\omega_j^2 - \omega^2)}. \tag{4.10}$$

Under the assumption that $\omega_1 \ll \omega \ll \omega_2$, the dispersion relation $k = n\omega/c$ can be rewritten as

$$k = \frac{n_0\omega}{c} - \frac{c_1}{\omega} - c_3\omega^3, \tag{4.11}$$

which is exactly the dispersion relation of the mKdV–sG equation (4.9), if we recall that the leading term $n_0\omega/c$ is included in the definition of the variable τ. It should be noticed that the same holds for the mKdV and sG models independently as derived above. Indeed, a Taylor expansion of the wavevector, taking into account the parity ($k(\omega)$ is even since the model is conservative), yields

$$k(\omega) = \frac{n\omega}{c} + \frac{1}{6}\frac{d^3k}{d\omega^3}\bigg|_{\omega=0}\omega^3 + \cdots \tag{4.12}$$

in which n is the linear index at $\omega = 0$ given by (3.8). Here again the leading term is absorbed by using the retarded time τ, and the following term exactly yields the dispersion relation of the mKdV equation (3.12). The dispersion relation of the sG model, system (3.30)–(3.32), is obtained by seeking a plane wave $E_0 = \mathcal{A}e^{i(\omega\tau - k\zeta)}$, $p = qe^{i(\omega\tau - k\zeta)}$, $w = w_i$, which yields

$$k = \frac{4\pi\Omega N|\mu|^2 w_i}{\hbar c\omega}. \tag{4.13}$$

The dispersion relation of the starting model in Section 3.2 is given by the refractive index of Eq. (2.22), if we assume $\alpha = 0$, in the case where all atoms are initially in the fundamental state ($W_i = -1$). Expanding $k = n\omega/c$ in a power series of $\omega/\omega_2 \ll 1$ shows that the latter dispersion relation exactly coincides with (4.13) in this limit.

The nonlinear susceptibility $\chi^{(3)} = \chi^{(3)}(\omega;\omega,\omega,-\omega)$ corresponding to the model (4.2)–(4.3)–(4.4) can be derived as follows. We set $E = \mathcal{A}e^{i\omega t} + \mathcal{A}^* e^{i(-\omega+\delta\omega)t}$. The frequency shift $\delta\omega \ll \omega$ is introduced to regularize a singularity in the computation. Eq. (4.3), or rather its counterpart in terms of U_j, is solved in a first approximation to yield $U_j = v_j e^{i\omega t} + cc$ with

$$v_j = \frac{-2dj\omega_j W_j(-\infty)}{\hbar\left(\omega_j^2 - \omega^2\right)}. \tag{4.14}$$

Then a solution of Eq. (4.4) is found in the form $W_j = W_j(-\infty) + W_j^{(2)}e^{2i\omega t} + W_j^{(0)}e^{i\delta\omega t} + W_j^{(-2)}e^{2i(-\omega+\delta\omega)t}$. After we take the limit $\delta\omega \longrightarrow 0$, a more accurate expression of U_j is found using the latter into Eq. (4.3), in the form $U_j = \left(v_j + v_j^{(1)}\right)e^{i\omega t} + v_j^{(3)}e^{3i\omega t} + cc$. The nonlinear polarization due to the transition j is $P_{NLj}(\omega) = 2d_j N_j v_j^{(1)} = 3\chi_j^{(3)}A|A|^2 e^{i\omega t}$ and consequently

$$\chi_j^{(3)}(\omega;\omega,\omega,-\omega) = \frac{8\omega_j d_j^4 N_j W_j(-\infty)}{\hbar^3\left(\omega_j^2 - \omega^2\right)^2}. \tag{4.15}$$

Obviously the total susceptibility is $\chi^{(3)} = \sum_{j=1}^{2}\chi_j^{(3)}$. Taking into account the relation between θ and E (Eq. (4.6)), it is seen that the coefficient of the mKdV-type nonlinear term in the mKdV–sG equation (4.9) is $B = -4d_1^2 c_2/\hbar^2$. Substituting the expression of c_2, and then that of c_3, and comparing with Eq. (4.15), it is found that $B = -2\pi/(n_0 c)\,\chi_2^{(3)}(\omega;\omega,\omega,-\omega)\big|_{\omega=0}$,

i.e. that the general formula (3.51) is valid, the 'non-resonant' transition only being taken into account. For the 'resonant' transition, no such simple expression of the coefficients can be proposed.

If we set $c_1 = 0$ in Eq. (4.9), i.e., if we neglect the 'resonant' term which represents both 'resonant' nonlinearity and dispersion, this equation reduces to the mKdV one. In turn, setting $c_2 = c_3 = 0$ transforms Eq. (4.9) into a sG equation by cutting off both 'non-resonant' nonlinearity and dispersion. Both nonlinear evolution equations are completely integrable by the IST method and have been extensively studied as a lowest-order approximation to the complete set of Maxwell–Bloch equations beyond the SVEA; see, e.g., Refs. [70,71,73–75].

Thus we arrived at the important result that the spatiotemporal evolution of the FCP having a pulse width such that $\omega_1 \ll 1/\tau_p \ll \omega_2$, will obey the evolution equation (4.9), which is in fact a superposition of the integrable mKdV and sG equations. This equation has already appeared in the dynamics of anharmonic crystals with dislocations. If $c_2 = c_3/2$, then Eq. (4.9) becomes completely integrable by the IST method; see Refs. [87,88]. This strict requirement reads in our case as $d_1 = d_2$. However we will show in what follows that by relaxing this severe condition we get *robust two-cycle solitons* in the nonintegrable case, too.

If we set $Z = c_3 z$ then the evolution equation (4.9) reduces to

$$\partial^2_{Z\tau}\theta - a\sin\theta + 3b\,(\partial_\tau\theta)^2\,\partial^2_\tau\theta + \partial^4_\tau\theta = 0, \tag{4.16}$$

where $a = -c_1/c_3$ and $b = c_2/c_3$. The integrability condition then expresses as $b = 1/2$.

4.2. The integrable modified Korteweg–de Vries–sine–Gordon equation: envelope, phase, and group velocities for the two-cycle pulses

We consider in this section the integrable mKdV–sG equation, in the normalized form

$$\partial^2_{Z\tau}\theta - a\sin\theta + \frac{3}{2}\,(\partial_\tau\theta)^2\,\partial^2_\tau\theta + \partial^4_\tau\theta = 0. \tag{4.17}$$

The discussion below is valid for mKdV and sG themselves with obvious adaptation. Following Ref. [88] we can write down the two-soliton solution of Eq. (4.16) as

$$\theta = -4\tan^{-1}\left[Q\left(e^{-s_1}, e^{-s_2}\right)\right],$$

where $s_j = 2A_{j0}Z + 2\eta_j\tau$, $A_{j0} = -4\eta_j^3 + a/(4\eta_j)$, $(j = 1,\ 2)$, and

$$Q(X, Y) = \left(\frac{c_{10}}{2\eta_1}X + \frac{c_{20}}{2\eta_2}Y\right)\left[1 - c_{10}c_{20}\frac{(\eta_1 - \eta_2)^2}{4\eta_1\eta_2(\eta_1 + \eta_2)^2}XY\right]^{-1}. \tag{4.18}$$

In the framework of the IST method, $i\eta_1$ and $i\eta_2$ are discrete eigenvalues, and the quantities $\eta_{1,2}$ must be real and positive; the real coefficients c_{10} and c_{20} are the corresponding initial scattering data. However, notice that the above exact two-soliton solution Q remains valid for any complex values of the quantities $\eta_{1,2}$, c_{10}, and c_{20}. However, since the pulse area θ is a real quantity, we must have $\eta_2 = \eta_1^*$ and $c_{20} = c_{10}^*$. If we next set $\eta_1 = (p + i\omega)/2$ and $c_{10}/(2\eta_1) = Ce^{i\phi}$, then $s_2 = s_1^*$, with $s_1 = \Psi + i(\Phi + \phi)$, where the quantities p, ω, C, ϕ, Φ, and Ψ are real. We will next see that the real quantities p and ω are actually the wave pulsation and the inverse of pulse duration, respectively. With these notations we thus get from the two-soliton solution, the breather solution of the mKdV–sG equation (4.16); see Ref. [68].

An important fact is that the above *breather solution* can be decomposed into a *carrier wave* and an *envelope*, not only in an approximate way in the SVEA limit, but also exactly, for a FCP solution, hence generalizing the notions of carrier and envelope beyond the SVEA regime. To this aim we notice that the quantity Q is a rational expression and can be written as $Q\left(e^{-s_1}, e^{-s_2}\right) = P\left(e^{-\Psi}, \cos\Phi\right)$, where P is another rational expression,

$$P(X, Y) = 2CXY/\left(1 + C^2p^2X^2/\omega^2\right). \tag{4.19}$$

In this way it appear explicitly a carrier wave $\cos\Phi$ and an envelope:

$$\theta_e = -4\tan^{-1}P\left(e^{-\Psi}, 1\right) = -4\tan^{-1}\left[2Ce^{-\Psi}/\left(1 + C^2p^2e^{-2\Psi}/\omega^2\right)\right]. \tag{4.20}$$

In Fig. 9(a), we show the fact that the wave envelope obtained above coincides with the extrema of the pulse shape. In Fig. 9(b) and (c) we present the scaled electric field $\frac{2d_1}{\hbar}E$ and the scaled 'resonant' population difference $W_2(\tau)/W_2(-\infty)$. The wave spectrum slightly differs from the spectrum of the field envelope; see Fig. 9(d). The parameters are the following: $C = 1$, $p = 2$, the carrier frequency $\omega = 8$, and $\phi = 0$. The expressions of Ψ and Φ are $\Psi = p\left(\tau - Z/V_g\right)$, $\Phi = \omega\left(\tau - Z/V_\phi\right) - \phi$, with

$$V_g^{-1} = p^2 - 3\omega^2 - a/(p^2 + \omega^2),\ V_\phi^{-1} = 3p^2 - \omega^2 + a/(p^2 + \omega^2). \tag{4.21}$$

where $\omega = \frac{1}{2}\mathrm{Im}(\eta_1)$ and $p = \frac{1}{2}\mathrm{Re}(\eta_1)$ are the wave pulsation and inverse of pulse duration, respectively. We notice that these group and phase velocities allow us to define a group velocity v_g and a phase velocity v_ϕ for the FCP itself,

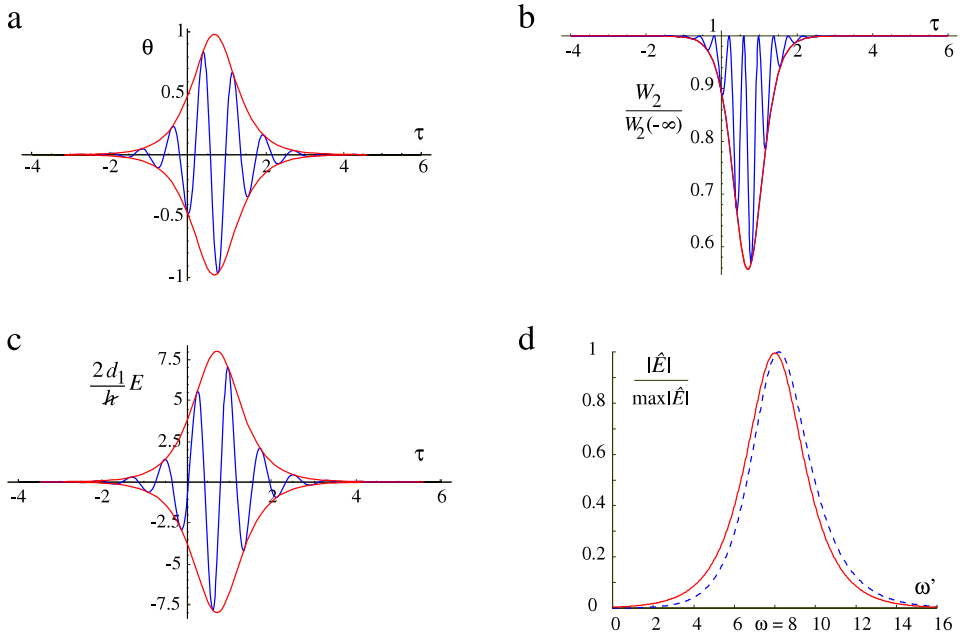

Fig. 9. (Color online) (a) The analytical two-cycle solution to Eq. (4.16) in the integrable case, and its envelope. (b) The electric field and its envelope. (c) The 'resonant' population difference and its envelope. (d) The optical spectrum (dashed line) compared to the spectrum of the field envelope, shifted to the carrier frequency (solid line). After Ref. [76].

$v_{g,\phi}^{-1} = \frac{n_0}{c} + c_3 V_{g,\phi}^{-1}$, which so far have been meaningful only within the SVEA regime. Notice that if we define the wave vector in the usual way as $k = \omega/v_\phi$, and if we then compute the derivative of ω with respect to the wave vector k we find that $d\omega/dk$ is not equal to the group velocity v_g, except in the limit $p \to 0$, which is the SVEA limit. This important remark could be expected, since the relationship $v_g = d\omega/dk$ is valid only within the framework of SVEA.

Note that the relations (4.21) were first derived by using the following procedure [68]. First, the linear dispersion relation is obtained by linearizing the governing equation (4.16):

$$\partial_{Z\tau}^2\theta - a\theta + \partial_\tau^4\theta = 0.$$

In order to get the linear dispersion equation we substitute $\theta \sim \exp[i(\omega\tau - kZ)]$ in the above equation and we arrive at the linear dispersion relation $k(\omega) = F(\omega) = \frac{a}{\omega} - \omega^3$. Then we use the method of analytically continuing the linear dispersion relation in the complex plane; see Refs. [141,68]. Thus replacing $\omega \to \omega + ip$, with $p = 1/\tau_p$, and $k \to k + i\kappa$, we get a complex linear dispersion relation $k + i\kappa = F(\omega + ip)$; the existence of the breather solution ensures the validity of this dispersion relation on the whole complex half plane. The total phase is then given by $(k+i\kappa)Z - (\omega+ip)\tau = k(Z - V_\phi\tau) + i\kappa(Z - V_g\tau)$, with $V_\phi = \omega/k$ and $V_g = p/\kappa$. Thus $V_g^{-1} = [F(\omega + ip) - F(\omega - ip)]/(2ip)$, $V_\phi^{-1} = [F(\omega + ip) + F(\omega - ip)]/(2\omega)$, and if we use the above expression of $F(\omega)$ we recover the relations (4.21) by using the above method of analytically continuing the dispersion relation in the complex plane; see Ref. [68]. The integrability by means of the IST ensures the validity of the procedure. Indeed, the evolution of the spectral data in the frame of the IST is given by the linear dispersion relation, which ensures that the latter is valid on the imaginary axis. The existence of the breather solution ensures the validity of the analytically continued dispersion relation on the remaining of the complex plane.

Next we get the envelope of the electric field. It can be easily obtained from the expression of the electric field of the FCP by using the corresponding expression of the two-soliton solution (see Ref. [87]) by setting Φ to a constant; here $\Phi = \pi/2$:

$$E_{env} = \frac{2\hbar}{d_1} p \ \mathrm{sech}\left(\Psi - \ln\frac{p}{C\omega}\right). \tag{4.22}$$

Within the SVEA, the mKdV–sG equation (4.16) can be reduced to the NLS equation:

$$i\partial_Z A + \mu\partial_T^2 A + \eta A|A|^2 = 0, \tag{4.23}$$

with $\mu = -3\omega + a/\omega^3$, $\eta = 3b\mu d_1^2/\hbar^2$, and $T = \tau + Z(3\omega^2 + a/\omega^2)$. Here $E \approx A\exp[i\omega(\tau - Z/v_\phi)] + cc$, where A is the solution of the NLS equation (4.23). It is well known that the single soliton solution of the NLS equation (4.23) is given by

$$A = 2q \ \mathrm{sech}\left\{2q\left[\sqrt{\frac{\eta}{2\mu}}\,(T - T_0) + 2\lambda\eta Z\right]\right\} \times \exp\left\{-i\left[2\lambda\sqrt{\frac{\eta}{2\mu}}\,T + 2\eta\left(\lambda^2 - q^2\right)Z\right]\right\} \tag{4.24}$$

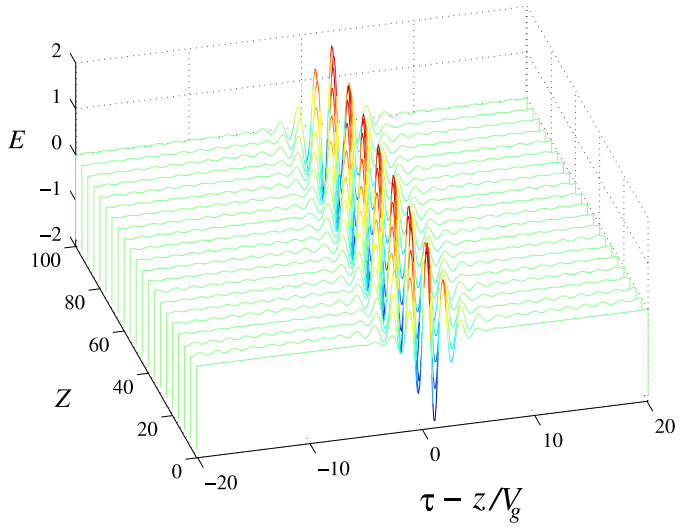

Fig. 10. (Color online) Robust, dispersion-free propagation of a two-cycle optical pulse for a large resonant term. The parameters are $a = -500$, $b = 2$, and $p_1 = 1 + 4i$. After Ref. [76].

where λ and q are arbitrary real parameters. Since λ is a shift between the central frequency of the pulse and that of the envelope, it must be set here to $\lambda = 0$. Next we identify the value of the parameter q as $q = p\hbar/d_1$ and we have $E_{env} = |A|$; in other words, the above equation reduces to $A = E_{env} \exp[ip^2(a/\omega^3 - 3\omega)Z]$, i.e., the envelope of the FCP coincides with that of the soliton of the NLS equation, not only in the SVEA limit $p \to 0$, as was already noticed in Ref. [68], but also in the two-cycle regime where the SVEA is not valid and the envelope soliton is merely meaningless; see Ref. [76]. We notice that it is possible to obtain a FCP with a constant relative carrier-envelope phase. The relative phase of the envelope and of the carrier is of much importance for a FCP and it is constant if the group and phase velocities $V_{g,\phi}$ are equal. This particular situation holds when $(p^2 + \omega^2)^2 + a = 0$, i.e., the parameter a should be a negative number. This conditions implies that $W_1(-\infty)W_2(-\infty) < 0$, i.e., an initial population inversion must be reached for one of the two transitions only; see Ref. [76].

4.3. The non-integrable mKdV–sG equation: robust two-cycle optical solitons

In Ref. [76] it was proved by numerical techniques the existence and robustness of two-cycle dispersion-free pulses in the two-cycle regime, in the general, nonintegrable case, i.e., when the coefficients $a \neq 0$ and $b \neq 1/2$ in the evolution equation (4.16). In order to perform this analysis the exact breather solution U_{two} of the mKdV equation was used as the input field; see Eq. (3.20). Note that for $a = 0$ and $b \neq 1/2$ the solution θ can be written as:

$$\partial_\tau \theta = \frac{2d_1}{\hbar} E = \frac{2}{\sqrt{2b}} U_{\text{two}}, \tag{4.25}$$

where $\eta_j = p_j\tau - p_j^3 z - \gamma_j$, for $j = 1, 2$, $p_2 = p_1^*$, and $\gamma_2 = -\gamma_1$.

For the numerical calculations a fixed value $b \neq 1/2$ was considered, and a negative value of the strength a of the resonance term was chosen. The *exponential time differencing method* (see Ref. [115]) along with absorbing boundary conditions in order to avoid numerical instability of the background was used in the computations. In Fig. 10 we show a typical robust propagation in the non-integrable case of the two-cycle pulse (4.25) in a medium with a relatively high concentration of the resonant atoms ($a = -500$). In this case the group-velocity V_g departs considerably from that of the mKdV breather, i.e., from $V_{g0} = [(\text{Re}p_1)^2 - 3(\text{Im}p_1)^2]^{-1}$. For the particular set of the parameter chosen in Fig. 10, it was numerically determined $V_g^{-1} = -32.25$ instead of $V_{g0}^{-1} = 47$ for the mKdV equation. Notice that for positive values of the parameter a, that is, when both of the initial population differences $W_{1,2}(-\infty)$ are of the same sign, the situation is somehow different, in the sense that a robust FCP still exists in this case, but appreciably differs from the mKdV breather; see Ref. [76] for more details. In Fig. 11 we show the stabilization of the carrier-envelope phase in the nonintegrable case for a value of the parameter $a = -292.55$ which is very close to $a = -(p^2 + \omega^2)^2 = -289$, which was predicted in the integrable case; see Ref. [76].

4.4. Few-optical-cycle solitons: the modified Korteweg–de Vries–sine–Gordon equation versus other non SVEA models

In this section we prove by both analytical and numerical methods that the general dynamical model based on the generic modified Korteweg–de Vries–sine–Gordon equation retrieves the main results reported so far in the literature, and so demonstrating its remarkable mathematical capabilities in describing the physics of few-cycle-pulse optical solitons; for a detailed study see Ref. [78].

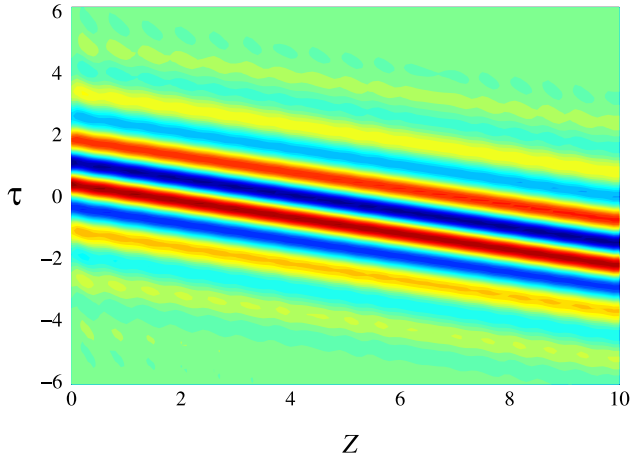

Fig. 11. (Color online) Stabilization of the carrier-envelope phase of the two-cycle pulse. The parameters are $a = -292.55$, $b = 2$, and $p_1 = 1 + 4i$. After Ref. [76].

As it was said in the Introduction the propagation of FCPs in nonlinear optical media can be described beyond the SVEA by using three main dynamical models: (a) the modified Korteweg–de Vries equation [70–72], (b) the sine–Gordon equation [73–75], and (c) the modified Korteweg–de Vries–sine–Gordon equation [76–79]. However, other non-SVEA models [141–143], especially the so-called short-pulse equation (SPE) [144], have been proposed in the literature. We next discuss the main features of the generic mKdV–sG model and the physical hypotheses it involves are described. We then show that both the SPE, and another model put forward in Refs. [141–143,81] can be considered as approximate versions of a generic mKdV–sG equation. However the FCP solitons obtained in [81] differ from the breather solutions of mKdV–sG equation considered in Ref. [76]. Indeed, in Ref. [76] it was assumed a self-focusing-type mKdV equation, whereas in Ref. [81] a self-defocusing one. The self-defocusing-type mKdV equation cannot support any breather solitons, but we show by approximate analytical methods and by numerical computation that the mKdV–sG equation containing a self-defocusing mKdV term is, within some approximation, equivalent to a pure sG equation, and therefore supports breather-type solitons very close to the sG ones. Then we obtain within the SVEA the linear dispersion relation $k = k(\omega)$, the group-velocity dispersion (GVD) and a rough approximation of the pulse shape for which self-focusing occurs. Numerical computations confirm the qualitative conclusions, and also that the FCP propagation strongly differs from that one predicted by the SVEA. We arrive at the conclusion that both the FCP solitons given in Ref. [81] as well as other soliton solutions can be adequately described by a generic mKdV–sG equation.

4.4.1. A comparison of mKdV, sG, and mKdV–sG models for describing few-cycle solitons

A temporal soliton, or more properly a temporal solitary wave, is a pulse which propagates in a highly dispersive medium in such a way that a certain nonlinear effect exactly compensates dispersion (in the sense of the natural tendency of spreading of the pulse), and the pulse shape remains unchanged during propagation. This unique phenomenon implies two essential conditions: (i) the medium is lossless, and (ii) the order of magnitude of propagation distance, wave amplitude, wavelength, dispersion and nonlinear characteristics of the medium are such that neither the dispersion nor the nonlinearity is negligible, and that both have effects comparable in magnitude. The two assumptions are unavoidable as soon as any kind of soliton is considered (except obviously the so-called 'dissipative solitons', but the latter require the mutual compensation of gain and loss effects).

Hence soliton propagation implies that damping can be neglected. In dielectric media, this occurs far from any resonance frequency. Let us first consider a two-level model with characteristic frequency Ω, and denote by ω a frequency characteristic for the FCP soliton under consideration. The transparency condition implies that either $\omega \ll \Omega$ or $\Omega \ll \omega$. The former case ($\omega \ll \Omega$) corresponds to the long-wave approximation. Assuming further that the wave amplitude is such that the nonlinear and dispersive effects are comparable, the reductive perturbation method [93] allows us to derive a mKdV evolution equation [70,73]: if, on the contrary, the characteristic frequency of the pulse is well above the resonance line ($\omega \gg \Omega$), the short-wave approximation allows us to derive a sG evolution equation, written in its dimensionless form as $\partial_z \partial_t v = \sin v$ [73].

In the case of a two-component medium, in which each component is described by a two-level model, there are two resonance frequencies, say $\Omega_1 < \Omega_2$. An appreciable change with respect to the previous situation arises if the transparency domain lies between Ω_1 and Ω_2. In this case assuming that $\Omega_1 \ll \omega \ll \Omega_2$, the propagation of FCPs can be described by a mKdV–sG equation, of the dimensionless form [76]

$$\partial_z u + c_1 \sin\left(\int^t u\right) + c_2 \partial_t \left(u^3\right) + c_3 \partial_t^3 u = 0. \tag{4.26}$$

It must be noticed that the coefficient c_1 of the sG-type term in Eq. (4.26) is proportional to the population difference. Especially, c_1 is usually positive, but becomes negative when a population inversion is realized, and vanishes if the two levels are equally populated.

The approximation used in deriving the above mKdV–sG equation is quite realistic in the general setting. Indeed, in order to get a soliton, the entire pulse spectrum must belong to the transparency domain. Hence, all optical transitions of the medium can be separated into two distinct groups, some transitions well below ω, and the other ones well above ω. If each of these two sets of resonance frequencies is approximated by a single transition, we exactly get the assumptions under which the mKdV–sG model has been derived. In the general case, it is reasonable to consider that the various lines will cumulate together to reconstruct the same terms in the mKdV–sG equation, however with more complicated coefficients. One notices that the quite general model equation (4.26) was first derived and studied in Refs. [68,145].

A few comments are needed at this point: it is well-known that both mKdV and sG equations are integrable by means of the inverse scattering transform method [113,86] and that both equations admit *breather solitons*, that are known to adequately describe FCPs; see Ref. [73]. These breather solutions have both spectrum and field profile analogous to the ones that can be obtained either experimentally or using other theoretical models. Moreover, from the established mathematical properties of these two completely integrable equations, any Gaussian-like input is expected to evolve into a FCP soliton [146]; hence breathers can be considered as the fundamental solutions of the two integrable equations mentioned above, as soon as the input is symmetrical with respect to a change in the sign of the field. The more general mKdV–sG equation (4.26) is also integrable if its coefficients obey the relationship $c_3 = 2c_2$; see Ref. [87]. However, for other values of its coefficients, it has been shown by numerical simulations that FCP solitons (or breathers) still exist, and their robustness has been investigated too; see Ref. [76].

4.4.2. The short-pulse equation: a special case of the mKdV–sG equation

Let us consider the so-called short-pulse equation (SPE), which was first introduced in [144], to describe FCP propagation in silica fibers:

$$\partial_z \partial_t U = U + \frac{1}{6}\partial_t^2 \left(U^3\right). \tag{4.27}$$

Note that the derivation of this equation performed in Ref. [144] was based on a parabolic approximation of the linear dispersion relation $\chi = \chi^{(1)}(\lambda)$, which is valid in silica glass for $1.55\,\mu\text{m} \leq \lambda \leq 3\,\mu\text{m}$, and on a purely cubic instantaneous nonlinear polarization. Also, the reduction of the bi-directional Maxwell equations to a uni-directional one was performed by means of a short wave approximation. The mathematical validity of the SPE as an asymptotics to Maxwell equations has been rigorously justified in Ref. [147]. The SPE is integrable by means of the IST method [148], and soliton solutions have been given in Ref. [149]; see also Refs. [150–157] for other aspects of the SPE. Vectorial versions of the SPE have been also proposed and their soliton solutions have been investigated too [158,82,159].

A third model, which is in fact the SPE with an additional dispersion term, has been first derived in Ref. [141] long before the introduction in the literature of the so-called SPE model:

$$\partial_z \partial_t U + U - \mu \partial_t^4 U + \partial_t^2 \left(U^3\right) = 0. \tag{4.28}$$

Note that a multi dimensional version of Eq. (4.28) was given in [142] and the self-focusing and pulse compression has been demonstrated in Ref. [143]. However, it has been recently considered in a vectorial version, which has shown pulse self-compression and FCP soliton propagation; see Ref. [81].

We then show that the mKdV–sG equation can be reduced to the SPE. Obviously, the mKdV–sG model (4.26) reduces to the mKdV one if $c_1 = 0$, and to the sG equation if $c_2 = c_3 = 0$. In the same way, Eq. (4.28) reduces to the SPE (4.27) if $\mu = 0$. It is easy to derive the SPE equation (4.27) from the mKdV–sG one (4.26): a small amplitude approximation yields $\sin(\int^t u) \simeq \int^t u$, the mKdV-type dispersion term is neglected ($c_3 = 0$), then setting $c_1 = -1$, $c_2 = -1/6$, Eq. (4.26) becomes, after derivation with respect to t, identical to Eq. (4.27). The same transform but with $c_1 = c_2 = 1$ and $c_3 = -\mu$ gives the alternative model equation (4.28).

The mKdV–sG model is able to predict pulse compression, as shown in Fig. 12, which is similar to the result presented in Ref. [81]. However, the concrete situation considered in Ref. [81] involves $\mu > 0$, i.e., $c_3 < 0$. If we disregard the term u coming from the sG equation or the 'resonant' part of the equation, this corresponds to a *defocusing mKdV equation*. It is worthy to mention that the mKdV–sG equation supports FCP solitons, but only the case of focusing mKdV equation was considered in Ref. [76]. However, the defocusing mKdV equation does not support FCP solitons, as we will see below. On the other hand, the pure sG equation admits breather solutions which allow us to describe the FCP solitons [73]. It is worthy to notice that the soliton put forward in Ref. [81] is nothing else than a soliton of the mKdV–sG equation by using the dispersion term of the sG equation and the nonlinearity term of the mKdV equation, whose relative signs correspond to the self-focusing case.

In Ref. [76] we considered the mKdV–sG equation (4.26) and we set $\int^t u = v$, in order to get the equation

$$\partial_z \partial_t v + c_1 \sin v + c_2 \partial_t \left(\partial_t v\right)^3 + c_3 \partial_t^4 v = 0. \tag{4.29}$$

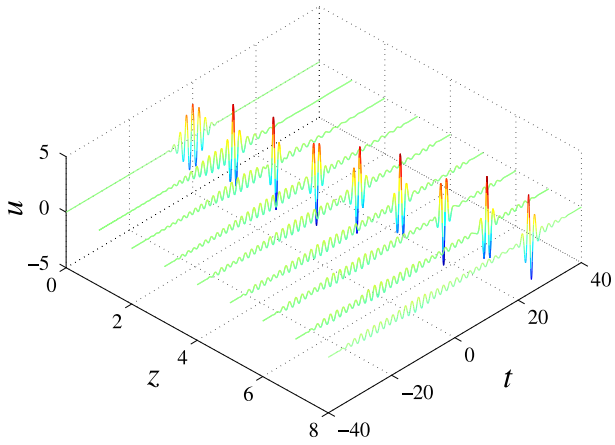

Fig. 12. (Color online) Compression of a long input pulse containing several optical cycles to a FCP soliton, as described by the mKdV–sG equation with parameters $c_1 = 50$, $c_2 = 0.5$, and $c_3 = 1$. After Ref. [78].

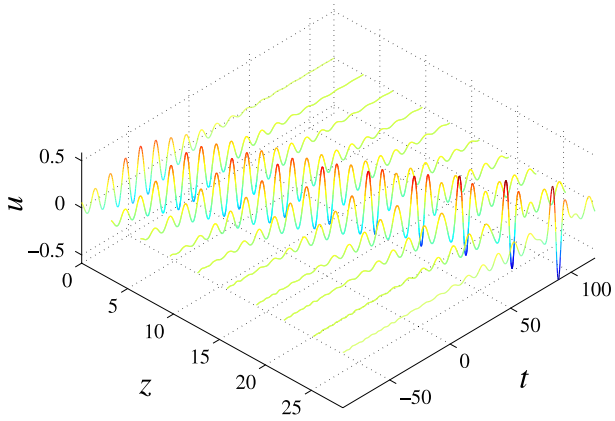

Fig. 13. (Color online) Pulse compression described by the mKdV–sG equation (4.29) with defocusing mKdV part. Input is a pulse with the hyperbolic secant envelope solution to the SVEA limit of mKdV–sG, with pulse length $\tau_0 = 25$ and angular frequency $\omega = 0.5$. Parameters are $c_1 = c_2 = 1, c_3 = -0.5$. After Ref. [78].

Note that for low amplitudes, the sG term in the above equation can be expanded in a power series of v to yield

$$\partial_z \partial_t v + c_1 \left(v - \frac{v^3}{6} \right) + c_2 \partial_t \left(\partial_t v \right)^3 + c_3 \partial_t^4 v = 0. \tag{4.30}$$

Due to the peculiar form of the third term in Eq. (4.30) containing the partial derivative $\left(v_t^3\right)_t$, the two nonlinear terms in Eq. (4.30) differ and cannot be straightforwardly compared; see Ref. [76]. Moreover, we have shown in Ref. [76] that the mKdV–sG model (4.26) with a true defocusing mKdV part, that is, when $c_3 < 0$ also possesses FCP soliton solutions and accounts for pulse self-compression. Thus in order to treat all equations at the same time, it was considered in Ref. [76] a more general equation

$$\partial_z \partial_t v + c_1 v - \frac{c_1'}{6} v^3 + c_2 \partial_t \left(\partial_t v \right)^3 + c_3 \partial_t^4 v = 0, \tag{4.31}$$

which becomes a mKdV–sG equation (4.30) if $c_1' = c_1$, and reduces to Eq. (4.28) if $c_1' = 0$. Note that the general Eq. (4.31) becomes (a) a sG equation (in the low-amplitude limit involved by the SVEA) if $c_2 = c_3 = 0$ and $c_1' = c_1$, (b) a mKdV equation if $c_1' = c_1 = 0$, (c) a SPE if $c_1' = c_3 = 0$, and has the normalized form (4.27) if, additionally, $c_1 = -1$ and $c_2 = -1/6$, (d) a normalized version of Eq. (4.28) if we put $c_1' = 0$, $c_1 = c_2 = 1$ and $c_3 = -\mu$, and (e) a mKdV–sG equation if $c_1' = c_1$.

In Fig. 13 we show pulse compression described by the mKdV–sG equation (4.29) with defocusing mKdV part. In this typical example, the pulse length $\tau_0 = 25$ is quite large and the angular frequency is $\omega = 0.5$. The velocity V_p of the pulse is computed from the numerical results, as $V_p \simeq 0.222$. It is close to, but still differs from the value of group velocity $d\omega/dk \simeq 0.229$ predicted by the SVEA by using the corresponding linear dispersion relation $k = -(c_1/\omega) - c_3\omega^3$.

Note that for shorter pulses the numerical solution to the mKdV–sG equation goes further away from the SVEA–NLS approximation, but the FCP soliton propagation still occurs; see Ref. [76]. As a typical situation, if we decrease the pulse length significantly to $\tau_0 = 8$ preserving the angular frequency $\omega = 0.5$, two FCP solitons, one taking the major part of the energy, and the other much smaller, are formed, while a non-negligible part of energy is radiated as dispersing waves; see

Ref. [76]. For this case the pulse velocity computed from the numerical data is $V_p \simeq 0.134$, while $d\omega/dk \simeq 0.229$ as above because we preserved the values of the linear coefficients c_1 and c_3. However, now the discrepancy is large, thus confirming the fact already evidenced in Ref. [73] that the usual expression of the group velocity is not valid any more for short FCP solitons.

Concluding this section we stress that it was proved in Ref. [76] that the dynamical model based on the modified Korteweg–de Vries–sine–Gordon partial differential equation was able to retrieve the results reported so far in the literature, and so demonstrating its remarkable mathematical capabilities in describing the physics of few-cycle-pulse optical solitons. Thus the generic modified Korteweg–de Vries–sine–Gordon equation contains all non-slowly varying envelope approximation model equations which have been earlier proposed for the description of $(1 + 1)$-dimensional few-cycle-pulse soliton propagation models.

5. Few-optical-cycle solitons: their interactions

In this section we consider the problem of few-optical-cycle soliton interactions. Following Ref. [77], by using the exact four-soliton solutions of the modified Korteweg–de Vries–sine–Gordon equation describing the propagation of few-optical-cycle pulses in transparent media with instantaneous cubic nonlinearity, we study the interaction of two such initially well-separated pulses. One notices that in Ref. [77] the shapes of soliton envelopes, the shifts in the location of envelopes maxima, and the corresponding phase shifts were explicitly calculated.

The more general mKdV–sG equation proved to describe fairly well the propagation of ultrashort optical pulses in a Kerr nonlinear medium and so demonstrating its remarkable mathematical capabilities in describing the physics of few-optical-cycle solitons; see the comprehensive studies reported in Refs. [76,78]. Though the mKdV and sG equations are completely integrable by means of the inverse scattering transform method [85], the mKdV–sG equation is completely integrable only if some condition between its coefficients is satisfied [87]. The general n-soliton solution of the mKdV–sG equation was obtained in a closed form in Ref. [140]; therefore we may easily get from it the general four-soliton solution and correspondingly, the two-breather solution (for specific sets of its parameters), from which can be drawn all features of the interaction between two FCPs. Note that the two-breather solution describes the interaction in a Kerr medium of two few-optical-cycle solitons initially well separated, in any physical setting where one of the three above mentioned integrable models (KdV, sG, mKdV–sG) is a realistic one. Moreover, thanks to the existence of analytic expression for the two-breather solution, the location and phase shifts resulting from the interaction were computed explicitly; see Ref. [77].

5.1. Exact four-soliton and two-breather solutions of the integrable mKdV–sG equation

Here we consider the propagation of optical FCPs in a one dimensional self-focusing Kerr medium, such as a highly nonlinear optical fiber. In any physical application, FCPs will be periodically launched in the medium, in such a way that they propagate as robust solitons. Due to the fluctuations of the intensity of the laser source, the consecutive FCPs may have different power and energies, and consequently different velocities. Therefore they are expected to interact and to cross each other. Here we briefly discuss what happens during the interaction of such ultrashort pulses; see Ref. [77].

The evolution of the electric field is governed by the mKdV–sG equation, which is in general a nonintegrable nonlinear evolution equation. However in the completely integrable case, for a special choice of its coefficients, it reads as

$$\partial_\tau \partial_z u + c_1 \sin u + 3c_2 \left(\partial_\tau u\right)^2 \partial_\tau^2 u + 2c_2 \partial_\tau^4 u = 0, \tag{5.1}$$

where the dimensionless variables u, z and τ are respectively proportional to the electric field, the propagation distance, and the retarded time, in a frame moving at the linear group velocity of the medium. Notice that u is not an amplitude, but is proportional to the electric field itself. Both constants c_1 and c_2 are related to the dispersion and nonlinear properties of the medium, see [76]. The integrable mKdV–sG equation (5.1) reduces to the integrable mKdV equation for $c_1 = 0$ and to the integrable sG equation for $c_2 = 0$.

The n-soliton solution of the above mKdV–sG equation is given by [140]:

$$u = 2i \ln\left(\frac{f^*}{f}\right), \tag{5.2}$$

where $f = \sum_{\mu_j = 0,\,1} E_\mu$, with $\mu = (\mu_1, \ldots, \mu_n)$,

$$E_\mu = \exp\left[\sum_{j=1}^{n} \mu_j \left(\xi_j + \frac{i\pi}{2}\right) + \sum_{l=1}^{n} \sum_{j=1}^{n} \mu_j \mu_l A_{j,l}\right], \tag{5.3}$$

and $A_{j,l} = \ln[(k_j - k_l)^2/(k_j + k_l)^2]$, $\xi_j = k_j \tau + \Omega_j z + \xi_{0j}$, $\Omega_j = -c_1/k_j - 2c_2 k_j^3$, here $j, l = 1, \ldots, n$ and the parameters k_j are arbitrary. These solutions are properly speaking solitons only for real values of the parameters k_j, but the solution holds for any complex values of k_j. For the particular case $n = 4$, and assuming that $k_3 = k_1^*$, $k_4 = k_2^*$, we are left with the two-breather solution of the integrable mKdV–sG equation. Next we set $k_1 = p_1 + i\omega_1$ and $k_2 = p_2 + i\omega_2$, so that ω_1 and

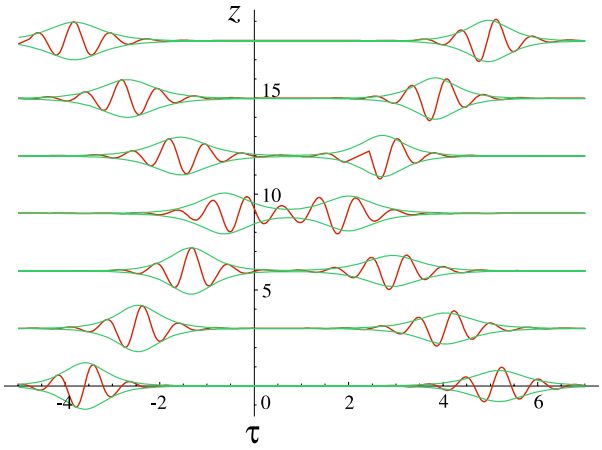

Fig. 14. (Color online) Interaction of two FCPs described by the two-breather solution of the mKdV–sG equation. The two envelopes are also shown. Here the parameters of the exact two-breather solution are $p_1 = 2$, $p_2 = 2.5$, and $\omega_1 = \omega_2 = 8$. After Ref. [77].

ω_2 are the characteristic frequencies of the two FCPs, and $1/p_1$, $1/p_2$ are their characteristic durations. The two-breather solution of the pure mKdV and the pure sG equations are recovered by setting either $c_1 = 0$ or $c_2 = 0$ in Eqs. (5.2)–(5.3), respectively.

5.2. Interaction of two few-cycle solitons

Fig. 14 shows the general envelope. Fig. 15(a) shows the two FCPs and their input and output envelopes, at $z = -15$. Here the output envelopes are defined as the envelope of the breather, at this propagation stage, which will coincide with the output of the interaction as $z \to +\infty$, after having propagated alone. Fig. 15(b) presents the same two-breather soliton and input and output envelopes, at $z = +15$. The coincidence between the FCPs and envelopes, at least in location, is checked for the numerical values. The shift in the location of the breathers appears clearly in Fig. 15. Input and output envelopes and the location of the maxima of the envelopes were obtained analytically in Ref. [77]. In Ref. [77], it was seen that the envelopes u_{j+e}, corresponding to the largest values of τ, did not have the correct amplitudes. The definition of the envelope implies indeed that the oscillation carrier is replaced by some constant φ_j adequately chosen, and in [77], this constant was taken as zero, which was the adequate value for the leftmost profiles (u_{j-e}), not for the rightmost ones (u_{j+e}). This feature brought forward the existence of the arising of a phase shift during the interaction. Seeking for the value of φ_j for which the maximum of the 'envelope' function becomes zero allowed to analytically compute the phase shift. The obtained value has been used in Fig. 15. Note that both the location and phase shifts vanish in the SVEA limit.

Numerical computations of Eq. (4.26) starting from an input yielded by a linear superposition of two breather solutions u_{two} of the mKdV equation is shown in Figs. 16 and 17. We see that the behavior of the interaction is qualitatively the same in the non-integrable case as in the integrable one. However, computation of the shifts in phase and location in the non-integrable case is possible for special values of parameters only, and involve lengthy numerical computations for each set of parameters.

Concluding this section we stress that the shapes of both input and output soliton envelopes as well as the phase and location shifts have been computed in Ref. [77] by using the exact expression for the four-soliton (two-breather) solution of the mKdV–sG equation. It was pointed out in that work the remarkable fact that, in contrast to the case of SVEA case (i.e., the case of envelope solitons), neither phase matching nor group-velocity matching are required for two few-cycle pulses to interact efficiently.

6. Circularly polarized few-optical-cycle solitons

6.1. Polarization effects in Kerr media: long wave approximation

In this section we consider the propagation of circularly polarized few-cycle pulses in Kerr media beyond the slowly varying envelope approximation. Assuming that the frequency of the transition is far above the characteristic wave frequency (long-wave-approximation regime), we show that propagation of FCPs, taking into account the wave polarization, is described by the non-integrable complex modified Korteweg–de Vries (cmKdV) equation. By direct numerical simulations we get robust localized solutions to the cmKdV equation, which describe circularly polarized few-cycle optical solitons, and strongly differ from the breather soliton of the modified Korteweg–de Vries equation, which represents linearly polarized FCP solitons. We found that the circularly polarized FCP soliton becomes unstable when the angular frequency is less than 1.5 times the inverse of the pulse length, which is about 0.42 cycles per pulse. The unstable subcycle pulse decays into a linearly polarized half-cycle pulse, whose polarization direction slowly rotates around the propagation axis.

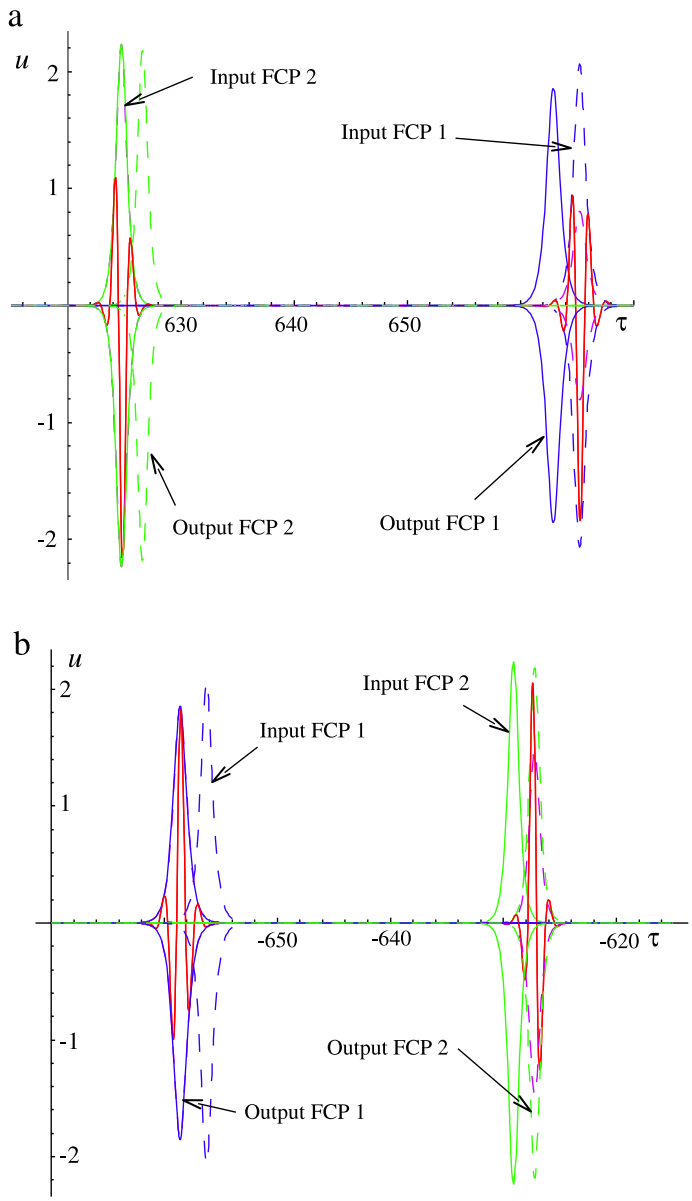

Fig. 15. (Color online) The FCPs and their initial and final envelopes before (15(a)) and after (15(b)) the interaction. The parameters are $c_1 = -1, c_2 = 1/2$, $p_1 = 2, p_2 = 2.5$, and $\omega_1 = \omega_2 = 4$. After Ref. [77].

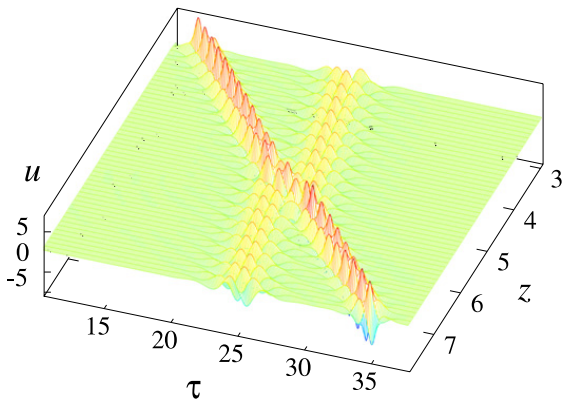

Fig. 16. (Color online). Interaction of two FCPs in the non-integrable case. The parameters are $c_1 = -1$, $c_2 = 0.5$, and $c_3 = 1$. The input is a linear superposition of two breather solutions u_{two} (given by Eq. (3.20)) of the mKdV equation obtained by setting $c_1 = 0$, with $p_1 = 1 + 2i$ and $p_2 = 2 + 2i$.

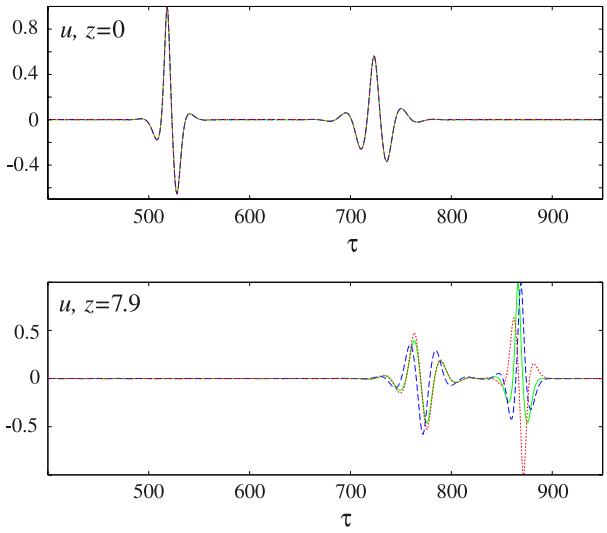

Fig. 17. (Color online) Interaction of two FCPs in the non-integrable case. The upper frame shows the input, normalized to its maximum value, and the bottom frame shows the output for several values of the coefficient c_2: $c_2 = 0.05$ (blue dashed line), 0.5 (red dotted line), 5 (green solid line). The other parameters are $c_1 = -1$ and $c_3 = 1$. The input is defined in the same way as in Fig. 16. Its total magnitude is proportional to $c_2^{(-1/2)}$.

6.1.1. Basic equations for an amorphous optical medium

As a simple model for a glass system we consider a set of two-level atoms with Hamiltonian H_0; $\Omega = \omega_b - \omega_a > 0$ is the frequency of the transition. The atoms may present some induced dipolar electric momentum $\vec{\mu}$, which is oriented randomly in space. Assuming a propagation along the z-axis, we can omit the component of $\vec{\mu}$ along the propagation direction z, and thus $\vec{\mu} = \mu\left(\cos\theta\vec{e}_x + \sin\theta\vec{e}_y\right)$, $\vec{e}_x$ and $\vec{e}_y$ being the unitary vectors along the x- and y-axis, respectively, and the 2×2 matrix μ is given by Eq. (3.1).

The evolution of the electric field $\vec{E}$ is governed by the Maxwell equations which, in the absence of magnetic effects, and assuming a plane wave propagating along the z axis, reduce to $\partial_z^2\vec{E} = c^{-2}\partial_t^2(\vec{E} + 4\pi\vec{P})$, where $\vec{P}$ is the polarization density. It is given by $\vec{P} = N\langle \mathrm{Tr}\,(\rho\vec{\mu})\rangle$, where N is the number of atoms per unit volume, ρ is the density matrix, and $\langle\cdot\rangle$ denotes the averaging over all directions in the x–y plane.

The evolution of the density-matrix is governed by the Schrödinger–von Neumann equation $i\hbar\partial_t\rho = [H, \rho]$, where $H = H_0 - \vec{\mu}\cdot\vec{E}$ includes the coupling between the atoms and the electric field. The relaxation effects can be neglected here as in the scalar approximation; see [73]. The physical values of the relaxation times are indeed in the picosecond range, or even slower, thus very large with regard to the pulse duration, which allows us to neglect them.

The typical frequency ω_w of the wave must be far away from the resonance frequency Ω because the transparency of the medium is required for soliton propagation. We therefore consider $\omega_w \ll \Omega$ (long-wave approximation regime). The typical length of the wave, say $t_w = 1/\omega_w$, is very large with respect to the characteristic time $t_r = 1/\Omega$ associated to the transition. Thus we are working in the long wave approximation regime, as defined in the framework of the reductive perturbation method [95,93]. Next we introduce a small parameter $\varepsilon = 1/(\Omega t_w)$, and the slow variables $\tau = \varepsilon(t - z/V)$, $\zeta = \varepsilon^3 z$. The retarded time variable τ describes the pulse shape, propagating at speed V in a first approximation. Its order of magnitude ε gives an account of the long-wave approximation, so that the corresponding values of retarded time have the same order of magnitude as $t_r/\varepsilon = t_w \gg t_r$ if τ is of the order of unity. The propagation distance is assumed to be very long with regard to the pulse length ct_w; therefore it will have the same order of magnitude as ct_r/ε^n, where $n \geqslant 2$. The value of n is determined by the distance at which dispersion effects occur. According to the general theory of the derivation of KdV-type equations [93], it is $n = 3$. The ζ variable of order ε^3 describes thus long-distance propagation, according to the general theory of the derivation of KdV-type equations [93].

The electric field $\vec{E}$, the polarization density $\vec{P}$, and the density matrix ρ are expanded in power series of ε as $\vec{E} = \sum_{n\geqslant 1}\varepsilon^n(u_n, v_n, 0)$, $\vec{P} = \sum_{n\geqslant 1}\varepsilon^n(P_n, Q_n, 0)$, $\rho = \sum_{n\geqslant 0}\varepsilon^n\rho_n$, in which the triplets of coordinates are given in the (x, y, z) frame, and the profiles u_1, v_1, etc., are functions of the slow variables τ and ζ. The components of ρ are denoted by

$$\rho = \begin{pmatrix} \rho_a & \rho_t \\ \rho_t^* & \rho_b \end{pmatrix}. \tag{6.1}$$

We assume that, in the absence of wave, all atoms are in the fundamental state (a), and hence all elements of ρ_0 are zero except $\rho_{0a} = 1$.

At lowest order ε^1, the Schrödinger–von Neumann equation yields

$$\rho_{1t} = \mu/(\hbar\Omega)(u_1\cos\theta + v_1\sin\theta).$$

The polarization density is $\vec{P} = (P, Q)$ with

$$P = N\left\langle \rho_t \mu^* \cos\theta + cc \right\rangle, \qquad Q = N\left\langle \rho_t \mu^* \sin\theta + cc \right\rangle$$

where cc denotes the complex conjugate. We get

$$(P_1, Q_1) = \left[N\,|\mu|^2 / (\hbar\Omega)\right](u_1, v_1)\,. \tag{6.2}$$

The Maxwell equation at leading order ε^3 gives the value of the velocity, $V = c/n$, with the refractive index $n = \sqrt{1 + 4\pi N\,|\mu|^2 / (\hbar\Omega)}$. The expression of n coincides with that obtained in the scalar model (cf. Ref. [73] and Eq. (3.8) above) if we take into account the fact that, for a linear polarization in the present framework, only one half of the dipoles would be active, being roughly aligned with the electric field. At the order ε^2, the Schrödinger–von Neumann equation yields $\rho_{1a} = \rho_{1b} = 0$ and $\rho_{2t} = \mu/(\hbar\Omega)\,(u_2\cos\theta + v_2\sin\theta) - i\mu/\left(\hbar\Omega^2\right)\partial_\tau\,(u_1\cos\theta + v_1\sin\theta)$. Consequently, we get similar expressions for P_2 and Q_2 as those for P_1 and Q_1, with the only difference that u_1 and v_1 are replaced by u_2 and u_2. The Maxwell equation at order ε^4 is automatically satisfied.

At order ε^3, the Schrödinger–von Neumann equation gives rise to

$$\rho_{2b} - \rho_{2a} = 2\,|\mu|^2 / \left(\hbar^2\,\Omega^2\right)(u_1\cos\theta + v_1\sin\theta)^2\,,$$

and a corresponding much longer expression for ρ_{3t}. By using

$$\left\langle \cos^4\theta \right\rangle = 3/8, \qquad \left\langle \cos^2\theta\,\sin^2\theta \right\rangle = 1/8,$$

the expression for the polarization density components P_3 is

$$P_3 = \frac{N\,|\mu|^2}{\hbar\Omega}u_3 - \frac{N\,|\mu|^2}{\hbar\Omega^3}\partial_\tau^2 u_1 - \frac{3N\,|\mu|^4}{2\,\hbar^3\,\Omega^3}\left(u_1^2 + v_1^2\right)u_1, \tag{6.3}$$

and we get an analogue expression for Q_3. Next, the Maxwell equation at order ε^5 yields the following pair of coupled equations:

$$\partial_\zeta u_1 = A\partial_\tau^3 u_1 + B\partial_\tau\left[\left(u_1^2 + v_1^2\right)u_1\right], \tag{6.4}$$

$$\partial_\zeta v_1 = A\partial_\tau^3 v_1 + B\partial_\tau\left[\left(u_1^2 + v_1^2\right)v_1\right], \tag{6.5}$$

in which we have set $A = 2\pi N\,|\mu|^2 / \left(nc\hbar\Omega^3\right)$, $B = 3\pi N\,|\mu|^4 / \left(nc\,\hbar^3\,\Omega^3\right)$. As in the scalar model [73], the dispersion coefficients A has the same expression as derived within the scalar model (Eq. (3.12)), if we consider that only one half of the dipoles are contributing. Regarding the nonlinear coefficient B, the ratio between the corresponding nonlinear coefficients is a bit smaller, 3/8, which is due to the averaging over θ.

Eqs. (6.4)–(6.5) can be written in the normalized form as

$$U_Z = U_{TTT} + \left[\left(U^2 + V^2\right)U\right]_T, \tag{6.6}$$

$$V_Z = V_{TTT} + \left[\left(U^2 + V^2\right)V\right]_T, \tag{6.7}$$

where the subscripts Z and T denote the derivatives, and the functions and variables are defined as $U = u_1/\mathcal{E}$, $V = v_1/\mathcal{E}$, $Z = z/\mathcal{L}$, $T = (t - z/V)/t_w$, with $\mathcal{L} = 2ct_w^3/n''$, and $\mathcal{E} = (1/2t_w)\sqrt{nn''/(-3\pi\,\chi^{(3)})}$.

Eqs. (6.6)–(6.7) are a set of coupled mKdV equations describing the propagation of optical FCPs in an amorphous medium presenting cubic nonlinearity and dispersion. They can be also seen as describing the interaction of two linearly polarized FCPs, U and V.

6.1.2. Basic equations for a crystal-like optical medium

A system of two coupled mKdV equations is derived above from a model of a glass, or an amorphous medium. This model involved some induced dipolar electric momentum $\vec{\mu}$, oriented randomly in the transverse plane (x, y), the polarization density $\vec{P}$ being averaged over all directions in this plane. We will show below that the same governing equations (6.6)–(6.7) can be derived from another model, which would rather correspond to a crystalline structure [161].

This alternative approach involves a two-level medium, in which the excited level is twice degenerated, with the induced dipole oriented either in the x or in the y direction. Precisely, the Hamiltonian is

$$H_0 = \hbar\begin{pmatrix}\omega_a & 0 & 0\\ 0 & \omega_b & 0\\ 0 & 0 & \omega_b\end{pmatrix}, \tag{6.8}$$

still with $\Omega = \omega_b - \omega_a > 0$. The dipolar momentum becomes

$$\vec{\mu} = \mu_x\vec{e}_x + \mu_y\vec{e}_y, \tag{6.9}$$

where $\vec{e}_x$ and $\vec{e}_y$ are the unitary vectors along the x axis and y axis, respectively, and

$$\mu_x = \begin{pmatrix} 0 & \mu & 0 \\ \mu^* & 0 & 0 \\ 0 & 0 & 0 \end{pmatrix}, \tag{6.10}$$

$$\mu_y = \begin{pmatrix} 0 & 0 & \mu \\ 0 & 0 & 0 \\ \mu^* & 0 & 0 \end{pmatrix}. \tag{6.11}$$

The evolution of the electric field $\vec{E}$ is governed by the Maxwell equations which, in the absence of magnetic effects, and assuming a plane wave propagating along the z axis, reduce to $\partial_z^2 \vec{E} = \frac{1}{c^2}\partial_t^2 \left(\vec{E} + 4\pi \vec{P}\right)$, where $\vec{P} = N\mathrm{Tr}\,(\rho\vec{\mu})$ is the polarization density, N is the number of atoms per unit volume, and ρ is the density matrix. There is no averaging over the transverse orientation of the dipolar momentum any more.

The evolution of the density-matrix is governed by the equation $i\hbar\partial_t \rho = [H, \rho]$, where $H = H_0 - \vec{\mu}\cdot\vec{E}$ describes the coupling between the atoms and the electric field. The relaxation effects can be neglected here as in the scalar approximation; see Ref. [73]. Notice that the physical values of the relaxation times are indeed in the picosecond range, or even slower (nanoseconds), thus very large with regard to the pulse duration, which allows us to neglect them.

As above, we assume that the typical frequency ω_w of the wave is much lower than the resonance frequency Ω, $\omega_w \ll \Omega$. Recall that, if ω_w is in the visible range, it means that the transition frequency is in the ultraviolet, and that the typical length of the wave, say $t_w = 1/\omega_w$, is very large with respect to the characteristic time $t_r = 1/\Omega$ associated to the transition. It is thus a long wave approximation, as defined in the framework of the reductive perturbation method [93,95]. Still as above, we introduce a small parameter ε, which can be here $\varepsilon = 1/(\Omega t_w) \ll 1$, and the slow variables $\tau = \varepsilon\left(t - \frac{z}{V}\right)$, $\zeta = \varepsilon^3 z$. The retarded time variable τ describes the pulse shape, propagating at speed V in a first approximation, and the ζ variable describes long-distance propagation.

The electric field $\vec{E}$, the polarization density $\vec{P}$, and the density matrix ρ are expanded in power series of ε as

$$\vec{E} = \sum_{n\geqslant 1} \varepsilon^n \vec{E}_n = \sum_{n\geqslant 1} \varepsilon^n (u_n, v_n, 0), \tag{6.12}$$

$$\vec{P} = \sum_{n\geqslant 1} \varepsilon^n (P_n, Q_n, 0), \tag{6.13}$$

$$\rho = \sum_{n\geqslant 0} \varepsilon^n \rho_n, \tag{6.14}$$

in which the triplets of coordinates are given in the (x, y, z) frame, and the profiles u_1, v_1, etc., are functions of the slow variables τ and ζ. The components of ρ_n are denoted by ρ_{ij}^n.

At lowest order ε^1, the Schrödinger–von Neumann equation yields

$$\rho_{12}^1 = \frac{\mu}{\hbar\Omega} u_1, \qquad \rho_{13}^1 = \frac{\mu}{\hbar\Omega} v_1, \tag{6.15}$$

and consequently

$$P_1 = \frac{2N|\mu|^2}{\hbar\Omega} u_1, \tag{6.16}$$

$$Q_1 = \frac{2N|\mu|^2}{\hbar\Omega} v_1, \tag{6.17}$$

which are the same expressions as in the glass model (Eq. (6.2) and [160]), except that N is replaced with $2N$.

At order ε^3 in the Maxwell equation, we get an expression of the refractive index with the same slight change:

$$n = \left(1 + \frac{8\pi N|\mu|^2}{\hbar\Omega}\right)^{\frac{1}{2}}, \tag{6.18}$$

which exactly coincides with (3.8).

At order ε^2 in the Schrödinger–von Neumann equation, we first notice that $\partial_\tau \rho_{23}^1 = 0$ and consequently $\rho_{23}^1 = 0$. In the same way, $\rho_{11}^1 = \rho_{22}^1 = \rho_{33}^1 = 0$. Then we get

$$\rho_{12}^2 = \frac{\mu}{\hbar\Omega} u_2 - \frac{i\mu}{\hbar\Omega^2}\partial_\tau u_1, \tag{6.19}$$

$$\rho_{13}^2 = \frac{\mu}{\hbar\Omega} v_2 - \frac{i\mu}{\hbar\Omega^2}\partial_\tau v_1, \tag{6.20}$$

which are the same expressions as in the case of the glass model [160], with the orientation angle of the dipolar momentum $\theta = 0$ for ρ_{12}^2 and $\theta = \pi/2$ for ρ_{13}^2. Consequently, we get

$$P_2 = \frac{2N|\mu|^2}{\hbar\Omega} u_2, \tag{6.21}$$

$$Q_2 = \frac{2N|\mu|^2}{\hbar\Omega} v_2, \tag{6.22}$$

and the Maxwell equation at order ε^4 is automatically satisfied.

At order ε^3 in the Schrödinger–von Neumann equation, the populations are computed as

$$\rho_{11}^2 = \frac{-|\mu|^2}{\hbar^2\,\Omega^2}\left(u_1^2 + v_1^2\right), \tag{6.23}$$

$$\rho_{22}^2 = \frac{|\mu|^2}{\hbar^2\,\Omega^2} u_1^2, \tag{6.24}$$

$$\rho_{33}^2 = \frac{|\mu|^2}{\hbar^2\,\Omega^2} v_1^2. \tag{6.25}$$

Notice that a nonzero coherence term between the two excited states appears, it is

$$\rho_{23}^2 = \frac{|\mu|^2}{\hbar^2\,\Omega^2} u_1 v_1. \tag{6.26}$$

Consequently, the coherence between the fundamental state and the state excited in the x direction at next order is

$$\rho_{12}^3 = \frac{\mu}{\hbar\Omega} u_3 - \frac{i\mu}{\hbar\Omega^2}\partial_\tau u_2 - \frac{\mu}{\hbar\Omega^3}\partial_\tau^2 u_1 - \frac{2\mu|\mu|^2}{\hbar^3\,\Omega^3}\left(u_1^2 + v_1^2\right) u_1. \tag{6.27}$$

The analogous expression, permuting u_1 and v_1, is obtained for the component ρ_{13}^3.

The expressions for the polarization density components P_3 and Q_3 are obtained, as

$$P_3 = \frac{2N|\mu|^2}{\hbar\Omega} u_3 - \frac{2N|\mu|^2}{\hbar\Omega^3}\partial_\tau^2 u_1 - \frac{4N|\mu|^4}{\hbar^3\,\Omega^3}\left(u_1^2 + v_1^2\right) u_1, \tag{6.28}$$

and analogously for Q_3. Apart from the change from N to $2N$ already noticed, the only discrepancy with respect to the corresponding equations in the glass model (Eq. (6.3) and [160]) is a coefficient value 4 instead of 3 in the nonlinear term in Eq. (6.28).

The Maxwell equation at order ε^5 yields the following pair of coupled equations:

$$\partial_\zeta u_1 = A\partial_\tau^3 u_1 + B\partial_\tau\left[\left(u_1^2 + v_1^2\right) u_1\right], \tag{6.29}$$

$$\partial_\zeta v_1 = A\partial_\tau^3 v_1 + B\partial_\tau\left[\left(u_1^2 + v_1^2\right) v_1\right], \tag{6.30}$$

in which we have set

$$A = \frac{4\pi N|\mu|^2}{nc\hbar\Omega^3}, \tag{6.31}$$

$$B = \frac{8\pi N|\mu|^4}{nc\,\hbar^3\,\Omega^3}. \tag{6.32}$$

Notice that the structure of the set of Eqs. (6.29)–(6.30) is the same as in the glass model (Eqs. (6.4)–(6.5) and [160]), with very slightly modified coefficients. The expressions of the two dispersion coefficients coincide (the ratio between the corresponding dispersion coefficients is therefore 1) if we consider that in the case of the glass model, only one half of the dipoles are contributing, while all of them are involved in the crystal model. The same feature is observed in the case of the refractive index. Regarding the value (6.32) of the coefficient B, the ratio between the corresponding nonlinear coefficients is a bit smaller, 3/8, which is nothing else but the average value $\langle\cos^4\theta\rangle$ of $\cos^4\theta$, which is involved in the averaging of the nonlinear polarization density over all orientations θ of $\vec{\mu}$ in the glass model (Eq. (3.12) and [160]). In fact, the coefficients A and B have here exactly the same expressions as in the scalar model [73].

One notices that Eqs. (6.29)–(6.30) in their normalized form coincide to Eqs. (6.6)–(6.7) where now the functions and variables are defined as

$$U = \frac{u_1}{\mathcal{E}}, \qquad V = \frac{v_1}{\mathcal{E}}, \qquad Z = \frac{z}{\mathcal{L}}, \qquad T = \frac{t - z/V}{t_w}, \tag{6.33}$$

with

$$\mathcal{L} = \frac{n\hbar c\Omega^3 t_w^3}{2\pi N\,|\mu|^2}, \tag{6.34}$$

$$\mathcal{E} = \sqrt{\frac{2}{3}}\frac{\hbar}{|\mu|\,t_w}. \tag{6.35}$$

6.1.3. The complex mKdV equation

Assuming that U and V vanish at infinity, the mKdV system of coupled partial differential equation (6.6)–(6.7) has four conserved quantities [163]:

$$I_1 = \int_{-\infty}^{+\infty} U dT, \qquad I_2 = \int_{-\infty}^{+\infty} V dT, \tag{6.36}$$

the momentum of the system

$$I_3 = \int_{-\infty}^{+\infty} \left(U^2 + V^2\right) dT, \tag{6.37}$$

and its Hamiltonian

$$I_4 = \frac{1}{2}\int_{-\infty}^{+\infty} \left\{\left(U^2 + V^2\right)^2 - 2\left[(\partial_T U)^2 + (\partial_T V)^2\right]\right\} dT, \tag{6.38}$$

which remain constant with Z.

Setting

$$f = U + iV, \tag{6.39}$$

Eqs. (6.6) and (6.7) reduce to

$$\partial_Z f = \partial_T^3 f + \partial_T\left(|f|^2 f\right), \tag{6.40}$$

which is known as the complex modified Korteweg–de Vries (cmKdV) equation. Confusion must be avoided between Eq. (6.40) and the other cmKdV equation

$$\partial_Z f = \partial_T^3 f + |f|^2\,\partial_T f. \tag{6.41}$$

Indeed, Eq. (6.41) is completely integrable [165] while Eq. (6.40) is not. Eqs. (6.40) and (6.41) are sometimes referred to as cmKdV I and cmKdV II equations, respectively. The integrable equation (6.41) has been extensively studied (see e.g. [164–168]), while less studies have been devoted to the non-integrable equation (6.40) [169,170]. In Ref. [169], using the Painlevé analysis, it is proved that Eq. (6.40) is not integrable, and an exhaustive list of analytical solutions is given. In the frame of the optics of FCPs, the field f must vanish at infinity. With this condition, there is no exact analytical solution to Eq. (6.40) but the solutions of the real mKdV equation. Indeed, setting $f = ue^{i\varphi}$, with $u = u(Z, T)$ and φ a constant, reduces the complex mKdV equation (6.40) to the real one. All linearly polarized FCP solitons are retrieved in this way. Their stability to a random perturbation of the polarization can be tested numerically. If we add to the constant φ a random noise (we used an amplitude of $0.1 \times 2\pi$), it is obtained that the pulse is not destroyed, and that its polarization remains linear. However, the direction of the linear polarization slowly rotates around the propagation direction.

More interesting would be a circularly polarized soliton, of the form

$$f = u(T - wZ)e^{i(\omega T - kZ)}. \tag{6.42}$$

However no exact, even numerical, steady state solution of this type do exist. To be ensured of this, just plug f given by the expression (6.42) in Eq. (6.40); separating real and imaginary parts and integrating once yields

$$\begin{aligned} \left(3\omega^2 - w\right) u &= \partial_T^2 u + u^3, \\ \left(\omega^2 - \frac{k}{\omega}\right) u &= 3\partial_T^2 u + u^3, \end{aligned} \tag{6.43}$$

which are not compatible. However, solutions having approximately the form (6.42) exist and are very robust. They are studied in detail in the next subsection.

6.1.4. Robust circularly polarized few-optical-cycle solitons

We will next compute an approximate analytic solution to the cmKdV equation (6.40), valid for long pulses, i.e. in the SVEA. Next we introduce again a small parameter ε and the slow variables

$$\xi = \varepsilon^2 Z, \qquad \eta = \varepsilon(T - wZ), \tag{6.44}$$

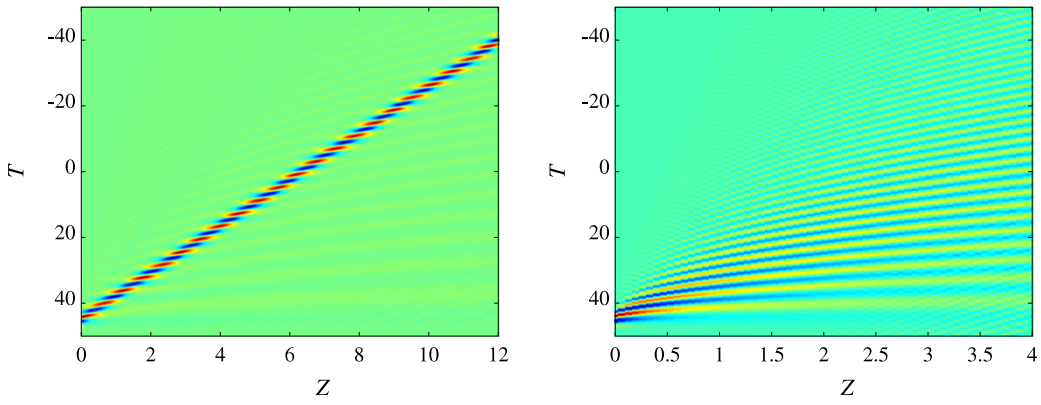

(a) Nonlinear. (b) Linear.

Fig. 18. Propagation of a circularly polarized FCP. The left panel shows the nonlinear propagation of the x-polarized component U. Initial data is given by Eq. (6.48) with $b = 1$ and $\omega = 2$. The right panel shows the propagation of the linearly dispersive FCP having the same initial profile but with very small amplitude. After Ref. [161].

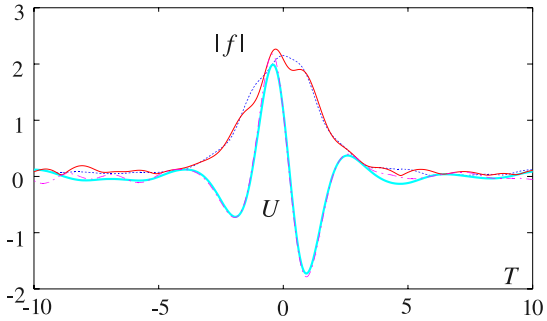

Fig. 19. (Color online) Initial ($Z = 100$) and final ($Z = 10000$) profiles of the FCP plotted on Fig. 18 for the input given by Eq. (6.48). Blue (dotted): initial $|f|$, light blue (thick gray): initial U, red (thin solid): final $|f|$, pink (dash-dotted): final U. After Ref. [161].

and expand f as

$$f = \varepsilon(f_0(\eta, \xi) + \varepsilon f_1(\eta, \xi) + \cdots)e^{i(\omega T - kZ)}, \tag{6.45}$$

and run the perturbative reduction procedure [93].

At leading order ε, we get $k = \omega^3$; at second order, we find the inverse velocity $w = 3\omega^2$, and at order ε^3 we get a nonlinear Schrödinger equation for f_0:

$$i\partial_\xi f_0 + 3\omega\partial_\eta^2 f_0 + \omega f_0 |f_0|^2 = 0. \tag{6.46}$$

Let us consider the fundamental soliton solution of the above written NLS equation:

$$f_0 = p\sqrt{6}\,\mathrm{sech}\,(p\eta)\, e^{i3p^2\omega\xi}. \tag{6.47}$$

Coming back to the initial variables, we obtain

$$f = b\sqrt{6}\,\mathrm{sech}\,\left[b\left(T - 3\omega^2 Z\right)\right] e^{i\omega\left[T - (\omega^2 - 3b^2)Z\right]}. \tag{6.48}$$

Eq. (6.48) gives an approximate solution to the mKdV equation (6.40), which is valid for long pulses ($b \ll \omega$).

The numerical resolution of the cmKdV equation is performed using the exponential time differencing second order Runge–Kutta (ETD–RK2) method [115]. The numerical scheme does not conserve exactly the $\mathcal{L}_2$-norm (or energy W) of the solution; however the error remains small (typically $\Delta W/W \sim 10^{-4}$ for $Z = 10000$). Due to the scale invariance of the cmKdV equation, only the ratio b/ω may modify the stability properties of the solution. Thus there is only one free parameter, which is the number of cycles in the pulse (the ratio ω/b being proportional to the number of optical cycles contained in the ultrashort pulse). For numerical calculations we fix $b = 1$ and decrease the frequency ω.

Figs. 18 and 19 shows the evolution of a FCP of this form, with $b = 1$ and $\omega = 2$. The propagation of the linearly dispersive FCP is also shown for the sake of comparison.

The FCP propagates without change in width and maximum amplitude after propagation over at least $z = 10000$ units, however, its shape is somehow distorted after propagation. The propagation speed is also quite different from the result of the above analytical approximate solution. In fact, since no steady state with linear phase exists, the pulse is not a true steady state, and consequently its velocity varies in a quite erratic way; nevertheless, it is a very robust FCP.

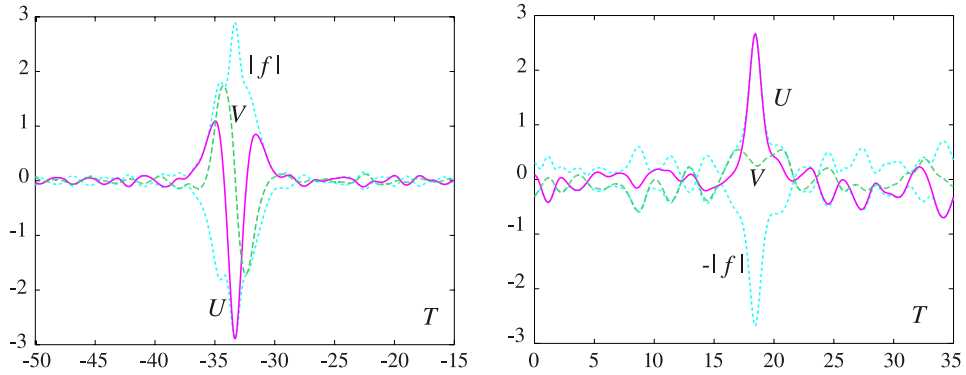

(a) Initial (at $Z = 100$). (b) Final (at $Z = 1300$).

Fig. 20. Normalized profiles of an unstable circularly polarized FCP. Initial data is defined by the breather soliton with $p_1 = 1 + i$, i.e. both pulse width and angular frequency equal to 1, for the polarization component U, and the same with a $\pi/2$ dephasing for V. Light blue (dotted): $|f|$ and $-|f|$, pink (solid): $U = \mathrm{Re}(f)$, green (dashed): $V = \mathrm{Im}(f)$. After Ref. [161].

We will next show by numerical simulations that we get robust circularly polarized FCP solitons. Notice that the approximate solution (6.48) has not a zero mean value, except at the SVEA limit $b \ll \omega$. However the mean value of the field is conserved. It is likely that the circularly polarized FCP soliton would have a zero mean value, and hence this would explain the discrepancy between the approximate analytical solution (6.48) and the direct numerical computation shown in Fig. 18.

In order to check this interpretation, let us consider an input having zero mean value. Such an alternative expression is found from the breather (or two-soliton) solution of the real mKdV equation [114]. Recall that the two-soliton solution u_{two} of the mKdV equation has the expression (3.20) with $\eta_j = p_j\tau - p_j^3\zeta - \gamma_j$, for $j = 1, 2$, and becomes a breather soliton if $p_2 = p_1^*$. Here $\mathrm{Re}(p_1)$ is the inverse of the pulse length, and $\mathrm{Im}(p_1)$ is the angular frequency, as are b and ω respectively in Eq. (6.48). The real part of the constant $\gamma_1 = \gamma_2^*$ determines the position of the center of the pulse, while its imaginary part is a phase. Taking for one polarization component, say U, the breather solution with $\gamma_{1U} = 0$, and for the second polarization component V the same expression, but with a $\pi/2$ dephasing, i.e. with $\gamma_{1V} = i\pi/2$, we get some expression which can be used as an input data for solving numerically the cmKdV equation. This pulse is very close to the approximate analytical solution (6.48), but has a zero mean value. Numerical resolution shows that the pulse, apart from small apparently chaotic oscillations, keeps its shape and characteristics during the propagation.

In what follows we will study the decay of the unstable circularly polarized FCP and the corresponding transition to a half-cycle soliton. The value $\omega/b \simeq 1.5$ appears to be the lower limit for the stability of the circularly polarized FCP soliton. Note that the ratio ω/b is proportional to the number of cycles contained in the pulse. More precisely, the number of optical cycles N_c is the ratio of the pulse duration ($\mathrm{FWHM} = 2\ln\left(1 + \sqrt{(2)}\right)/b$) divided by the optical period $2\pi/\omega$, i.e. $N_c \simeq 0.28\omega/b$. The stability limit of the circularly polarized FCP soliton is thus about $N_c = 0.42$. Hence circularly polarized FCP are stable down to the sub-cycle range. For smaller values of the ratio ω/b, the FCP becomes unstable, and decays into a linearly polarized single-humped (half-cycle) pulse, in the form of a fundamental soliton of the real mKdV.

The transition occurs, for $\omega/b = 1.4$, between $Z = 19100$ and 19200, for $\omega/b = 1.3$, between $Z = 9300$ and 9400, but for $\omega/b = 1$, between $Z = 400$ and 500. Further, it occurs very abruptly, and involves a strong modification of the spectrum; see Ref. [160,161].

The transition to a half-cycle soliton is shown in Figs. 20 and 21. It is a single pulse, whose profile accurately coincides with that of the fundamental soliton solution to the real mKdV equation

$$U = \sqrt{2}b\,\mathrm{sech}\left(bT - b^3Z\right), \tag{6.49}$$

but which slowly rotates around the propagation axis.

As a final remark we notice that half-cycle optical solitons were also put forward in quadratic nonlinear media; thus a few-cycle pulse launched in a quadratic medium may result in a half-cycle soliton in the form of a single hump, with no oscillating tails [120].

Concluding this section, we point out that the multiscale perturbation analysis was used in Refs. [160,161] to derive approximate evolution equations governing the propagation of circularly polarized femtosecond optical solitons in cubic (Kerr-like) media beyond the slowly varying envelope approximation. Thus we took into account the vectorial character of the electric field and therefore we properly considered the wave polarization effects. In the long-wave-approximation regime we have found that the two interacting waveforms corresponding to such vector few-optical-cycle solitons are adequately described by a coupled pair of complex modified Korteweg–de Vries equations at the third-order approximation of the perturbation approach.

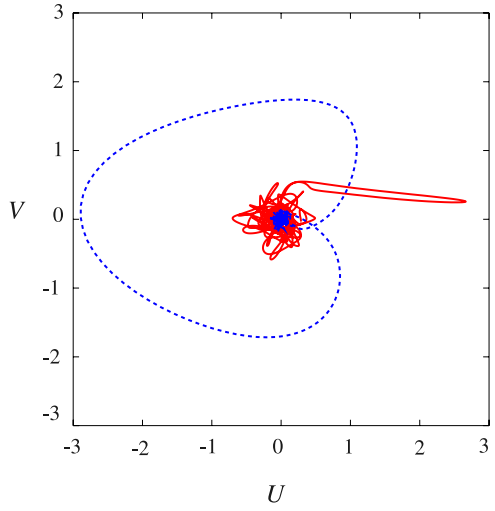

Fig. 21. Evolution of the polarization of the unstable circularly polarized FCP with both angular frequency and pulse length 1. Blue (dotted): initial circularly polarized pulse (at $Z = 100$), red (solid): final linearly polarized pulse (at $Z = 1300$). After Ref. [161].

6.2. Circularly polarized few-optical-cycle solitons: short wave approximation

In this section we consider the propagation of few-cycle pulses beyond the slowly varying envelope approximation, in media in which the dynamics of constituent atoms is described by a two-level Hamiltonian, by taking into account the wave polarization and in the short-wave approximation regime. Therefore we assume that the resonance frequency of the two-level atoms is well below the inverse of the characteristic duration of the optical pulse, it should thus belong to the infrared range if the latter is in the visible range. By using the reductive perturbation method (multiscale analysis) we then derive from the Maxwell–Bloch–Schrödinger equations the governing evolution equations for the two polarization components of the electric field in the first order of the perturbation approach. We show that propagation of circularly polarized few-optical-cycle solitons is described by a rather complicated system of coupled nonlinear equations [162], which reduces in the scalar case to the standard sine–Gordon equation describing the dynamics of linearly polarized FCPs in the short-wave-approximation regime. By direct numerical simulations we then calculate the lifetime of circularly-polarized FCPs and we study the transition to two orthogonally polarized single-humped pulses as a generic route of their instability; for a comprehensive study of this issue see Ref. [162]. It is worth mentioning that other vectorial non-SVEA models have been also proposed [158,142], however they were only built from a direct analogy with common SVEA models. It is also worth mentioning that circularly polarized short pulse propagation in a system of two-level atoms has been studied more than two decades ago in the framework of the self-induced transparency [172] and the existence of localized solutions of Maxwell–Bloch type systems beyond the SVEA has been considered too [173,174]. However, not all the coupling mechanisms between the polarization components were taken into account in these earlier studies. However, the authors of Ref. [174] took an essential coupling term into account through the out-of-phase polarization, which allowed them to show that the pulse solution valid within the SVEA could not be generalized beyond it by means of some corrections terms.

6.2.1. Basic equations and the short-wave approximation

We consider a two level model, in which the excited state is degenerated twice, corresponding to oscillations along the x and y axes. The free Hamiltonian is thus given by Eq. (6.8). The resonance angular frequency is $\Omega = \omega_b - \omega_a > 0$. The electric field $\vec{E}$ is coupled with the atoms by the Hamiltonian $H = H_0 - \vec{\mu}\vec{E}$, in which the dipolar momentum operator is $\vec{\mu} = \mu_x\vec{e}_x + \mu_y\vec{e}_y$; μ_x and μ_x are given by Eqs. (6.10) and (6.11).

Then the evolution of the atoms is governed by the Schrödinger–von Neumann equation $i\hbar\partial_t\rho = [H, \rho]$, in which ρ is the density matrix, and the evolution of the electric field $\vec{E}$ is governed by the Maxwell equation $\partial_z^2\vec{E} = c^{-2}\partial_t^2\left(\vec{E} + 4\pi\vec{P}\right)$, where c is the speed of light in vacuum and the polarization density $\vec{P}$ is given by $\vec{P} = N\mathrm{Tr}\,(\rho\vec{\mu})$.

The short-wave approximation is performed according to the general theory developed in Refs. [73,175,176]. We denote by $(u, v, 0)$ the components of the electric field $\vec{E}$ in the (xyz) frame, by $(P, Q, 0)$ the ones of $\vec{P}$, and by ρ_{ij}, $i, j = 1, 2, 3$, the elements of the Hermitian matrix ρ. All these quantities are expanded in power series of a small parameter ε as $\vec{E} = \vec{E}^0 + \varepsilon\vec{E}^1 + \varepsilon^2\vec{E}^2 + \cdots$, and so on. We introduce fast and slow variables $\tau = \left(t - \frac{z}{V}\right)$ and $\zeta = \varepsilon z$, so that $\partial_t = \partial_\tau$ and $\partial_z = -V^{-1}\partial_\tau + \varepsilon\partial_\zeta$. The above series expansions and fast and slow variables are reported into the Maxwell and Schrödinger–von Neumann equations and the perturbative scheme is solved order by order.

The Schrödinger–von Neumann equation at order ε^0 yields $i\hbar\partial_\tau\rho^0 = -\left[\vec{\mu}\cdot\vec{E}_0, \rho^0\right]$, that is,

$$i\hbar\partial_\tau\rho_{11}^0 = -\left(\mu\rho_{12}^{0*} - \rho_{12}^0\mu^*\right)u_0 - \left(\mu\rho_{13}^{0*} - \rho_{13}^0\mu^*\right)v_0, \tag{6.50}$$

$$i\hbar\partial_\tau \rho_{22}^0 = -\left(\mu^* \rho_{12}^0 - \rho_{12}^{0*}\mu\right) u_0, \tag{6.51}$$

$$i\hbar\partial_\tau \rho_{33}^0 = -\left(\mu^* \rho_{13}^0 - \rho_{13}^{0*}\mu\right) v_0, \tag{6.52}$$

$$i\hbar\partial_\tau \rho_{12}^0 = -\mu\left(\rho_{22}^0 - \rho_{11}^0\right) u_0 - \mu\rho_{23}^{0*} v_0, \tag{6.53}$$

$$i\hbar\partial_\tau \rho_{13}^0 = -\mu\rho_{23}^0 u_0 - \mu\left(\rho_{33}^0 - \rho_{11}^0\right) v_0, \tag{6.54}$$

$$i\hbar\partial_\tau \rho_{23}^0 = -\mu^* \rho_{13}^0 u_0 + \rho_{12}^{0*}\mu v_0. \tag{6.55}$$

It is easy to check that Eqs. (6.50)–(6.52) satisfy the normalization condition for the density matrix, i.e. $\partial_\tau \mathrm{Tr}\rho^0 = 0$.

Assuming that the electric field components u and v vanish as τ tends to $-\infty$, integrating (6.53) and (6.54), and incorporating them into (6.50) we get

$$\partial_\tau \rho_{11}^0 = \frac{2|\mu|^2}{\hbar^2}\left[u_0 \int_{-\infty}^{\tau} \{w_1 u_0 + \sigma v_0\} + v_0 \int_{-\infty}^{\tau} \{\sigma u_0 + w_2 v_0\}\right], \tag{6.56}$$

where we have defined the population differences as $w_1 = \rho_{22}^0 - \rho_{11}^0$, $w_2 = \rho_{33}^0 - \rho_{11}^0$, and we set $\sigma = \mathrm{Re}\rho_{23}^0$.

Then by incorporating (6.53) into (6.51), we get

$$\partial_\tau \rho_{22}^0 = -\frac{2|\mu|^2}{\hbar^2} u_0 \int_{-\infty}^{\tau} (w_1 u_0 + \sigma v_0). \tag{6.57}$$

Integrating Eq. (6.54) and incorporating it into (6.52) yield

$$\partial_\tau \rho_{33}^0 = -\frac{2|\mu|^2}{\hbar^2} v_0 \int_{-\infty}^{\tau} (\sigma u_0 + w_2 v_0). \tag{6.58}$$

The x and y components P_0 and Q_0 of the zero order polarization density $\vec{P}_0$ are given by $P_0 = N\left(\rho_{12}^0 \mu^* + \rho_{12}^{0*}\mu\right)$, $Q_0 = N\left(\rho_{13}^0 \mu^* + \rho_{13}^{0*}\mu\right)$. By integrating (6.53) and (6.54), incorporating them into the expressions of P_0, and Q_0 and setting $\kappa = \mathrm{Im}\left(\rho_{23}^0\right)$ we get

$$P_0 = \frac{2|\mu|^2 N}{\hbar} \int_{-\infty}^{\tau} \kappa v_0, \tag{6.59}$$

$$Q_0 = -\frac{2|\mu|^2 N}{\hbar} \int_{-\infty}^{\tau} \kappa u_0. \tag{6.60}$$

By integrating Eqs. (6.53) and (6.54), incorporating them into (6.55), and separating real and imaginary parts, we obtain evolution equations for $\sigma = \mathrm{Re}\rho_{23}^0$ and $\kappa = \mathrm{Im}\rho_{23}^0$, as

$$\partial_\tau \sigma = -u_0 P_y - v_0 P_x, \tag{6.61}$$

where we have set

$$P_x = \frac{|\mu|^2}{\hbar^2} \int_{-\infty}^{\tau} (w_1 u_0 + \sigma v_0), \tag{6.62}$$

$$P_y = \frac{|\mu|^2}{\hbar^2} \int_{-\infty}^{\tau} (w_2 v_0 + \sigma u_0), \tag{6.63}$$

and

$$\partial_\tau \kappa = -\frac{|\mu|^2}{\hbar^2}\left(u_0 \int_{-\infty}^{\tau} \kappa u_0 + v_0 \int_{-\infty}^{\tau} \kappa v_0\right). \tag{6.64}$$

Then a simple analysis shows that $\kappa = 0$ and consequently, ρ_{23}^0 is a real quantity. Thus we find out that $\vec{P}_0 = \vec{0}$ and incorporating this value into the Maxwell wave equation at order ε^0, we get that the wave velocity is $V = c$ at the zero order of the series expansion in the small parameter ε.

We next get the polarization density at order ε^1 from the Schrödinger–von Neumann equation at order ε^1. The polarization density components P_1 and Q_1 involve the density matrix elements ρ_{12}^1 and ρ_{13}^1, respectively and are given by $P_1 = N\left(\rho_{12}^1 \mu^* + \rho_{12}^{1*}\mu\right)$ and $Q_1 = N\left(\rho_{13}^1 \mu^* + \rho_{13}^{1*}\mu\right)$. If we set $\hat{\kappa} = \mathrm{Im}\left(\rho_{23}^1\right)$ we get the following expressions for P_1 and Q_1:

$$P_1 = -\frac{2|\mu|^2 \Omega N}{\hbar} \int_{-\infty}^{\tau}\int_{-\infty}^{\tau} (w_1 u_0 + \sigma v_0) + \frac{2|\mu|^2 N}{\hbar} \int_{-\infty}^{\tau} \hat{\kappa} v_0, \tag{6.65}$$

$$Q_1 = -\frac{2|\mu|^2 \Omega N}{\hbar} \int_{-\infty}^{\tau}\int_{-\infty}^{\tau} (\sigma u_0 + w_2 v_0) - \frac{2|\mu|^2 N}{\hbar} \int_{-\infty}^{\tau} \hat{\kappa} u_0. \tag{6.66}$$

From the wave equation at order ε^1 we get the evolution equations for the fields u_0 and v_0 as $\partial_\zeta u_0 = (-2\pi/c)\partial_\tau P_1$ and $\partial_\zeta v_0 = (-2\pi/c)\partial_\tau Q_1$. The equations for w_1, w_2 are deduced straightforwardly from the equations for the diagonal elements of ρ^0, as $\partial_\tau w_1 = -4u_0P_x - 2v_0P_y$ and $\partial_\tau w_2 = -2u_0P_x - 4v_0P_y$. Then we get the equation for $\hat{\kappa}$:

$$\partial_\tau \hat{\kappa} = -\Omega \left(u_0 \int_{-\infty}^{\tau} P_y - v_0 \int_{-\infty}^{\tau} P_x \right). \tag{6.67}$$

Summarizing the analysis of Maxwell–Schrödinger–von Neumann equations, we are left with a coupled system of ten nonlinear integro-differential equations:

$$\partial_\zeta u_0 = \frac{-2\pi}{c}\partial_\tau P_1, \tag{6.68}$$

$$\partial_\zeta v_0 = \frac{-2\pi}{c}\partial_\tau Q_1, \tag{6.69}$$

$$\partial_\tau P_1 = -2N\hbar\Omega P_x + \frac{2N|\mu|^2}{\hbar} v_0\hat{\kappa}, \tag{6.70}$$

$$\partial_\tau Q_1 = -2N\hbar\Omega P_y - \frac{2N|\mu|^2}{\hbar} u_0\hat{\kappa}, \tag{6.71}$$

$$\partial_\tau P_x = \frac{|\mu|^2}{\hbar^2}\left(w_1u_0 + \sigma v_0\right), \tag{6.72}$$

$$\partial_\tau P_y = \frac{|\mu|^2}{\hbar^2}\left(w_2v_0 + \sigma u_0\right), \tag{6.73}$$

$$\partial_\tau \hat{\kappa} = \frac{1}{2N\hbar}\left(u_0Q_1 - v_0P_1\right), \tag{6.74}$$

$$\partial_\tau w_1 = -4u_0P_x - 2v_0P_y, \tag{6.75}$$

$$\partial_\tau w_2 = -2u_0P_x - 4v_0P_y, \tag{6.76}$$

$$\partial_\tau \sigma = -\left(u_0P_y + v_0P_x\right). \tag{6.77}$$

We then write down this nonlinear system in its normalized (dimensionless) form by introducing the following dimensionless functions and variables: $(u, v) = (u_0, v_0)/E_0$, $T = \tau/T_0$, $Z = \zeta/D$, where the reference electric field E_0, the reference propagation distance D and the reference time T_0 are related through $T_0 = \hbar/(|\mu|E_0)$, $D = E_0c/(4\pi N\Omega|\mu|)$, $(m, n) = (\hbar/\mu)\left(P_x, P_y\right)$ and $(p, q) = [E_0/(2N\hbar\Omega)]\,(P_1, Q_1)$. One notices that the short-wave assumption mainly expresses in the fact that the reference propagation distance D is large.

If we set $w = (w_1 + w_2)/2$, $r = (w_2 - w_1)/2$, the system (6.68)–(6.77) reduces to the dimensionless form:

$$\partial_Z u = -\partial_T p, \tag{6.78}$$

$$\partial_Z v = -\partial_T q, \tag{6.79}$$

$$\partial_T p = -m + vK, \tag{6.80}$$

$$\partial_T q = -n - uK, \tag{6.81}$$

$$\partial_T m = (w - r)u + Sv, \tag{6.82}$$

$$\partial_T n = (w + r)v + Su, \tag{6.83}$$

$$\partial_T K = uq - vp, \tag{6.84}$$

$$\partial_T w = -3(um + vn), \tag{6.85}$$

$$\partial_T r = um - vn, \tag{6.86}$$

$$\partial_T S = -un - vm. \tag{6.87}$$

By defining four new complex quantities $P = p + iq$, $M = m + in$, $U = u + iv$ and $s = r - iS$, the nonlinear system (6.78)–(6.87) of ten coupled equations reduces to a more compact system of only six coupled nonlinear equations:

$$\partial_Z U = -P_T \tag{6.88}$$

$$\partial_T P = -M - iUK \tag{6.89}$$

$$\partial_T M = wU - sU^* \tag{6.90}$$

$$\partial_T K = \mathrm{Im}\left(U^*P\right) \tag{6.91}$$

$$\partial_T s = UM \tag{6.92}$$

$$\partial_T w = -3\mathrm{Re}\left(U^*M\right). \tag{6.93}$$

The above nonlinear system of coupled partial differential equations in its normalized form describing vectorial ultrashort solitons in the short-wave propagation regime is the central result of this section and it can be considered as the natural generalization of the sine–Gordon equation. We will indeed show below that it reduces to the usual sine–Gordon equation in the scalar case when the second component $v = v_0/E_0$ of the electric field is equal to zero.

Now we write down two conservation laws for the above physical system. First, denoting by $I = u^2 + v^2$ the normalized intensity we straightforwardly get $\partial_Z I = -(2/3)\partial_T w$, that is, when the homogeneous population difference w has its value corresponding to the thermal equilibrium both before and after the pulse $\partial_T w = 0$, the power $\int_{-\infty}^{+\infty} I dt$ is conserved during propagation. This equation for the evolution of intensity I also shows that the energy transfer inside the pulse is entirely governed by the homogeneous population difference w. Second, we show that there is an additional conservation law which can be obtained by mimicking the obtaining of a second conservation law in the scalar case, when a sine–Gordon equation is obtained from the above complicated system of ten coupled nonlinear equations. To this aim let us consider the scalar case $v = 0$. It is seen that K, S, n, q are equal to 0 and $w = -3r$. Then the system (6.78)–(6.87) reduces to

$$\partial_Z u = -\partial_T p, \tag{6.94}$$

$$\partial_T p = -m, \tag{6.95}$$

$$\partial_T m = -4ru, \tag{6.96}$$

$$\partial_T r = um. \tag{6.97}$$

The nonlinear system of coupled equations (6.94)–(6.97) reduces to the sine–Gordon equation as follows [116]. If we set $m = A\sin\theta$ and $r = (-A/2)\cos\theta$, then a direct computation shows that $\partial_T A = 0$, hence A is a constant. From Eqs. (6.94)–(6.96) it is seen that $\partial_Z u = A\sin\theta$. On the other hand, $\partial_Z\partial_T u$ can be computed, either by taking the T-derivative of $\partial_Z u$, which yields $\partial_Z\partial_T u = -2r\partial_T\theta$, or by combining (6.94) and (6.96) which yields $\partial_Z\partial_T u = -4ru$. Comparison between both expressions shows that $u = \partial_T\theta/2$ and we get the sine–Gordon equation

$$\partial_Z\partial_T\theta = 2A\sin\theta. \tag{6.98}$$

From this derivation, it is seen that the reduction of system (6.94)–(6.97) to a sine–Gordon equation is based on the conservation law $\partial_T A^2 = \partial_T\left(m^2 + 4r^2\right) = 0$. This conservation law can be straightforwardly generalized to the vectorial case as follows: $\mathcal{A} = m^2 + n^2 + \frac{1}{3}w^2 + r^2 + S^2$ in terms of the normalized real variables, or equivalently, $\mathcal{A} = |M|^2 + \frac{1}{3}w^2 + |s|^2$ in terms of the normalized complex ones.

It is easily shown that the general vectorial model introduced above allows us to retrieve the linear polarization model as a particular case of it. We now look for an approximate expression of circularly polarized pulses. One notices that a circularly polarized FCP is described by means of the complex system of nonlinear equations (6.88)–(6.93). An expression of the form $U = F\left(T - Z/v_g\right)e^{i(kZ-\omega T)}$ might be a solution of this system. However, a direct substitution of this expression into the system (6.88)–(6.93) shows, that no exact solution of this form exist. It is worthy to notice that the non-existence of exact non-SVEA circularly polarized pulse solutions to the Maxwell–Bloch equations was already pointed out in [173], although in the framework of slightly different model.

However, in the following we seek for an approximate solution of circularly polarized pulses in the limit of large ω, i.e., in the SVEA limit, by means of a multiscale expansion very similar to the standard one for deriving a NLS equation model in the SVEA limit [93]. To this aim we consider some small parameter ε, so that $1/\varepsilon$ is of the order of magnitude of the number of optical cycles in the pulse, which is assumed to be large in the SVEA limit. We expand U in power series $U = \sum_{r,n}\varepsilon^n e^{ir\varphi}U_{r,n}$, with $\varphi = kZ - \omega T$, and introduce slow variables $\tau = \varepsilon\left(t - z/v_g\right)$, and $\zeta = \varepsilon^2 Z$. At leading order (ε^1), we assume that $U_{1,1} = F$ is the only nonzero term in this expansion. After a standard procedure, we are left with a NLS equation for the variable F, from which we finally get the approximate expression for the circularly polarized soliton, as

$$U = be^{i\left[\left(k-\frac{b^2k}{\omega^2}\right)Z-\omega T\right]}\,\mathrm{sech}\left[b\left(T + \frac{k}{\omega}Z\right)\right], \tag{6.99}$$

in which the soliton parameter b is assumed to be small. As concerning the stability of the circularly polarized soliton (6.99) within the SVEA, it can be addressed analytically; see Ref. [162]. A direct consequence of the properties of NLS solitons implies that the circularly polarized pulses are stable within the SVEA.

6.2.2. *Lifetime of circularly polarized few-cycle pulses and transition to single-humped ones*

One notices that the existence and stability of the circularly polarized FCP does not ensure either its stability or even its existence beyond SVEA [173]. In the following we study numerically the stability of circularly polarized few-cycle pulses beyond the SVEA. The Z evolution of u and v is computed by means of a standard fourth-order Runge–Kutta algorithm, at each step and substep of the scheme, the eight other components are computed using the same algorithm but relative to the T variable. We assume that all atoms are initially in the fundamental state, that is, $w = -1$ at $T = 0$. We use the approximate circularly polarized pulse (6.99) as an input, with $\omega = 5$, and vary the pulse duration b. We found that the input FCP decays into two linearly polarized single-humped pulses. In general, two orthogonally polarized pulses with different amplitudes are obtained (see Figs. 22–24). For the shortest sub-cycle pulses, the instability occurs very fast, the amplitudes of the two

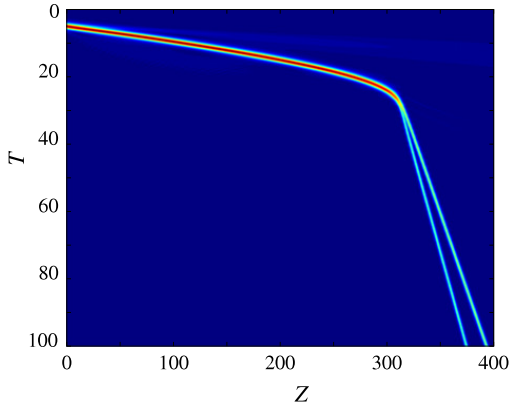

Fig. 22. (Color online) The circularly polarized FCP and its decay into orthogonally polarized single-humped pulses. Parameters: $\omega = 5$ and $b = 2$. Here $Z_{disp} = 37$. After Ref. [162].

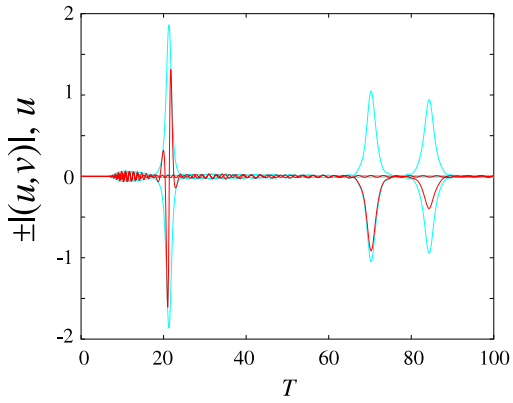

Fig. 23. (Color online) The circularly polarized FCP and its decay into two orthogonally polarized single-humped pulses. The shape of the FCP at $Z = 280$ (left) and $Z = 360$ (right). Light blue (gray): the amplitude $|U| = \sqrt{u^2 + v^2}$ (and $-|U|$), red (black): $u = \mathrm{Re}(U)$. After Ref. [162].

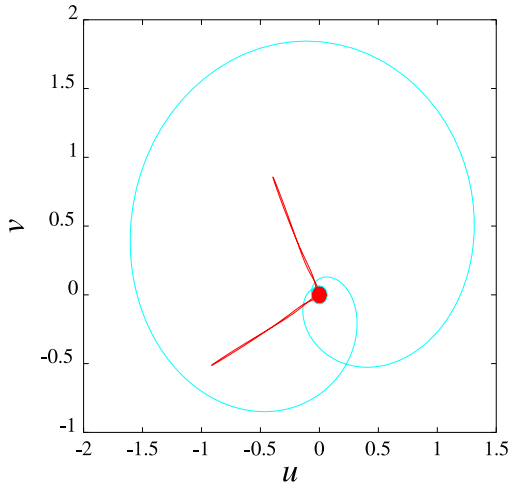

Fig. 24. (Color online) The circularly polarized FCP and its decay into two orthogonally polarized single-humped pulses. The trajectories of the tip of the normalized electric field vector (u, v) in the transverse plane, for two values of Z, showing the polarization. Light blue (gray): at $Z = 280$, red (black): at $Z = 360$. After Ref. [162].

single humped pulses strongly differ, and the angle between their polarization directions is not close to $\pi/2$. It is worthy to notice at this point that the single-humped pulses are in fact fundamental solitons of the sG equation (6.98) to which the system reduces in the case of linear polarizations (scalar case). However, no stability threshold for the circularly polarized FCPs can be evidenced by these numerical calculations. The lifetime of circularly-polarized FCPs becomes very large when the number N_c of optical cycles in the pulse is greater than one; see Ref. [162].

Concluding this section devoted to circularly polarized few-cycle solitons in the short-wave regime we stress that we took into account the vectorial nature of the electric field, and therefore we properly considered the wave polarization effects.

We have found that the two interacting waveforms corresponding to such vector few-optical-cycle solitons are adequately described by a coupled system of nonlinear equations at the first-order approximation of the perturbation approach. By direct numerical simulations we calculated the lifetime of circularly polarized few-optical-cycle solitons and we studied their decay into two orthogonally polarized single-humped pulses as a generic route of their instability.

A challenging extension suggested by these studies is to consider the case of two transitions, one below and one above the range of propagated wavelengths. Another interesting issue is the generalization of the present work to one or even to two spatial transverse dimensions, in addition to time and spatial longitudinal coordinates, that is, the study of formation and robustness of vector few-optical-cycle spatiotemporal solitons, alias ultrashort vector light bullets, beyond the slowly varying envelope approximation, both in the long- and short-wave regimes (for an overview of theoretical and experimental studies of spatiotemporal solitons in several relevant physical settings, see Ref. [171]).

7. Few-optical-cycle dissipative solitons

In this section by using the powerful reductive perturbation technique, a generalized modified Korteweg–de Vries (gmKdV) partial differential equation is derived, which describes the physics of few-optical-cycle dissipative solitons beyond the slowly-varying envelope approximation; see Ref. [38] for a detailed study of this problem. We also briefly discuss the output of numerical simulations showing the formation of stable dissipative solitons from arbitrary breather-like few-cycle pulses. Though there are a lot of papers devoted to FCPs in conservative physical settings, there are only a few works devoted to the study of *few-optical-cycle dissipative solitons*. It is worthy to mention the works of Rosanov et al. [49,50], where both the formation of few-optical-cycle dissipative solitons in active nonlinear optical fibers and the collisions between them were investigated. The theory of mode-locked lasers essentially relies on mean field models derived within the SVEA. One of the most important of such models is Haus' *master equation* [177], which is in fact the stationary version of the complex Ginzburg–Landau (CGL) equation [178–181]; see, e.g., the comprehensive reviews [182,183] on the CGL equation and its various applications. The short pulses are fairly well described by soliton solutions to the CGL equation, which are unstable for the cubic CGL equation and stable for the cubic-quintic CGL model. Both the cubic and the cubic-quintic CGL models have been derived from a detailed description of the laser cavity, in the case of fiber lasers that are mode-locked by means of nonlinear polarization rotation, or figure-eight ones [184–186]. One notices that, for such lasers, descriptions of the cavity by means of full numerical resolution of propagation equations along it have also been used; see e.g. [187]. The Lorentz–Haken equations, commonly considered as a general model of a laser setup, have been reduced to the Swift–Hohenberg equation [188], which can be considered as a perturbed CGL equation [182]. It is commonly admitted that mode-locking requires some saturable absorber [189] or some setup having an equivalent effect; nonlinear polarization rotation and nonlinear loop mirror have been mentioned above. An alternative technique is the Kerr lens mode-locking (KLM) [190–192], which combines self-focusing due to the Kerr effect and the use of an aperture to select the highest intensities. KLM is not a mere effective amplitude-dependent gain/loss effect, but a complex phenomenon which involves the spatiotemporal intra-cavity pulse dynamics. The existing theory of KLM is based on nonlinear geometrical optics for Gaussian beams, hence within the SVEA, and the initial approach of Refs. [190–192] was not fundamentally modified in more recent studies (see e.g. Refs. [193,194]). The technique is very efficient even in the case of strong self-focusing and two-cycle pulses (see e.g. Ref. [111]), in which the validity of the approximations used in the theoretical developments is not ensured.

In this section we derive a generic partial differential equation describing the dynamics of dissipative FCP solitons in a laser cavity filled with two-level atoms, beyond SVEA model equations [38]. Starting from the Maxwell–Bloch equations, by using a multiscale perturbation approach [93] we derive a non-SVEA version of the Lorenz–Haken equations [195,196]. We are left with a generic equation describing dissipative few-optical-cycle solitons in the form of a gmKdV equation containing additional terms accounting for gain and losses. Thus in addition to the standard term accounting for linear losses (proportional to the optical field) we get a term proportional to the second-order derivative of the optical field with respect to the time variable, which accounts for gain and a second, regularizing term, proportional to the fourth-order derivative with respect to the time variable of the optical field, which accounts for losses; see Ref. [38].

7.1. Maxwell–Bloch equations and their multiscale analysis

In an important work published more than three decades ago, Haken [196] used a single-mode unidirectional ring laser model (with a homogeneously broadened line) described by the Maxwell–Bloch equations, and after some approximations showed its mathematical equivalence with an appropriate model of the Lorenz oscillator [195]. In the following we derive a non-SVEA version of the Lorenz–Haken equations. We start from the Maxwell–Bloch equations for the simple case of linear polarizations: $\partial_z^2 E = c^{-2}\partial_t^2\left(E + 4\pi\hat{P}\right)$ with $\hat{P} = N\mathrm{Tr}\left(\hat{\rho}\hat{\mu}\right)$, where N is the atomic density, $\hat{\mu}$ is the dipolar momentum operator, and $\hat{\rho}$ is the density matrix, which obeys the Schrödinger–von Neumann equation

$$i\hbar\partial_t\hat{\rho} = \left[\hat{H}_0 - \hat{\mu}\hat{E}, \hat{\rho}\right] + i\hat{\Lambda} - i\hat{R}, \tag{7.1}$$

$\hat{\Lambda}$ accounts for gain, and $\hat{R}$ for relaxation of the components of the density matrix $\hat{\rho}$.

In Eq. (7.1) $\hat{H}_0$ is the free Hamiltonian of the atomic system under consideration. However, losses must be also taken into account. A phenomenological loss term has to be introduced, in such a way that it can be compensated by gain. It is necessary that the time evolution of losses (or their spectral profile) be able to adjust to the gain. Hence not only losses due to reflection at the cavity boundaries, which will be evaluated below, but also the ones of the medium must be taken into account. Therefore we need to introduce a second transition, independent of the former (pumped) one, which only produces absorption. The corresponding free Hamiltonian is thus

$$\hat{H}_0 = \begin{pmatrix} H_0 & 0 \\ 0 & H_0' \end{pmatrix} = \hbar \begin{pmatrix} \omega_a & 0 & 0 & 0 \\ 0 & \omega_b & 0 & 0 \\ 0 & 0 & \omega_a' & 0 \\ 0 & 0 & 0 & \omega_b' \end{pmatrix}. \tag{7.2}$$

Here, as we said before, we consider a set of four-level atoms with the Hamiltonian $\hat{H}_0$, corresponding to two distinct two-level transitions with frequencies $\Omega = \omega_b - \omega_a$ and $\Omega' = \omega_b' - \omega_a'$, respectively. The dipolar momentum is thus given by

$$\hat{\mu} = \begin{pmatrix} \mu & 0 \\ 0 & \mu' \end{pmatrix} = \begin{pmatrix} 0 & \mu & 0 & 0 \\ \mu^* & 0 & 0 & 0 \\ 0 & 0 & 0 & \mu' \\ 0 & 0 & \mu'^* & 0 \end{pmatrix}. \tag{7.3}$$

The gain is

$$\hat{\Lambda} = \begin{pmatrix} \Lambda & 0 \\ 0 & 0 \end{pmatrix} = \hbar \begin{pmatrix} \lambda_a & 0 & 0 & 0 \\ 0 & \lambda_b & 0 & 0 \\ 0 & 0 & 0 & 0 \\ 0 & 0 & 0 & 0 \end{pmatrix}, \tag{7.4}$$

and the relaxation term is

$$\hat{R} = \begin{pmatrix} R & 0 \\ 0 & R' \end{pmatrix} = \hbar \begin{pmatrix} \gamma_a(\rho_a - 1) & \gamma_t \rho_t & 0 & 0 \\ \gamma_t \rho_t^* & \gamma_a \rho_b & 0 & 0 \\ 0 & 0 & \gamma_a'(\rho_a' - 1) & \gamma_t \rho_t' \\ 0 & 0 & \gamma_t' \rho_t'^* & \gamma_a' \rho_b' \end{pmatrix}, \tag{7.5}$$

and the density matrix is

$$\hat{\rho} = \begin{pmatrix} \rho_a & \rho_t & \rho_{13} & \rho_{14} \\ \rho_t^* & \rho_b & \rho_{23} & \rho_{24} \\ \rho_{31} & \rho_{32} & \rho_a' & \rho_t' \\ \rho_{41} & \rho_{42} & \rho_t'^* & \rho_b' \end{pmatrix}. \tag{7.6}$$

Next it can be easily shown that the density matrix $\hat{\rho}$ is block diagonal (the components of the two off-diagonal 2×2 blocks in $\hat{\rho}$ are zero):

$$\hat{\rho} = \begin{pmatrix} \rho & 0 \\ 0 & \rho' \end{pmatrix}.$$

Thus the Schrödinger–von Neumann equation (7.1) splits into two equations of the same form for the two diagonal blocks of the matrix $\hat{\rho}$; note that each of these equations describes a two-level transition.

Now we briefly show how to evaluate the mirror losses. In order to derive an additional term in the Maxwell wave equation which can account for the losses due to the mirrors, we consider a simplified cavity model, in which only the mirrors are taken into account. Consider thus a cavity with length L, and mirrors with amplitude reflection coefficients r. It can be seen as a periodic medium with period L and periodically localized losses with a loss factor $(1 - r^2)$. We intend to describe this in a continuous way as distributed losses. Let z be the variable along the cavity axis, c and v the light velocity in vacuum and in the cavity, respectively. A simple analysis shows that the initial Maxwell equation should be replaced with a modified one, which take into account the mirror loss through the parameter $\beta = -v \ln r/L$; see Ref. [38]. Consequently, we consider here the modified Maxwell equation

$$\partial_z^2 E = \frac{1}{c^2} (\beta + \partial_t)^2 \left[E + 4\pi \left(P + P' \right) \right]. \tag{7.7}$$

Here P and P' are the two polarization terms corresponding to the two distinct transitions.

We have shown in the preceding sections that the reductive perturbation method is a very powerful way of deriving simplified, generic models describing nonlinear wave propagation and interaction in various physics settings [93]. We will

apply this mathematical method to the study of dissipative few-cycle optical solitons. To this aim we first introduce scaled variables corresponding to a long-wave approximation of mKdV type, as

$$\tau = \varepsilon\left[t - z\left(\frac{1}{V} + \varepsilon W\right)\right], \qquad \zeta = \varepsilon^3 z. \tag{7.8}$$

One notices that with respect to the standard mKdV-type scaled variables, the above expression (7.8) involves an additional correction W of order ε to the inverse velocity V^{-1}. We will next see that this correction W of order ε to the inverse velocity is proportional to the correction w_1 of order ε to the population difference. We expand the optical field E in a power series of a small parameter ε as $E = \varepsilon E_1(\zeta, \tau) + \varepsilon^2 E_2(\zeta, \tau) + \cdots$. The corresponding power series expansions of ρ and ρ' start with the order ε^0 quantity ρ_0. The gain Λ and R are also expanded in this way. We will consider here a laser setup, hence the characteristic frequency ω_0 of the wave must be close to the resonance line, say $\Omega = \omega_b - \omega_a$, and especially fall within the gain curve. Since we use a long-wave approximation, we have $\omega_0 \simeq 0$. Hence the spectral line, which expresses typically as $[(\omega - \Omega)^2 + \gamma_t^2]^{-1}$, must extend down to $\omega = \omega_0 \simeq 0$, which happens only if its width γ_t has the same order of magnitude as the central line Ω. The second transition, with central line Ω', has been introduced to account for cavity losses. Further, losses must be compensated by gain. Therefore it is necessary that the bandwidth of both gain and losses have the same order of magnitude. Thus γ_t' must have the same order of magnitude as γ_t. One notices that the long-wave approximation used here means that the characteristic frequency ω_0 of the wave is small with respect to γ_t, or conversely, that γ_t is large with respect to ω_0. Thus the long-wave approximation can be seen as an approximation of broad bandwidth. This is consistent with the fact that a very wide bandwidth is required to produce ultrashort pulses in commercially available laser systems. On the other hand, the mirror loss parameter β is expanded as $\beta = \varepsilon\beta_1 + \varepsilon^2\beta_2 + \cdots$. Hence we assume that β is small, i.e., the good cavity condition. However, the order of magnitude of β which allows dissipative soliton propagation is not specified *a priori*; it will arise as a result of the computation, see below the details of it.

In the following we will perform the order by order resolution of the governing Maxwell–Bloch equations. At order ε^0 the Schrödinger–von Neumann equation for the first transition (let us call it equation (S)) is $[H_0, \rho_0] + i\Lambda_0 - iR_0 = 0$. Using

$$[H_0, \rho_0] = \begin{pmatrix} 0 & -\hbar\Omega\rho_t \\ \hbar\Omega\rho_t^* & 0 \end{pmatrix},$$

we get $\rho_{0t} = 0$, $\rho_{0a} = 1 + \lambda_{0a}/\gamma_a$, and $\rho_{0b} = \lambda_{0b}/\gamma_a$. Due to the condition $\mathrm{Tr}\rho = 1$, we see that $\lambda_{0b} = -\lambda_{0a}$. We define the population difference as $w_j = \rho_{jb} - \rho_{ja}$ for all j, then $w_0 = (2\lambda_{0b}/\gamma_a) - 1$. We will assume that $w_0 > 0$, hence $\lambda_{0b} > \alpha\gamma_a/2$, and $\lambda_{0b} > 0$.

For the Schrödinger equation for the second transition, which we call equation (S'), we get the same results, but without pumping, and with the corresponding 'prime' quantities, i.e., $\rho_{0a}' = 1$, $\rho_{0b}' = 0$, $\rho_{0t}' = 0$ and $w_0' = \rho_{0b}' - \rho_{0a}' = -1$.

At order ε^1 equation (S) is $i\hbar\partial_\tau\rho_0 = [H_0, \rho_1] - E_1[\mu, \rho_0] + i\Lambda_1 - iR_1$, then by calculating the corresponding commutators and taking into account that $\rho_{0t} = 0$, we get $w_1 = -2\rho_{1a} = 2\rho_{1b} = 2\lambda_{1b}/\gamma_a$ and $\rho_{1t} = (-\mu w_0 E_1)/[\hbar(\Omega + i\gamma_t)]$. The polarization term P_1 at order 1 is given by

$$P_1 = \frac{-2N\Omega\,|\mu|^2\, w_0 E_1}{\hbar\left(\Omega^2 + \gamma_t^2\right)}.$$

For equation (S'), we get analogous formulas, with λ_{1b} replaced by 0 and $w_0' = -1$.

From the Maxwell wave equation at leading order ε^3 we get $\beta_1 = 0$ and the expression of velocity $V = c/n$ with the refractive index

$$n = \left[1 + \frac{8\pi N\Omega'\left|\mu'\right|^2}{\hbar(\Omega'^2 + \gamma_t'^2)} - \frac{8\pi N\Omega\,|\mu|^2\, w_0}{\hbar\left(\Omega^2 + \gamma_t^2\right)}\right]^{1/2}. \tag{7.9}$$

The refractive index n has a similar expression as in the conservative two level-model (see Eq. (3.8) above and Ref. [73]), except that (i) there are two terms in the above equation, one term for each of the two transitions, (ii) the line widths γ_t, γ_t' are not neglected here as was done in Ref. [73], and (iii) $w_0 > 0$, which accounts for gain which should be present in the present physical setting.

Next at order 2 we get equation (S) in the form: $i\hbar\partial_\tau\rho_1 = [H_0, \rho_2] - E_2[\mu, \rho_0] - E_1[\mu, \rho_1] + i\Lambda_2 - iR_2$. From this equation we get the corresponding values of w_2 and the polarization P_2 at order ε^2:

$$w_2 = 2\rho_{2b} = -2\rho_{2a} = \frac{2\lambda_{2b}}{\gamma_a} - \frac{4\gamma_t\,|\mu|^2\, w_0 E_1^2}{\hbar^2\,\gamma_a\left(\Omega^2 + \gamma_t^2\right)}, \tag{7.10}$$

$$P_2 = \frac{-2N\Omega\,|\mu|^2}{\hbar\left(\Omega^2 + \gamma_t^2\right)}(E_2 w_0 + E_1 w_1) + \frac{4N\Omega\gamma_t\,|\mu|^2\, w_0}{\hbar\left(\Omega^2 + \gamma_t^2\right)^2}\partial_\tau E_1. \tag{7.11}$$

One notices that from equation (S'), we get similar results, except that there is no pumping, that is, λ_{2b} is replaced by zero, $w_0' = -1$, and $w_1' = 0$.

The wave equation at perturbation order ε^4 reduces to

$$\frac{2W}{V}\partial_\tau^2 E_1 = \frac{1}{c^2}\partial_\tau^2\left[\frac{-8\pi N\Omega\,|\mu|^2}{\hbar\left(\Omega^2+\gamma_t^2\right)}E_1 w_1 + \frac{16\pi N\Omega\gamma_t\,|\mu|^2\,w_0}{\hbar\left(\Omega^2+\gamma_t^2\right)^2}\partial_\tau E_1 - \frac{16\pi N\Omega'\gamma_t'\,|\mu'|^2}{\hbar(\Omega'^2+\gamma_t'^2)^2}\partial_\tau E_1\right] + \frac{2\beta_2}{V^2}\partial_\tau E_1. \tag{7.12}$$

First, a simple analysis of the above equation involving the following three derivatives with respect to τ of the field E_1, that is, $\partial_\tau E_1$, $\partial_\tau^2 E_1$ and $\partial_\tau^3 E_1$, shows that the second order correction to the mirror loss parameter β is equal to zero ($\beta_2 = 0$), which implies that mirror losses are even smaller as previously estimated. Second, we obtain a relationship between W and w_1

$$W = \frac{-4\pi N\Omega\,|\mu|^2}{n\hbar c\left(\Omega^2+\gamma_t^2\right)}w_1 \tag{7.13}$$

(the refractive index n being given by (7.9)), i.e. a correction w_1 of order ε to the population difference induced a correction of the same order to the velocity. Third, we are left with the relationship

$$\frac{\Omega\gamma_t\,|\mu|^2\,w_0}{\left(\Omega^2+\gamma_t^2\right)^2} = \frac{\Omega'\gamma_t'\,|\mu'|^2}{\left(\Omega'^2+\gamma_t'^2\right)^2}, \tag{7.14}$$

i.e., the gain induced by the pumped transition compensates the losses induced by the unpumped one, at this perturbation order. Eq. (7.14) determines the laser threshold. An essential feature of laser pulse propagation is the excess of gain above the threshold. It is due to the correction term w_1 to the population difference, and fixes the magnitude of the gain term in the evolution equation governing the dynamics of few-optical-cycle dissipative solitons, as in SVEA models of Ginzburg–Landau type [186]. We anticipate that we are left with a generalized modified KdV partial differential equation which describes the evolution of few-cycle dissipative solitons.

At order 3 we write down the equation (S) as

$$i\hbar\partial_\tau\rho_2 = [H_0,\rho_3] - E_3[\mu,\rho_0] - E_2[\mu,\rho_1] - E_1[\mu,\rho_2] + i\Lambda_3 - iR_3. \tag{7.15}$$

From the above equation we are left with a rather complicated expression for the polarization P_3 at order ε^3 and an analogous expression for the polarization P_3' where $w_0' = -1$, $w_1' = 0$, and λ_{2b} is replaced with 0. From the wave equation at perturbation order ε^5 we get a rather complicated evolution equation for E_1. One notices that $\beta_1 = \beta_2 = 0$ and the terms involving the field E_3 cancel out each other due to the condition expressing the value of velocity V. The terms involving the field E_2 cancel out due to the condition (7.13) giving the correction W to the velocity V and due to the condition (7.14) that gain compensates losses.

As a result of this reductive perturbation analysis we are finally left with the following equation for the field E_1 at the first perturbation order ε^1:

$$\partial_\zeta E_1 = -A\partial_\tau E_1^3 - B\partial_\tau^3 E_1 - C\partial_\tau^2 E_1 + D\partial_\tau E_1 - \Gamma E_1, \tag{7.16}$$

with

$$A = \frac{16\pi N}{nc\,\hbar^3}\left[\frac{\Omega\gamma_t\,|\mu|^4\,w_0}{\gamma_a\left(\Omega^2+\gamma_t^2\right)^2} - \frac{\Omega'\gamma_t'\,|\mu'|^4}{\gamma_a'\left(\Omega'^2+\gamma_t'^2\right)^2}\right], \tag{7.17}$$

$$B = \frac{4\pi N}{nc\hbar}\left[\frac{\Omega\left(\Omega^2-3\gamma_t^2\right)|\mu|^2\,w_0}{\left(\Omega^2+\gamma_t^2\right)^3} - \frac{\Omega'\left(\Omega'^2-3\gamma_t'^2\right)|\mu'|^2}{\left(\Omega'^2+\gamma_t'^2\right)^3}\right], \tag{7.18}$$

$$C = \frac{8\pi N}{nc\hbar}\frac{\Omega\gamma_t\,|\mu|^2\,w_1}{\left(\Omega^2+\gamma_t^2\right)^2}, \tag{7.19}$$

$$D = \frac{8\pi N}{nc\hbar}\frac{\lambda_{2b}\Omega\,|\mu|^2}{\gamma_a\left(\Omega^2+\gamma_t^2\right)} + \frac{VW^2}{2}, \tag{7.20}$$

and $\Gamma = \beta_3/V$. For $C = D = \Gamma = 0$, Eq. (7.16) reduces to the mKdV equation. An inspection of this equation gives us the physical significance of different terms involved in it. Thus the term containing the second-order derivative with respect to the time variable τ looks like a diffusion term in a partial differential equation of Burgers' type (see, for example, Refs. [85,86]). However, if we assume $\lambda_{1b} = \gamma_a w_1/2 > 0$, i.e., for a pumping slightly above the threshold characterized by Eq. (7.14), then $C > 0$ and this term becomes a gain one. The term proportional to first-order derivative with respect to the time variable τ corresponds to a pumping term of lower order, but its concrete contribution here is a mere change in velocity. Thus the parameter D can be changed to any value at our convenience by means of adequate Galilean transform. Finally, the term $(-\Gamma E_1)$ corresponds to the losses due to the mirrors, with $\beta_3 > 0$ and $\Gamma > 0$.

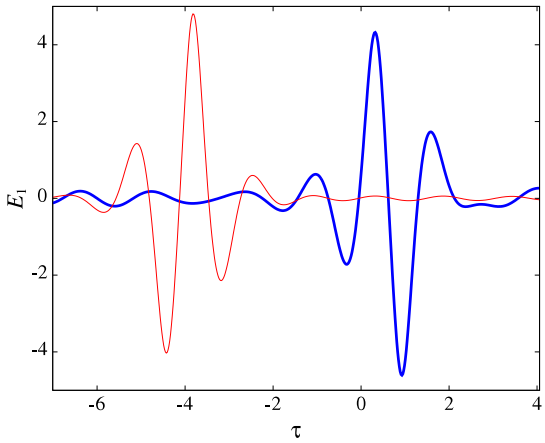

Fig. 25. Evolution of a dissipative FCP soliton. Thick (blue) line: $z = 26$, thin (red) line: $z = 50$. After Ref. [38].

However, a serious problem with the above written generalized modified KdV equation is that Eq. (7.16) is highly unstable when C is positive. Indeed, the gain increases as the frequency tends to infinity, which is an unphysical consequence of the perturbation formalism. Therefore an additional regularizing term is necessary to be incorporated in Eq. (7.16); see Ref. [38] for more details of this issue. As a result, Eq. (7.16) should be replaced with a regularized one

$$\partial_\zeta E_1 = -A\partial_\tau E_1^3 - B\partial_\tau^3 E_1 - C\partial_\tau^2 E_1 + D\partial_\tau E_1 - G\partial_\tau^4 E_1 - \Gamma E_1, \tag{7.21}$$

where

$$G = \frac{16\pi\varepsilon N}{n\hbar c}\left[\frac{\Omega\gamma_t\left(\gamma_t^2 - \Omega^2\right)|\mu|^2 w_0}{\left(\Omega^2 + \gamma_t^2\right)^4} - \frac{\Omega'\gamma_t'\left(\gamma_t'^2 - \Omega'^2\right)|\mu'|^2}{\left(\Omega'^2 + \gamma_t'^2\right)^4}\right]. \tag{7.22}$$

At this point we note the misprint in Eqs. (72)–(74) of Ref. [38]. The partial differential evolution equation (7.21), which is a non-SVEA version of Lorenz–Haken laser equation, adequately describes the physics of few-optical-cycle dissipative solitons beyond the SVEA. This nonlinear evolution equation is a generalized modified Korteweg–de Vries partial differential equation. Note that the nonlinear term $-A\partial_\tau E_1^3$ accounts for the Kerr effect, while the term $-B\partial_\tau^3 E_1$ accounts for dispersion. These terms and the corresponding coefficients A and B have the same expressions as in the conservative counterpart of Eq. (7.21), which is the mKdV equation derived in [73] by using a reductive perturbation approach. The term $D\partial_\tau E_1$ describes a change in the pulse (phase and group) velocity. Expression (7.20) of D shows that this velocity change is due to a gain effect. The three other terms account for a frequency-dependent gain–loss: the main term is $-C\partial_\tau^2 E_1$, which accounts for a broadband gain. However, the width of the gain spectrum must be finite, which is ensured by the term $-G\partial_\tau^4 E_1$. On the other hand linear losses must be introduced to avoid excessive amplification, they are accounted for by the term $-\Gamma E_1$. It is thus seen that Eq. (7.21) contains all terms involved by a one-dimensional description of a laser setup, as nonlinearity, dispersion, and frequency-dependent gain and losses, except one term: the nonlinear gain, or effective saturable absorber. However, from numerical simulations we will see that this term is not necessary for stabilization of the dissipative few-cycle pulses; see Ref. [38].

7.2. Robust ultrashort dissipative optical solitons

The generalized modified KdV dynamical equation (7.21) was solved numerically in Ref. [38] by means of an exponential time differencing scheme, of second order Runge–Kutta type [115]. Absorbing boundary conditions were implemented in the numerical simulations (see Ref. [38]) and numerical values of the parameters were fixed as follows: the nonlinear coefficient $A = 1$ (a self-focusing optical medium was considered), the third-order dispersion coefficient $B = 1, C = 0.1$ (corresponding to gain), $G = 0.002$ (corresponding to losses), $D = -48.836$ (a velocity adjusted in such a way that the soliton remained in the computation box), and $\Gamma = 1$ (corresponding to losses). For this specific set of parameters stable few-optical-cycle dissipative soliton propagation was obtained; see Fig. 25. The initial field distribution was a breather solution of the underlying modified KdV equation, which displays only a few oscillation cycles. The above FCP propagates thus in a stable way, that is, a robust few-optical-cycle dissipative soliton was put forward. Note that its stabilization does not require any effective saturable absorber, or nonlinear gain term in Eq. (7.21).

The numerical simulation described above uses an initial pulse close to the final one; hence this result shows the stability of the FCP rather in a medium used as an optical amplifier than really in a laser cavity. In order to study the latter issue, it was used a random input and it was investigated whether a self-starting behavior can be observed [38]. Using periodic boundary conditions, it was found in Ref. [38] that FCPs form spontaneously, however their number in the numerical box

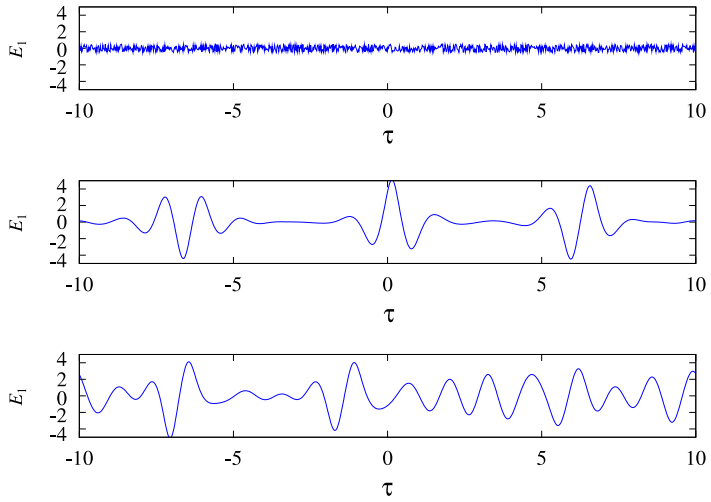

Fig. 26. Evolution of the electric field from noise. (a) The input ($z = 0$). (b) Three dissipative FCP solitons are formed ($z = 31.9$). (c) The interaction of many FCP solitons appears as chaotic ($z = 75$). After Ref. [38].

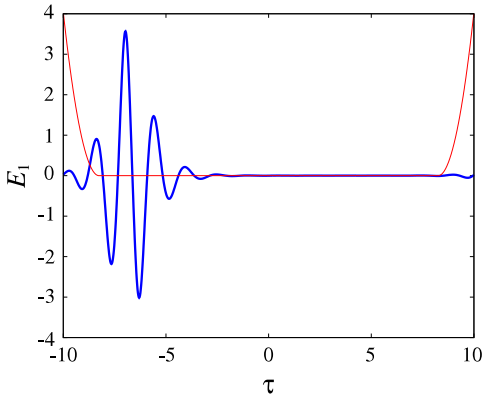

Fig. 27. The FCP soliton formed from noise in the presence of velocity filtering yielded by absorbing boundary conditions (thick blue line). The thin red line shows the transverse variations of the linear absorption coefficient α producing the absorbing boundary conditions (more exactly $\alpha/15$). After Ref. [38].

increases during propagation; see Fig. 26. The result of the interaction and superposition of a many FCPs appear as irregular oscillations, with an apparently chaotic behavior; see Fig. 26(c). It is incoherent light, and in this sense incoherent light can be seen as a superposition of FCPs. Thus, in order to produce a FCP laser, the question is not, how a FCP can be produced, but how it can be isolated. It was shown in Ref. [38] that the absorbing boundary conditions achieve it. However, the obtained FCP soliton is locked to the edge of the pumped zone; see Fig. 27. Hence the mechanism of stabilization is closely related to the temporal localization of pumping realized this way. It strongly differs from the situation of Fig. 25, in which was set an initial pulse distribution close to the final FCP.

In a recent paper [39], Farnum and Kutz proposed a 'master mode-locking equation' for few-cycle pulses. Their equation reads as

$$\partial_x \partial_t u - u - \frac{1}{6}\partial_x^2 u^3 = \partial_x \left(g(t) \mathcal{F}^{-1} \left(P(k) \hat{u} \right) - \gamma u + \beta u^3 \right) \tag{7.23}$$

in which x is the variable which accounts for the pulse shape, proportional to our variable τ, t is the propagation variable, proportional to our variable ζ, u is the normalized laser electric field. $\mathcal{F}$ is the Fourier transform with k the variable conjugated to x and $\mathcal{F}(u) = \hat{u}$. Here

$$g(t) = \frac{2g_0}{1 + \|u\|^2/I_0},$$

with $\|u\|$ the $\mathcal{L}_2$-norm of u, is the saturated gain, and $P(k) = 1 - a\,(|k| - b)^2$ is the spectral gain profile.

In addition to Eq. (7.21), this phenomenological equation takes into account the dispersion term due to the infrared resonances, it is the term $-u$ on the left-hand side of Eq. (7.23). It also takes into account gain saturation, through the expression of $g(t)$, and the effect of some instantaneous saturable absorber, through the term $\partial_x \left(\beta u^3 \right)$. However, the spectral profile of the gain is essential for dissipative FCP soliton formation. In [39], the gain–loss spectrum is given by $P_g(k) = gP(k) - \gamma$. In Eq. (7.21), it is $Q(\omega) = C\omega^2 - G\omega^4 - \Gamma$. Let us consider the same numerical values of C, G, Γ as above, and $a = 0.75$, $b = 1.6$ as used in [39]. The proportionality coefficient between k and ω is fixed so that the maxima of

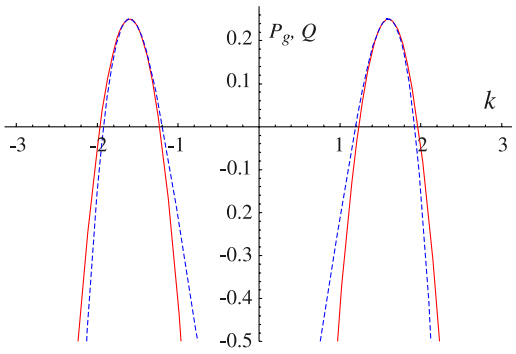

Fig. 28. The spectral profile of the gain involved by Eq. (7.21) (dashed blue line), compared to the one used in the 'master mode-locking equation' for FCPs of Ref. [39] (solid red line).

$P_g(k)$ and $Q(\omega)$ coincide, then g and γ are fixed so that both the maximum amplitude and the width of the two functions coincide. They are plotted versus k in Fig. 28. Comparison between the two curves show that both approaches are in fact very close together.

We conclude this section with a few comments on these studies of dissipative FCPs. First, we recall that in Ref. [38] it was introduced a model based on the Maxwell–Bloch equations for an ensemble of 2×2-level atoms, which takes into account both the losses due to the optical field reflection at the laser cavity mirrors and the ones occurring in the optical medium itself. The multiscale perturbative approach up to the third-order in a certain small perturbation parameter was used. As a result of this powerful reductive perturbation method, a generalized modified Korteweg–de Vries equation containing gain and loss terms has been derived and has been solved by adequate numerical methods. The simulations have clearly proved its suitability for describing the physics of few-optical-cycle dissipative solitons. Second, a remarkable feature of the model introduced in Ref. [38] is that no nonlinear gain/loss term accounting for some effective saturable absorber is required in order to get robust ultrashort dissipative solitons; it was found that absorbing boundary conditions are the only way to stabilize the FCP. Note that a precise identification of the physical mechanism that such specific boundary conditions are modeling requires a separate study. Third, it was shown in Ref. [38] that a single dissipative FCP soliton can be formed only if some velocity filtering or temporal localization of pumping is introduced in the model equation. We believe that these results can also be generalized to $(2+1)$-dimensional few-cycle-pulse propagation models for dissipative optical solitons.

8. Spatiotemporal few-optical-cycle solitons

In this section we will systematically use the reductive perturbation technique to obtain generic nonlinear equations which describe the evolution of $(2+1)$-dimensional spatiotemporal few-optical-cycle solitons in both quadratic and cubic nonlinear optical media, beyond the SVEA. First, we will consider ultrashort spatiotemporal optical solitons in quadratic nonlinear media and the generation of both line and lump solitons from few-cycle input pulses [31]. Second, in the case of nonlinear Kerr media, we will describe the collapse of ultrashort spatiotemporal pulses described by the cubic generalized Kadomtsev–Petviashvili (KP) equation [32]. Third, we consider the problem of ultrashort light bullets described by the two-dimensional sine–Gordon equation in the short-wave approximation regime [33]. By using a reductive perturbation technique applied to a two-level model, it was obtained in Ref. [33] a generic two-dimensional sine–Gordon evolution equation governing the propagation of femtosecond spatiotemporal optical solitons in Kerr media beyond the SVEA. One notices that in contrast to the long-wave approximation, no collapse occurs, and that robust $(2+1)$-dimensional ultrashort light bullets may form from adequately chosen few-cycle input spatiotemporal waveforms. Also, in contrast to the case of quadratic nonlinearity, the light bullets oscillate in both space and time, and are therefore not steady-state lumps [33]. (See Fig. 36.)

8.1. Ultrashort light bullets in quadratic nonlinear media: the long-wave approximation regime

A FCP launched in a quadratically nonlinear medium may result in the formation of a $(1+1)$-dimensional half-cycle soliton (with a single hump) and without any oscillating tails [120]. It was proved in Ref. [120] that the FCP soliton propagation in quadratic nonlinear media can be adequately described by a KdV equation and not by a mKdV equation as in the case of cubic (Kerr) nonlinear media. Note that in Ref. [120] it was considered a quadratic nonlinearity for a single wave (frequency), and that no effective third order nonlinearity was involved (due to cascaded second order nonlinearities). This is in sharp contrast with the nonlinear propagation of standard *quadratic solitons* (alias two-color solitons) within the SVEA where two different frequencies are involved, namely a fundamental frequency and a second harmonic [197–208].

It is to be mentioned that there are only a few works devoted to the study of multidimensional few-optical-cycle solitons (spatiotemporal few-cycle solitons), where additional spatial transverse dimensions are incorporated into the model; see e.g., the earlier works [72,74,75], where the propagation of few-cycle optical pulses in a collection of two-level atoms was

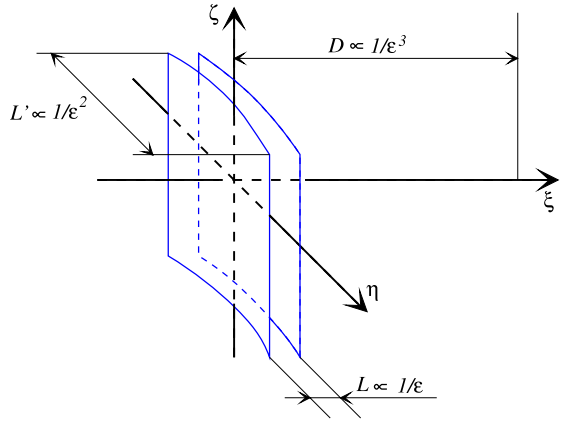

Fig. 29. (Color online) The different length scales of the KP soliton. After Ref. [31].

investigated beyond the traditional SVEA in a $(2+1)$-dimensional model. The extensive numerical simulations have shown that in certain conditions, a femtosecond pulse can evolve into a stable few-optical-cycle spatiotemporal soliton [72,74,75].

In the following we derive the generic KP equation governing the propagation of femtosecond spatiotemporal solitons in quadratic nonlinear media beyond the SVEA. The powerful reductive perturbation technique up to sixth order in a small parameter ε will be used [31]. When the resonance frequency is well above the inverse of the typical pulse width, which is of the order of a few femtoseconds, the long-wave approximation leads to generic KP I and KP II evolution equations. We then briefly discuss the known analytical solutions of these KP equations, such as line and lump solitons. Direct numerical simulations of the nonlinear evolution equations show the generation of stable line solitons (for the KP II equation) and of stable lumps (for the KP I equation). As concerning the problem of instability of such solitons, a typical example of the decay of the perturbed unstable line soliton of the KP I equation into stable lumps is also given in what follows.

The derivation of the KP equation closely follows the corresponding derivation of the KdV equation describing the $(1+1)$-dimensional model of the propagation of ultrashort solitons in quadratic nonlinear media; see Section 3.3 and Ref. [120]. As we explained in the latter case, transparency implies that the characteristic frequency ω_w of the considered radiation (in the optical range) strongly differs from the resonance frequency Ω of the atoms, hence it can be much higher or much lower. We consider here the latter case, i.e., we assume that ω_w is much smaller than Ω. This motivates the introduction of the temporal and spatial slow variables

$$\tau = \varepsilon\left(t - \frac{z}{V}\right), \qquad \zeta = \varepsilon^3 z, \qquad \eta = \varepsilon^2 y, \tag{8.1}$$

ε being a small parameter. The delayed time τ involves propagation at some speed V to be determined. It is assumed to vary slowly in time, according to the assumption $\omega_w \ll \Omega$. The pulse shape described by the variable τ is expected to evolve slowly in time, the corresponding scale being that of variable ζ. The different length scales for the soliton of the KP-type nonlinear evolution equations are shown in Fig. 29. The smallest scale determines the direction of the wave surface, and the propagation direction, which is normal to it. Consequently, the transverse spatial variable y must have an intermediate scale: ε^2 and not ε^3 as for the longitudinal spatial coordinate z; these three different scalings of the variables t, y, and z are usual in KP-type expansions; see Ref. [93].

A weak amplitude assumption is needed in order that the nonlinear effects arise at the same propagation distance scale as the dispersion does. According to the reductive perturbation method as developed in Ref. [93], the electric field E is expanded in a power series of a small parameter ε: $E = \varepsilon^2 E_2 + \varepsilon^3 E_3 + \varepsilon^4 E_4 + \cdots$, as in the standard KdV-type expansions [93,120]. Also, the polarization density P is expanded in a similar way.

If we proceed with the order by order resolution of the corresponding Schrödinger–von Neumann density matrix evolution equation and the Maxwell wave equation we find that the computation is exactly the same as in Ref. [120] up to order ε^4 in the Schrödinger–von Neumann equation and up to order ε^5 in the wave equation. Then the Maxwell wave equation at order ε^6 yields the evolution equation for the electric field amplitude E_2, as

$$\partial_\zeta \partial_\tau E_2 = A\partial_\tau^4 E_2 + B\partial_\tau^2 (E_2)^2 + \frac{V}{2}\partial_\eta^2 E_2, \tag{8.2}$$

which is a generic KP equation. One notices that the dispersion coefficient A and the nonlinear coefficient B can be written in a general form as $A = [1/(2c)]\left.\frac{d^2 n}{d\omega^2}\right|_{\omega=0}$, and $B = -[2\pi/(nc)]\,\chi^{(2)}(2\omega;\omega,\omega)\big|_{\omega=0}$, where n is the refractive index of the medium and ω is the wave pulsation. $V = c/n$ is the velocity.

The KP equation (8.2) is reduced to

$$\partial_Z \partial_T u = \partial_T^4 u + \partial_T^2 u^2 + \sigma\partial_Y^2 u, \tag{8.3}$$

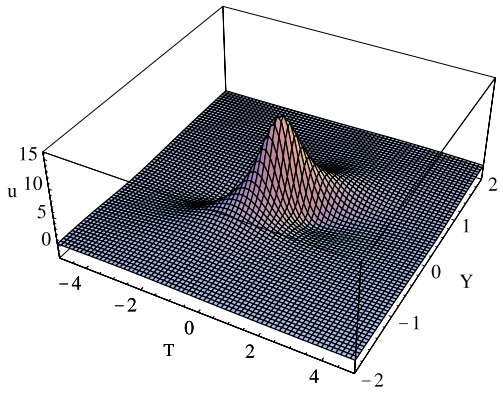

Fig. 30. (Color online) The typical lump solution of the KP I equation. The parameters are $A = -1$, $B = -1$, $V = 1$, $p_r = -1$, and $p_i = 2$. After Ref. [31].

where $\sigma = \mathrm{sgn}(A)$, by the change of variables

$$\zeta = Z, \qquad \tau = A^{1/3}T, \qquad \eta = |A|^{1/6}\sqrt{\frac{V}{2}}Y, \qquad E_2 = \frac{A^{1/3}}{B}u. \tag{8.4}$$

Typically, in the case of the two-level model, the dispersion coefficient A is a positive number, i.e., we are in the normal dispersion case. Hence $\sigma = +1$ and Eq. (8.3) is the so-called KP II equation. If Eq. (8.2) is generalized to other physical situations, we can assume an anomalous dispersion, i.e. $n'' < 0$ and $A < 0$. Then $\sigma = -1$, and Eq. (8.3) becomes the so-called KP I equation.

Both KP I and KP II are completely integrable by means of the inverse scattering transform method [86], however the mathematical properties of the solutions differ. The KP II equation admits stable nonlocalized *line solitons*, but not stable localized soliton solutions. The line soliton solution has the known analytical expression

$$E_2 = \frac{6p^2A}{B}\,\mathrm{sech}^2\left\{p\left[\tau + a\eta + \left(\frac{a^2V}{2} + 4p^2A\right)\zeta\right]\right\}, \tag{8.5}$$

where a and p are arbitrary constants and A, B are the coefficients given above. For the KP I equation, the above line soliton is not stable, but KP I admits stable *lumps* [209,210], which are two-dimensionally localized solutions, as

$$E_2 = \frac{12A}{B}\frac{\left[-\left(t' + p_r y'\right)^2 + p_i^2 y'^2 + 3/p_i^2\right]}{\left[(t' + p_r y')^2 + p_i^2 y'^2 + 3/p_i^2\right]^2}, \tag{8.6}$$

with $t' = \tau + \left(p_r^2 + p_i^2\right)A\zeta$ and $y' = \eta(-2A/V)^{1/2} - 2p_rA\zeta$, where p_r and p_i are arbitrary real constants. In Fig. 30 we plot the analytical lump solution, which was written above.

In what follows we give typical examples of numerical simulations of both KP I and KP II equations. The KP equation (8.3) is solved by means of the fourth order Runge–Kutta exponential time differencing (RK4ETD) scheme [115]. Let us first consider a normal dispersion ($n'' > 0$), for which Eq. (8.2) is a KP II equation. We start from an input in the form of a Gaussian plane wave packet

$$u = u_0 \exp\left[-\frac{(T - T_1)^2}{w_t^2}\right]\cos\left[\frac{2\pi}{\lambda}(T - T_1)\right] \tag{8.7}$$

where $T_1 = (-\lambda/2)\exp\left(-Y^2/w_y^2\right)$ accounts for a transverse initial perturbation. As a result of these numerical simulations we show in Fig. 31 that (a) the FCP input transforms into a half-cycle pulse (a line soliton solution of KP II equation), whose temporal profile is a sech-square shaped KdV soliton, plus the accompanying dispersing–diffracting waves, and that (b) the initial transverse perturbation vanishes and the line soliton becomes straight again during propagation.

If we now assume a quadratic nonlinear medium with anomalous dispersion ($n'' < 0$), the KP equation (8.2) reduces to Eq. (8.3) with $\sigma = -1$, i.e., a KP I equation. Now we consider initial data of the form

$$u = u_0 \exp\left(-\frac{T^2}{w_t^2} - \frac{Y^2}{w_y^2}\right)\cos\left(\frac{2\pi}{\lambda}T\right), \tag{8.8}$$

with arbitrary values of the initial amplitude u_0, width w_y, and duration w_t of the pulse. The evolution of the input FCP into a lump is shown in Fig. 32; we clearly see the accompanying dispersive waves, which remain captured in the computation box due to the periodic boundary conditions used in the T-direction. In the Y-direction, absorbing boundary conditions have been used, and consequently, the dispersive waves propagating transversely or obliquely vanish from the computation box as they move away from the lump.

Fig. 33 shows the decay of a perturbed unstable line soliton of KP I equation into lump solitons. The input is given by Eq. (8.7), with the transverse perturbation $T_1 = (-\lambda/2)\cos(2\pi Y/L)$, where the wavelength L of the transverse perturbation

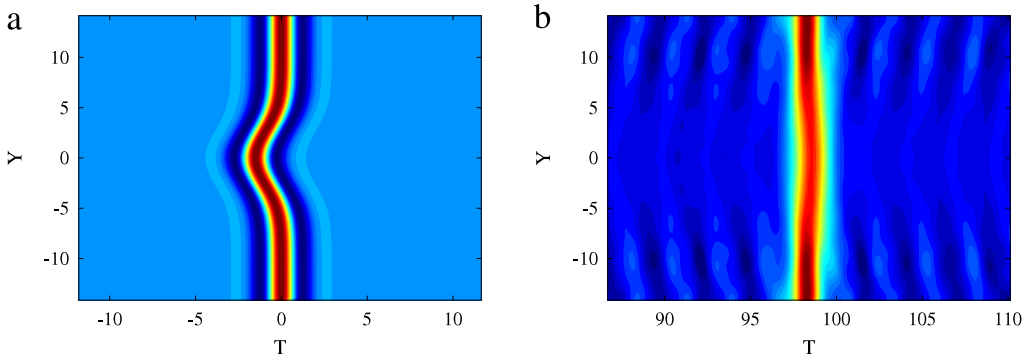

Fig. 31. (Color online) Shape and profile of the line soliton. (a) input, (b) after propagation ($Z = 14.95$). The parameters are $\lambda = 3$, $u_0 = 10.7$, $w_t = 1.4$, and $w_y = 3.87$. After Ref. [31].

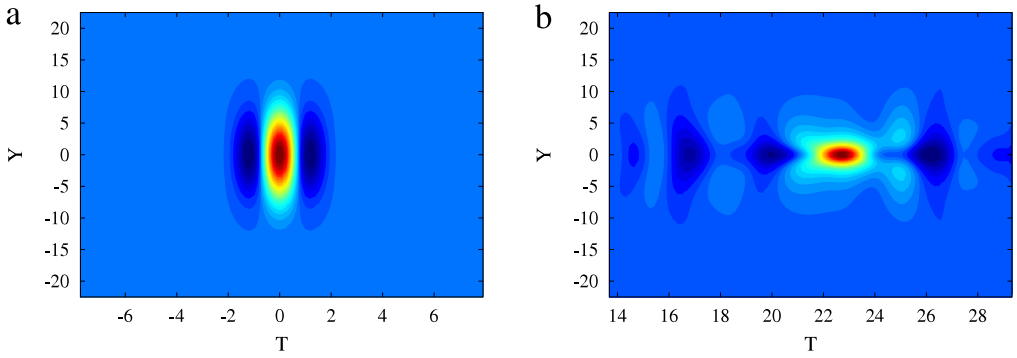

Fig. 32. (Color online) Shape and profile of the lump. (a) input, (b) after propagation ($Z = 14.95$). Parameters are $\lambda = 3$, $u_0 = 6.12$, $w_t = 1.2$, and $w_y = 6.36$. After Ref. [31].

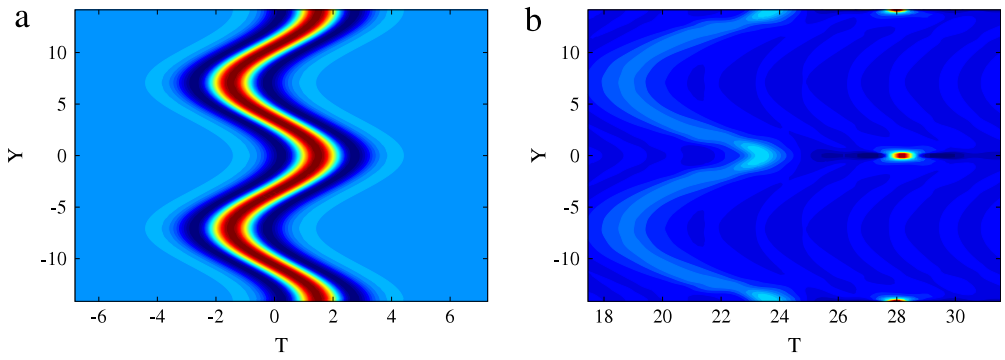

Fig. 33. (Color online) Generation of lumps from a perturbed unstable line soliton. (a) input, (b) after propagation $Z = 1.45$. Parameters are $\lambda = 3$, $u_0 = 10.7$, $w_t = 1.4$, and $L = 14.14$. After Ref. [31].

is chosen so that $2L = 28.3$ is the width of the numerical box, in accordance with the periodic boundary conditions used in the numerical computations; see Ref. [31] for more details. Note also that this transversely perturbed line soliton, in contrast with the case of KP II equation for normal dispersion shown in Fig. 31, does not recover its initial straight line shape and transverse coherence, but breaks up into localized lumps. We conclude this study by noting that ultrashort $(2 + 1)$-dimensional spatiotemporal quadratic solitons may form from an adequately chosen FCP input, their transverse focusing results from any transverse perturbation of the incident Gaussian plane-wave packet. Though we restricted this study to $(2 + 1)$ dimensions, however, due to the known properties of the Kadomtsev–Petviashvili equation in $(3 + 1)$ dimensions [211,212], analogous behavior is expected in three dimensions, i.e., stability of the spatial coherence of a plane wave few-cycle quadratic soliton for normal dispersion, and spontaneous formation of spatiotemporal few-cycle 'light bullets' in the case of anomalous dispersion.

8.2. Collapse of ultrashort spatiotemporal optical pulses

In this subsection, following Ref. [32] a cubic generalized Kadomtsev–Petviashvili (CGKP) equation for describing ultrashort spatiotemporal optical pulse propagation in cubic (Kerr-like) media, without the use of the slowly varying

envelope approximation, is derived by using a reductive perturbation method. The collapse threshold for the propagation of few-cycle spatiotemporal pulses is calculated by a direct numerical method, and compared to the analytic results based on a rigorous virial theorem. Note also that the evolution of the optical spectrum (integrated over the transverse spatial coordinate) evidenced a strongly asymmetric spectral broadening of ultrashort spatiotemporal pulses during collapse.

As in the preceding subsection we consider a set of two-level atoms and, since transparency of the medium implies that the characteristic frequency ω_w of the considered radiation (in the optical range) strongly differs from the resonance frequency Ω of the atoms, we assume that ω_w is much smaller than Ω, i.e., we work in the long-wave-approximation regime. We introduce the same kind of temporal and spatial slow variables as in the preceding subsection; see Eq. (8.1).

A weak amplitude assumption is needed in order that the nonlinear effects arise at the same propagation distance scale as the dispersion does, however, in the present case of cubic (Kerr) media the expansion of the electric field E as power series of a small parameter ε is different: $E = \varepsilon E_1 + \varepsilon^2 E_2 + \varepsilon^3 E_3 + \cdots$. Indeed, as it is well known within the SVEA, the quadratic nonlinear effects require much less intensity than cubic ones. That is why the amplitude required for the quadratic nonlinearity is of order ε^2, which is small with respect to the amplitude of order ε required in the present case of the cubic nonlinearity.

The above expansion is a standard one in mKdV-type series expansions [93]. Also, the polarization density P is expanded in the same way: $P = \varepsilon P_1 + \varepsilon^2 P_2 + \varepsilon^3 P_3 + \cdots$. The resolution of the perturbative scheme is very close to the $(1+1)$-dimensional case (see Ref. [73] and Section 3.1 above) in what concerns nonlinearity and dispersion, while the treatment of dispersion and the dependency with respect to the transverse (spatial) variable η is fully analogous to the case of quadratic nonlinear media; see Ref. [31] and the previous subsection. After a straightforward algebra, we are left with

$$\partial_\zeta \partial_\tau E_1 = A\partial_\tau^4 E_1 + B\partial_\tau^2 (E_1)^3 + \frac{V}{2}\partial_\eta^2 E_1, \tag{8.9}$$

which is a CGKP equation. Here the dispersion and nonlinear coefficients A and B in the above $(2+1)$-dimensional evolution equation are given by the same expressions as in the $(1+1)$-dimensional case, see Section 3.1 (Eq. (3.12)). The coefficient $V = c/n$ in Eq. (8.9) is the velocity, where the refractive index n has the same expression as in the $(1+1)$-dimensional case (Eq. (3.8)).

Rescaling the CGKP equation (8.9) we get its normalized form

$$\left(u_Z + \sigma_1 u^2 u_T + \sigma_2 u_{TTT}\right)_T = u_{YY}, \tag{8.10}$$

where $\sigma_1 = \mathrm{sgn}(-B)$ and $\sigma_2 = \mathrm{sgn}(-A)$.

Generally speaking, there are four different CGKP equations [Eq. (8.10)], depending on the signs σ_1 and σ_2. If the dispersion is anomalous ($n'' < 0, A < 0$ and $\sigma_2 = +1$), then depending on the sign of nonlinearity, (i.e. of B and σ_1), it is either focusing for both space and time, or defocusing for both space and time. The corresponding situation for quadratic nonlinearity is KP I, while, within the SVEA, it would be the elliptic NLS equation in two dimensions. For normal dispersion ($n'' > 0, A > 0$ and $\sigma_2 = -1$), the CGKP equation is focusing in space and defocusing in time or conversely; it corresponds to KP II for quadratic nonlinearity, and to a hyperbolic NLS equation in two dimensions within the SVEA.

In the framework of the Maxwell–Bloch equations, the dispersion is normal ($A > 0$) and $B > 0$ ($\sigma_1 = \sigma_2 = -1$), hence the nonlinearity and dispersion yield temporal self-compression, but nonlinearity and diffraction tend to defocus the FCP. In this case we observe the typical nonlinear diffraction; see Fig. 34. The CGKP equation (8.10) was solved by means of the fourth order Runge–Kutta exponential time differencing (RK4ETD) scheme [115] and the input field distribution was taken in the form:

$$u(T, Y, Z = 0) = A\ \exp(-T^2/p^2 - Y^2/q^2)\ \sin(\omega T). \tag{8.11}$$

The nonlinear effect strongly increases the diffraction: compare the panels (c) and (d) in Fig. 34. The conjugated effect of temporal self-compression and diffraction may lead to an intermediary stage, in which the pulse is very well localized temporally, and strongly widens spatially; see the characteristic crescent shape in panel (b) of Fig. 34. In this situation, the CGKP is a KP II with cubic nonlinearity, and consequently the existence of stable line soliton might be expected. Line solitons have been derived analytically [213], however their stability has not yet been studied. In fact, preliminary computations indicate that they might be unstable.

For normal dispersion, but the opposite sign for nonlinearity ($\sigma_1 = +1, \sigma_2 = -1$), focusing occurs spatially, but the pulse should be spread out in the time domain due to dispersion. This situation may be relevant for some experiments: although no stable state can be reached from an initial pulse localized in time and space, the dispersion is able to prevent the collapse (even in $(3+1)$ D), and it may result in a relative stabilization of the beam profile in space. However, we did not study this situation in detail. Note that the line solitons are not regular in this case [213].

In the case of anomalous dispersion and defocusing nonlinearity ($\sigma_1 = -1, \sigma_2 = +1$), both nonlinear diffraction and nonlinear dispersion occur. Any pulse will be spread out in all directions, which is of little interest, and we will not discuss this situation further.

More interesting is the situation where the medium presents anomalous dispersion and focusing nonlinearity ($A,\ B < 0$ and $\sigma_1 = \sigma_2 = +1$). In this case, spatiotemporal self-focusing occurs. Numerical simulations of the CGKP equation have been performed in Ref. [32] for the following set of parameters $\omega = -2.1909$, $p = 1.8257$, $q = 1.414$, and for several

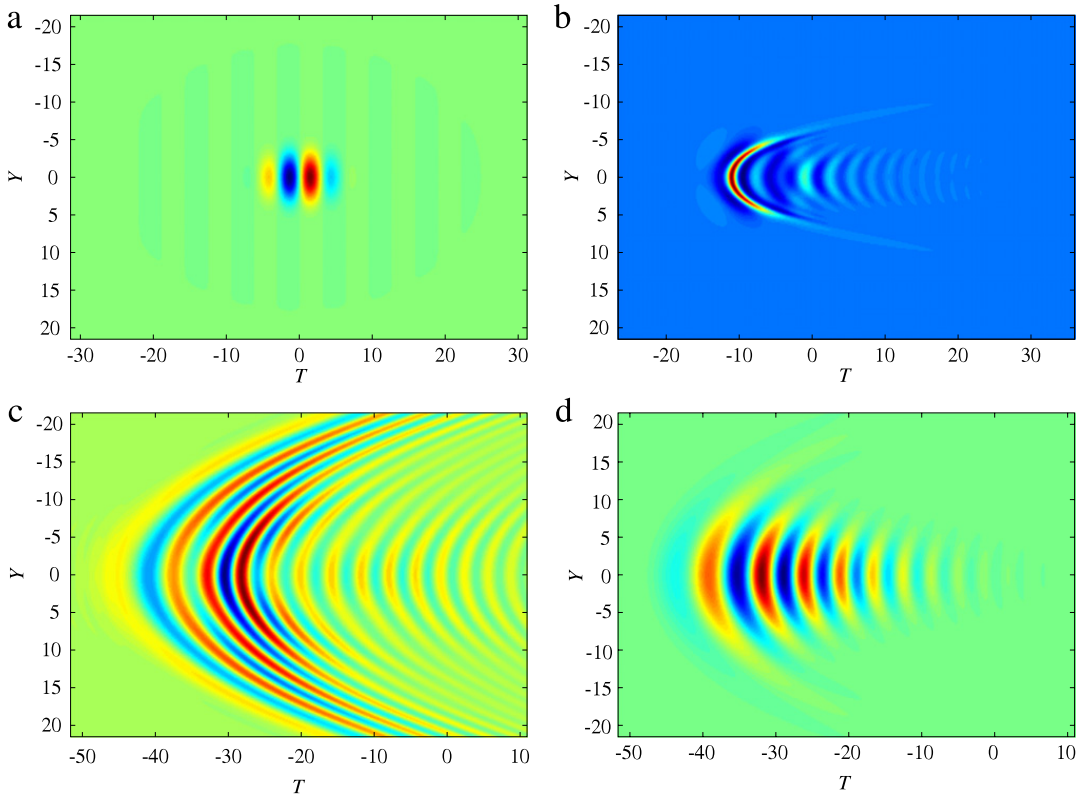

Fig. 34. (Color online) Nonlinear diffraction of a spatiotemporal FCP. (a) Initial ($Z = 0$), (b) an intermediary stage, with a typical crescent shape ($Z = 0.9594$), (c) nonlinear diffraction at $Z = 3.984$, (d) linear diffraction at the same propagation distance for the sake of comparison. The input field distribution is given by the expression (8.11) with $p = 4.0825$, $q = 2.8868$, $\omega = 1$, $A = 4.8990$ (a), (b), and (c), and $A = 10^{-7}$ (d). After Ref. [32].

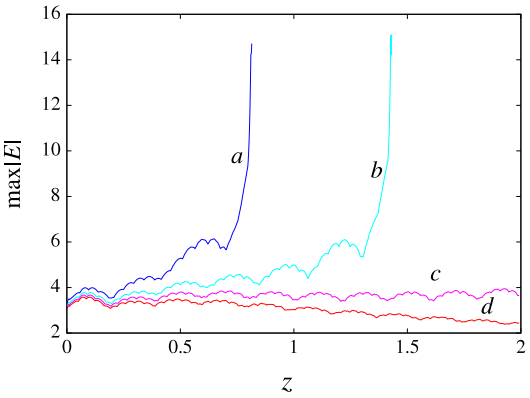

Fig. 35. (Color online) Evolution of the maximal value of the electric field for a few values of the initial amplitude. The collapse occurs above some amplitude threshold. Input data is expression (8.11) with $\omega = -2.1909$, $p = 1.8257$, $q = 1.414$, and several values of the amplitude A, namely $A = 3.80$ (a), 3.65 (b), 3.57 (c) 3.50 (d). After Ref. [32].

values of the initial field amplitude A; clear numerical evidence for collapse was found; see Fig. 35. Collapse occurs for the two highest values of the input spatiotemporal field amplitude A (curves a and b in Fig. 35), and not for the two lowest ones (curves c and d in Fig. 35). Hence the occurrence of some input amplitude threshold A_{th} is evidenced, and for the considered pulse shape, frequency, length and width, we get the numerical estimation $3.57 < A_{th} < 3.65$. This numerical value for the collapse threshold was compared in Ref. [32] with the corresponding value given by using a virial theorem. Thus a rigorous mathematical analysis of the CGKP equation (8.9) based on a virial theorem has proved that wave collapse do occurs (for a comprehensive review of wave collapse in optics and plasma waves, see Ref. [214]); also, for more details concerning CGKP equation, see Refs. [215–218].

It was possible to derive from the virial theorem some threshold value $\tilde{A}_{th}$ of the amplitude [32]. For the specific values of parameters used in that work, this value is $\tilde{A}_{th} = 7.567$. However, the threshold $A_{th} \simeq 3.6$ found by numerical methods is about half of the value $\tilde{A}_{th}$, found using the assumptions of the virial theorem. On the other hand, it was found in Ref. [32] that for initial amplitude below threshold A_{th}, the self-focusing stops after a while and the collapse is inhibited. This feature is due to the dispersion (both linear and nonlinear), which tends to increase the temporal length of the pulse at the same time as it

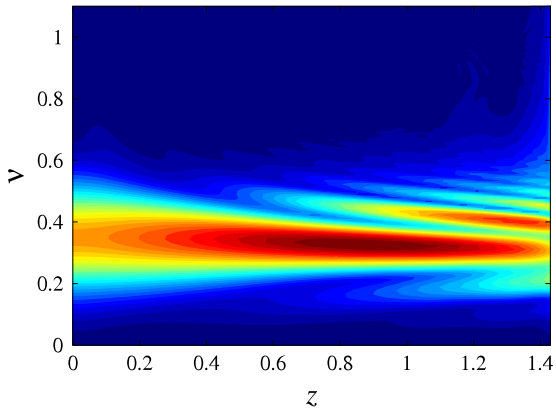

Fig. 36. (Color online) Evolution of the spectrum integrated over Y during collapse. The input data correspond to the case (b) in Fig. 35. After Ref. [32].

self-focuses. Note that below the threshold, the dispersion dominates and collapse is prevented, while above the threshold, self-focusing dominates and collapse occurs; it is worth mentioning that the arrest of collapse due to dispersion was actually found in a previous work; see Ref. [72]. The discrepancy between the analytic and numerical thresholds for collapse found in Ref. [32] may be justified qualitatively as follows: between the two values for threshold ($A_{th} \simeq 3.6 \lesssim A \lesssim 7.6 \simeq \tilde{A}_{th}$), at the beginning of the process, the amplitude is not properly speaking sufficient to initiate collapse but, due to the shape of the pulse, a nonlinear lens effect induces a transverse self-focusing of the pulse, which increases the maximal pulse amplitude. At the same time, both linear and nonlinear dispersion occur, which tend to decrease the amplitude. If dispersion dominates, the growth of the amplitude stops and collapse does not occur. If, on the contrary, self-focusing dominates, the peak amplitude reaches a value which is sufficient to induce the collapse as such. It is worth noting that in Fig. 35, the collapsing curves show two distinct parts, the first part, which is oscillating corresponds rather to self-focusing and the second part corresponds rather to collapse *stricto sensu*. The numerical value of the amplitude at the boundary between the two distinct domains is rather close to the threshold value for collapse ($\tilde{A}_{th} \simeq 7.6$) found from a rigorous mathematical condition; see Ref. [32] for more details of this issue.

Concluding this subsection we stress that we have introduced a model beyond the SVEA of the commonly used nonlinear Schrödinger-type evolution equations, for describing the propagation of $(2+1)$-dimensional spatiotemporal ultrashort optical solitons in Kerr (cubic) nonlinear media. Our approach was based on the Maxwell–Bloch equations for an ensemble of two level atoms and on the multiscale approach, and as a result of using the powerful reductive perturbation method [93], a generic cubic generalized Kadomtsev–Petviashvili partial differential evolution equation was introduced and was analyzed by both analytical and numerical technique. Moreover, the evolution of the spectrum (integrated over the transverse spatial coordinate) was also calculated and a strongly asymmetric spectral broadening of ultrashort pulses during collapse was also put forward [32], in contrast to the case of long spatiotemporal waveforms described within the SVEA.

8.3. Ultrashort light bullets in cubic nonlinear media: the short-wave approximation regime

In this subsection we consider the problem of existence and robustness of ultrashort light bullets described by the two-dimensional sine–Gordon equation. A reductive perturbation technique applied to a two-level model was used in Ref. [33] in order to get the corresponding nonlinear evolution equation. A generic two-dimensional sine–Gordon evolution equation governing the propagation of femtosecond spatiotemporal optical solitons in Kerr media beyond the SVEA was derived in Ref. [33] and direct numerical simulations have shown that, in contrast to the long-wave approximation, no collapse occurs. Robust $(2+1)$-dimensional ultrashort light bullets may form from adequately chosen few-cycle input spatiotemporal waveforms. One notices that in contrast to the case of quadratic nonlinearity, the light bullets oscillate in both space and time and are therefore not steady-state lumps.

One notices that there exist in the published literature several generalizations to $(2+1)$ dimensions of the generic sG equation. Such evolution equations can be derived in the short-wave approximation regime; some of them support localized solitons which are not oscillating as either the sG breathers or as the one-dimensional FCP solitons in Kerr media [219–222]. The question whether the $(2+1)$-dimensional generalization of sG equation, which is valid for FCP propagation in cubic nonlinear media, is one of the nonlinear dynamical systems discussed in Refs. [219–222] or some other one, can only be decided by means of a rigorous derivation starting from the basic equations. We will show below that we get a nonlinear system of equations which cannot be reduced to any of the equations obtained by using the same reductive perturbation method in the case of electromagnetic wave propagation in ferromagnetic media; see Refs. [219–222].

We consider the so-called short-wave approximation, by assuming that ω_w is much larger than Ω. In [33] the short wave approximation was presented through a rescaling of the time, based on the assumption that Ω is small, considering a small reductive perturbation parameter $\varepsilon \sim \Omega/\omega_w$. It is equivalent to state that the typical wave frequency ω_w is very large, and corresponds thus to a fast variable $\tau = (1/\varepsilon)(t - z/V)$, as in the standard short-wave approximation defined

in Refs. [93,175,176]. The delayed time τ involves propagation at some speed V to be determined. It is assumed to vary rapidly in time according to the assumption $\omega_w \gg \Omega$. This motivates the introduction of the new scaled variables $\zeta = z$ and $\eta = y/\sqrt{\varepsilon}$. The pulse shape described by the variable τ evolves more slowly in time, the corresponding scale being that of variable ζ. The transverse spatial variable y has an intermediate scale, comparable to what is usually considered in long-wave approximations [93]. In fact, the situation presented in Fig. 29 still holds as concerns the relative order of magnitude of the various characteristic lengths; only their relation with the reference length (which defines the order ε^0) is changed.

Thus we expand the electric field E, the polarization density P and the density matrix ρ as power series of a small parameter ε: $E = (1/\varepsilon)\left(E_0 + \varepsilon E_1 + \varepsilon^2 E_2 + \varepsilon^3 E_3 + \cdots\right)$, $P = (1/\varepsilon)\left(P_0 + \varepsilon P_1 + \varepsilon^2 P_2 + \varepsilon^3 P_3 + \cdots\right)$, and $\rho = \left(\rho_0 + \varepsilon\rho_1 + \varepsilon^2\rho_2 + \varepsilon^3\rho_3 + \cdots\right)$.

The large amplitude assumption plays the same role as the rescaling used in Ref. [33]; see Section 3.2 above. These expansions are then introduced into the Schrödinger–von Neumann and Maxwell equations, which are solved order by order. The computation follows the same steps as the $(1+1)$-dimensional case; see Ref. [73].

At order $1/\varepsilon$, the Schrödinger–von Neumann equation for the evolution of the density matrix reduces to $i\hbar\partial_\tau\rho_0 = -E_0[\mu, \rho_0]$. In what follows we label the components of any Hermitian matrix u as

$$u = \begin{pmatrix} u_a & u_t \\ u_t^* & u_b \end{pmatrix}. \tag{8.12}$$

We assume that the coherences ρ_{jt} are zero long before the pulse, i.e., as $z \to +\infty$ or $\tilde{t} \to -\infty$ we have $\lim_{\tau\to-\infty}\rho_{jt} = 0$ for any $j \geq 0$. Then one can express the coherence ρ_{0t} as

$$\rho_{0t} = \frac{i\mu}{\hbar}\int_{-\infty}^{\tau} E_0 w_0 d\tau', \tag{8.13}$$

where $w_0 = \rho_{0b} - \rho_{0a}$ is the population difference. We do not assume a pumping, hence $\lim_{\tau\to-\infty} w_0 = w_{th}$, where $-1 < w_{th} < 0$ is the population difference at thermodynamic equilibrium. If all atoms are initially in the fundamental state, then we have $w_{th} = -1$. Note that the higher order terms of the population difference ($w_j = \rho_{jb} - \rho_{ja}$ with $j \geq 1$) vanish at infinity. Using the above boundary conditions and definitions, we get from the Schrödinger–von Neumann equation at order $1/\varepsilon$ the evolution equation for w_0, as

$$\partial_\tau w_0 = \frac{-4|\mu|^2}{\hbar^2} E_0 \int_{-\infty}^{\tau} E_0 w_0 d\tau'. \tag{8.14}$$

Since the polarization density at this order is $P_0 = N(\rho_{0t}\mu^* + cc) = 0$, where cc denotes the complex conjugate, we see from the wave equation at leading order $1/\varepsilon^3$ that the velocity V should be $V = c$ up to this order. Next, the Schrödinger–von Neumann equation at order ε^0 gives

$$i\hbar\partial_\tau\rho_1 = \left[\tilde{H}_0, \rho_0\right] - E_0[\mu, \rho_1] - E_1[\mu, \rho_0],$$

and the off-diagonal terms of the above equation yield

$$\rho_{1t} = i\tilde{\Omega}\int_{-\infty}^{\tau}\rho_{0t}d\tau' + \frac{i\mu}{\hbar}\int_{-\infty}^{\tau}(E_0 w_1 + E_1 w_0)\, d\tau'. \tag{8.15}$$

It allows us to compute the leading term of the polarization density

$$P_1 = N\left(\rho_{1t}\mu^* + cc\right),$$

as

$$P_1 = \frac{-2N\tilde{\Omega}|\mu|^2}{\hbar}\int_{-\infty}^{\tau}\int_{-\infty}^{\tau'} E_0 w_0 d\tau'' d\tau'. \tag{8.16}$$

If we insert the polarization P_1 into the Maxwell wave equation at order $1/\varepsilon^2$ we finally get the evolution equation for the electric field E_0:

$$\left(\partial_\eta^2 - \frac{2}{\tilde{c}}\partial_\zeta\partial_\tau\right)E_0 = \frac{-8\pi N\tilde{\Omega}|\mu|^2}{\hbar\tilde{c}^2} E_0 w_0. \tag{8.17}$$

Eq. (8.17) together with Eq. (8.14) yield the sought nonlinear system of equations for the variables E_0 and w_0.

At this point we put the coupled nonlinear equations (8.14) and (8.17) in their normalized form as

$$\partial_Z\partial_T B = AB + \partial_Y^2 B, \tag{8.18}$$

$$\partial_T A = -BC, \tag{8.19}$$

$$\partial_T C = AB, \tag{8.20}$$

by setting $Y = y/l_r, Z = z/L_r, T = (t - z/c)/T_r, A = w_0/w_r, B = E_0/E_r$, with L_r a reference length in the micrometer range,

$$l_r = L_r/\sqrt{2}, \qquad T_r = L_r/c, \qquad w_r = (\hbar c^2)/(4\pi N\Omega|\mu|^2 L_r^2), \qquad E_r = (\hbar c)/(2|\mu|L_r).$$

The boundary conditions, are then $\lim_{T\to-\infty} C = 0$, and $\lim_{T\to-\infty} A = w_{th}/w_r$.

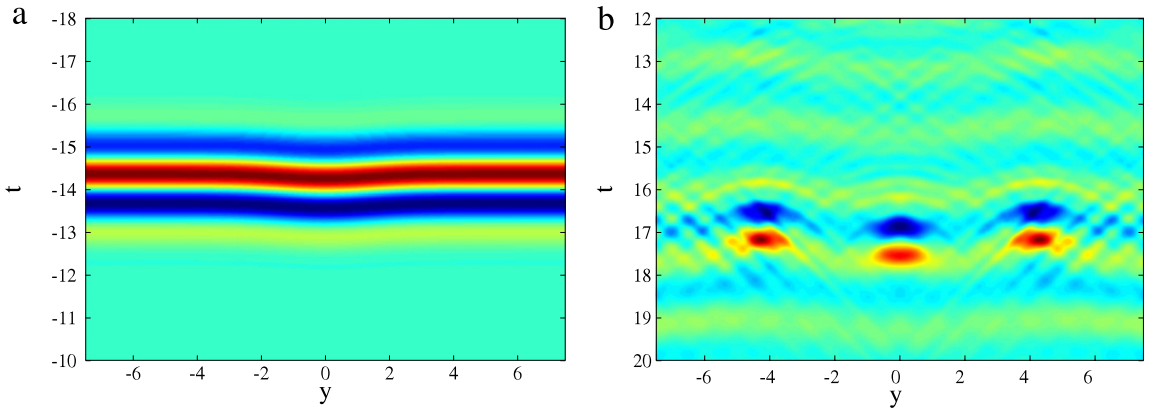

Fig. 37. (Color online) Evolution of a perturbed input FCP plane wave into two-dimensional FCP solitons. (a) Input ($Z = 0$), (b) output ($Z = 52.2$). After Ref. [33].

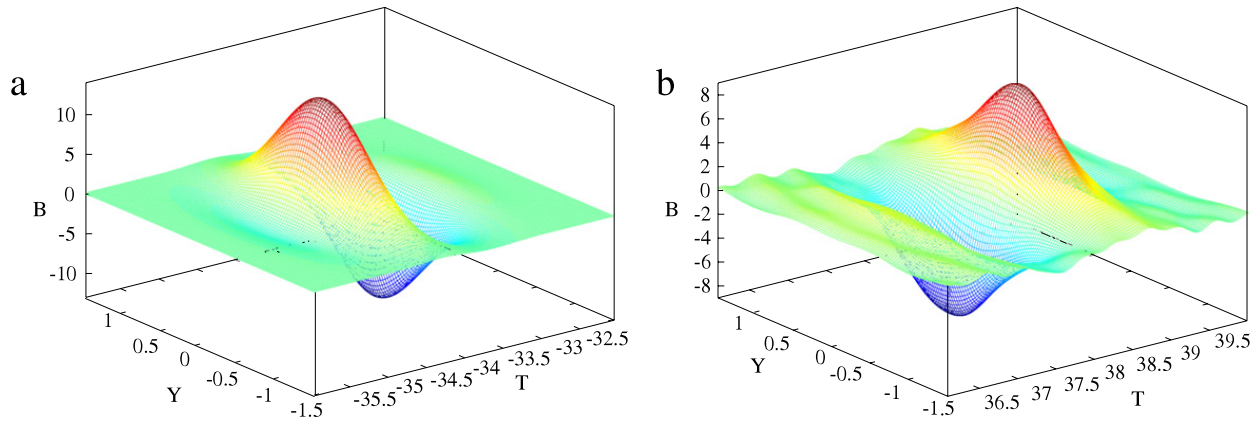

Fig. 38. (Color online) The evolution of a two-dimensional soliton, from an input roughly reproducing it. (a) Input ($Z = 0$), (b) output ($Z = 316.8$). After Ref. [33].

We note that the coupled system of partial differential equations (8.18)–(8.20) is a two-dimensional generalization of the sine–Gordon equation [33]. It is worthwhile to compare it to the set of equations derived by the same reductive perturbation method in the case of electromagnetic wave propagation in ferromagnetic media [219–222]; however a careful analysis shows that system (8.18)–(8.20) cannot be reduced to any of these equations.

Next it is seen from Eqs. (8.19)–(8.20) that $\partial_T \left(A^2 + C^2\right) = 0$. This allows us to introduce a function $\psi = \psi(Z, T)$ as $A = U \cos\psi$, $C = U \sin\psi$, where U depends on Z only. From the above written boundary conditions, we see that $\lim_{T\to-\infty} \psi = 0$ and thus $U = w_{th}/w_r$, and is independent of Z (except if inhomogeneous pumping is present, but this situation is excluded here as we have said above). By a straightforward manipulation of the above equations we get $\psi_T = B$ and after integration over T of Eq. (8.18), we are left with the evolution equation

$$\psi_{ZT} = U \sin\psi + \psi_{YY}, \tag{8.21}$$

which is known as the two-dimensional sG equation; see Ref. [33].

In Ref. [33] the two-dimensional sG equation was solved numerically starting from an input field distribution in the form of a FCP plane wave with temporal shape as

$$B = \beta \exp\left[-\frac{(T - T_1 - T_0)^2}{w_T^2}\right] \cos\left[\frac{2\pi}{\theta}(T - T_1) + \pi/2\right], \tag{8.22}$$

in which $T_1 = 0.1 \exp\left(-Y^2/w_Y^2\right)$ yields a transverse perturbation. The set of parameters was $w_T = 1$, $w_Y = 2$, $T_0 = -0.2$, $\theta = 1.5$, $\beta = 8$, and $U = -10$. The numerical calculations clearly show that we get the formation of robust localized two-dimensional sG solitons; see Fig. 37. Note that the two-dimensional sG solitons are oscillating structures, which are localized in both space and time. These two-dimensional FCP solitons were fitted by an expression of the form

$$B = \beta \exp\left[-(T^2/w_T^2) - (Y^2/w_Y^2)\right] \sin\left[\omega(T - T_1)\right],$$

in which the coefficients were chosen to fit the obtained numerical data. For the above numerical data, the following values were obtained in Ref. [33]: $w_T = 0.7$, $w_Y = 0.75$, $\omega = 3.5$, $\beta = -18$, and $T_1 = 0.04$. Then the fit was used as input; its evolution is shown in Fig. 38. We see that the input spatiotemporal waveform stably propagates, being neither affected

by dispersion nor by diffraction; after a transitory stage in which the pulse radiates energy, and its amplitude decreases, stabilization is reached eventually. Note that light bullets in the two-dimensional sG model have been also introduced in Ref. [223], and even interactions have been studied in Ref. [224]. In Ref. [223], the two-dimensional sG equation was also derived from the Maxwell–Bloch equations, but the derivation was performed from a reduced form of the Maxwell–Bloch equations, and the physical assumptions were not so clearly given. In Ref. [33] we clearly demonstrated that the short wave approximation of the Maxwell–Bloch equations is indeed the two-dimensional sG equation, and not one of the nonlinear system of equations found in the study of nonlinear electromagnetic waves in ferromagnets [219,221]. In Ref. [223] ultrashort light bullets were also simulated numerically, but on a rather short propagation distance; it was stated in that work that the light bullets loose energy and will become destroyed eventually. However, according to the computations reported in Ref. [32] on propagation distances twenty times larger than in Ref. [223], in which stabilization of the energy occurs, the energy loss seems rather to be due to the reshaping of the input pulse, and the light bullet is expected to be a remarkable robust physical object.

As we already mentioned in this review, soliton propagation in a nonlinear medium implies that damping can be neglected (we are not considering here the case of the so-called dissipative solitons where gain and loss effects also compensate each other in order to get a solitonic waveform in a dissipative medium). In dielectric media, the damping effects can be neglected when the propagation occurs at a given frequency which is far from any resonance frequency. Let us consider a two-level model with characteristic frequency Ω, and denote by ω_w a frequency characteristic for the FCP soliton under consideration. The transparency condition implies that either $\omega_w \ll \Omega$ or $\Omega \ll \omega_w$. The former case ($\omega_w \ll \Omega$) corresponds to the *long wave approximation*, whereas the latter case corresponds to the *short wave approximation*. We have shown in Section 3.1 that in the framework of a two-level model, a mKdV equation is obtained if the frequency of the transition Ω is far above the characteristic wave frequency ω_w (the long-wave approximation regime), while a sG model is valid if Ω is much smaller than ω_w (the short-wave approximation regime); see Section 3.2. However, some of the transition frequencies Ω_j are much smaller than ω_w, and the other ones much larger than ω_w. This more realistic situation can be modeled by considering two transitions only, with different frequencies Ω_1 and Ω_2. The physical system is thus equivalent to a two-component medium, each of the two components being described by a two-level model. As a result, a mKdV–sG model was put forward [68,76], which is completely integrable in certain particular cases by means of the inverse scattering transform. It admits stable solutions of 'breather' type, which also give a good description of few-optical-cycle soliton propagation.

The propagation of FCPs in a quadratic medium has also been described by either a KdV or a KP equation, in $(1+1)$ or $(2+1)$ dimensions, respectively, which evidenced either the stability of a plane wavefront, for a normal dispersion, or the formation of a localized spatiotemporal half-cycle soliton, for an anomalous dispersion [120,31]. By using a multiscale analysis, a generic KP evolution equation governing the propagation of femtosecond spatiotemporal optical solitons in quadratic nonlinear media beyond the SVEA was put forward [31]. Direct numerical simulations showed the formation, from adequately chosen few-cycle input pulses, of both stable line solitons (in the case of a quadratic medium with normal dispersion) and of stable lumps (for a quadratic medium with anomalous dispersion). The perturbed unstable line solitons decay into stable lumps for a quadratic nonlinear medium with anomalous dispersion [31]. However, in Ref. [31] it was considered a set of two-level atoms and it was assumed that the characteristic frequency ω_w of the considered electromagnetic wave in the optical spectral range is much less than the transition frequency Ω of the atoms (long-wave approximation regime). Thus in the *long wave approximation regime*, in a medium with a quadratic nonlinearity, half-cycle light bullets in the form of single lumps may exist, while in a medium with a cubic nonlinearity collapse occurs. However, in the *short wave approximation regime* and considering the wave propagation in a nonlinear medium with a cubic nonlinearity, a third physical situation occurs: $(2+1)$-dimensional *few-cycle light bullets* may form, oscillating in both space and time. Such ultrashort spatiotemporal optical solitons are adequately described by a $(2+1)$-dimensional sine–Gordon equation.

Concluding this subsection, we point out that this study can be generalized by taking into account both resonant and non-resonant optical nonlinearities. Moreover, the generalization to two transverse spatial dimensions, in addition to time and longitudinal coordinates, in order to study the formation of $(3+1)$-dimensional few-optical-cycle spatiotemporal solitons (alias light bullets) can also be envisaged; see Refs. [130,225] and some recent theoretical and experimental works in the area of $(3+1)$-dimensional solitons in different physical settings [226–243].

9. Conclusions

The above theory is relevant for all phenomena involving ultra-short pulses or very broad spectrum, for which the SVEA fails to be valid. An important phenomenon in this class is *supercontinuum generation*. Preliminary studies have shown that the mKdV–sG model is adapted to the description of supercontinuum generation, especially in the later stage of the process, when the width of the supercontinuum spectrum exceeds the initial central frequency. It is also suited to the description of supercontinuum generation from femtosecond pulses, which have a broad spectrum from the beginning of the process. Especially, it allows to take into account the generation of high harmonics, and their own spectral broadening, which seems to have an important effect, which cannot be accounted for within the SVEA.

Refinements of the theory to make it closer to realistic experimental situations is important. The derivation of the mKdV model in a general medium has recently been performed [112], the same study for a quadratic nonlinearity was also reported [112]. Within the long-wave approximation, the effects of the various transitions combine themselves so that

the general model keeps the same form, the coefficients merely involve the general linear and nonlinear susceptibilities. Regarding the infrared transitions, or more generally the transitions with frequencies below the wave one, the relevant approach is the short wave approximation. The question, how the various transitions will combine in the general case is still open.

The theory of few-cycle dissipative solitons is still at its very beginning, and requires to be developed. In particular, the experimental setups frequently use the Kerr-lens mode-locking. This phenomenon is clearly a multidimensional one, and it is unlikely that it can be accounted for by a phenomenological modification of the one-dimensional evolution equation, even in first approximation. The study of the evolution of multidimensional few-cycle pulses in a gain medium seems to be required for such a study.

Given the rapid growth of studies in the past decade in the area of few-optical-cycle pulses, extreme nonlinear optics and interaction of matter with strong optical fields, one can expect many new and exciting developments over the next years. No doubt, soon one can expect a maturity of these fast growing research fields, leading to new and interesting physical phenomena and to the utilization of their huge technological potential. We conclude with the hope that this overview on recent developments in the area of few-optical-cycle solitons will inspire further theoretical and experimental investigations.

Acknowledgments

The authors acknowledge collaborative work with colleagues Igor V. Mel'nikov, François Sanchez and Houria Triki. The work of D.M. was supported in part by a Senior Chair Grant from the Région Pays de Loire, France, and by Romanian Ministry of Education and Research, CNCS-UEFISCDI, project number PN-II-ID-PCE-2011-3-0083.

D.M. aknowledges useful discussions with Gaetano Assanto, Jerzy Jasiński, Bozena Jaskorzyńska, Mirosław Karpierz, Fedor Mitschke, Roberto Morandotti, Ulf Peschel, Ewa Weinert-Raczka, and George Stegeman during the XI International Workshop "Nonlinear Optics Applications-NOA 2011" (Toruń, Poland, September 14–17, 2011).

References

[1] L. Gallmann, D.H. Sutter, N. Matuschek, G. Steinmeyer, U. Keller, C. Iaconis, I.A. Walmsley, Characterization of sub-6-fs optical pulses with spectral phase interferometry for direct electric-field reconstruction, Opt. Lett. 24 (1999) 1314.
[2] U. Morgner, F.X. Kärtner, S.H. Cho, Y. Chen, H.A. Haus, J.G. Fujimoto, E.P. Ippen, V. Scheuer, G. Angelow, T. Tschudi, Sub-two-cycle pulses from a Kerr-lens mode-locked Ti: sapphire laser, Opt. Lett. 24 (1999) 411.
[3] D.H. Sutter, G. Steinmeyer, L. Gallmann, N. Matuschek, F. Morier-Genoud, U. Keller, V. Scheuer, G. Angelow, T. Tschudi, Semiconductor saturable-absorber mirror-assisted Kerr-lens mode-locked Ti: sapphire laser producing pulses in the two-cycle regime, Opt. Lett. 24 (1999) 631.
[4] A. Shirakawa, I. Sakane, M. Takasaka, T. Kobayashi, Sub-5-fs visible pulse generation by pulse-front-matched noncollinear optical parametric amplification, Appl. Phys. Lett. 74 (1999) 2268.
[5] M. Wegener, Extreme Nonlinear Optics, Springer, Berlin, 2005.
[6] E. Goulielmakis, M. Schultze, M. Hofstetter, V.S. Yakovlev, J. Gagnon, M. Uiberacker, A.L. Aquila, E.M. Gullikson, D.T. Attwood, R. Kienberger, F. Krausz, U. Kleineberg, Single-cycle nonlinear optics, Science 320 (2008) 1614.
[7] A. Scrinzi, M.Yu. Ivanov, R. Kienberger, D.M. Villeneuve, Attosecond physics, J. Phys. B 39 (2006) R1.
[8] F. Krausz, M. Ivanov, Attosecond physics, Rev. Modern Phys. 81 (2009) 163.
[9] T. Brabek, F. Krausz, Intense few-cycle laser fields: frontiers of nonlinear optics, Rev. Modern Phys. 72 (2000) 545.
[10] G.A. Mourou, T. Tajima, S.V. Bulanov, Optics in the relativistic regime, Rev. Modern Phys. 78 (2006) 309.
[11] G.A. Mourou, T. Tajima, More intense, shorter pulses, Science 331 (2011) 41.
[12] D. Strickland, G. Mourou, Compression of amplified chirped optical pulses, Opt. Commun. 56 (1985) 219.
[13] A. Dubietis, G. Jonusauskas, A. Piskarskas, Powerful femtosecond pulse generation by chirped and stretched pulse parametric amplification in BBO crystal, Opt. Commun. 88 (1992) 437.
[14] V.M. Malkin, G. Shvets, N.J. Fisch, Fast compression of laser beams to highly overcritical powers, Phys. Rev. Lett. 82 (1999) 4448.
[15] G.A. Mourou, N.J. Fisch, V.M. Malkin, Z. Toroker, E.A. Khazanov, A.M. Sergeev, T. Tajima, Exawatt–Zettawat pulse generation and applications, Opt. Commun. 285 (2012) 720.
[16] J.K. Ranka, R.S. Windeler, A.J. Stentz, Visible continuum generation in air-silica microstructure optical fibers with anomalous dispersion at 800 nm, Opt. Lett. 25 (2000) 25.
[17] T.A. Birks, W.J. Wadsworth, P.St.J. Russel, Supercontinuum generation in tapered fibers, Opt. Lett. 25 (2000) 1415.
[18] A.V. Husakou, J. Herrmann, Supercontinuum generation of higher-order solitons by fission in photonic crystal fibers, Phys. Rev. Lett. 87 (2001) 203901.
[19] J.M. Dudley, G. Genty, S. Coen, Supercontinuum generation in photonic crystal fiber, Rev. Modern Phys. 78 (2006) 1135.
[20] D.V. Skryabin, A.V. Gorbach, Colloquium: looking at a soliton through the prism of optical supercontinuum, Rev. Modern Phys. 82 (2010) 1287.
[21] G. Krauss, S. Lohss, T. Hanke, A. Sell, S. Eggert, R. Huber, A. Leitenstorfer, Synthesis of a single cycle of light with compact erbium-doped fibre technology, Nat. Photonics 4 (2010) 33.
[22] G. Cerullo, A. Baltuska, O.D. Mücke, C. Vozzi, Few-optical-cycle light pulses with passive carrier-envelope phase stabilization, Laser and Photonics Revi 5 (2011) 323.
[23] Shu-Wei Huang, G. Cirmi, J. Moses, Kyung-Han Hong, S. Bhardwaj, J.R. Birge, Li-Jin Chen, Enbang Li, B.J. Eggleton, G. Cerullo, F.X. Kärtner, High-energy pulse synthesis with sub-cycle waveform control for strong-field physics, Nat. Photon. 5 (2011) 475.
[24] M. Bache, O. Bang, B.B. Zhou, J. Moses, F.W. Wise, Optical Cherenkov radiation by cascaded nonlinear interaction: an efficient source of few-cycle energetic near- to mid-IR pulses, Opt. Express 19 (2011) 22557.
[25] J.-P. Likforman, M. Mehendale, D.M. Villeneuve, M. Joffre, P.B. Corkum, Conversion of high-power 15-fs visible pulses to the mid infrared, Opt. Lett. 26 (2001) 99.
[26] D. Brida, M. Marangoni, C. Manzoni, S.D. Silvestri, G. Cerullo, Two-optical-cycle pulses in the mid-infrared from an optical parametric amplifier, Opt. Lett. 33 (2008) 2901.
[27] B.B. Zhou, A. Chong, F.W. Wise, M. Bache, Ultrafast and octave spanning optical nonlinearities from strongly phase-mismatched quadratic interactions, Phys. Rev. Lett. 109 (2012) 043902.

[28] Chuang Li, Ding Wang, Liwei Song, Jun Liu, Peng Liu, Canhua Xu, Yuxin Leng, Ruxin Li, Zhizhan Xu, Generation of carrier-envelope phase stabilized intense 1.5 cycle pulses at 1.75 μm, Opt. Express 19 (2011) 6783.
[29] M. Schultze, T. Binhammer, G. Palmer, M. Emons, T. Lang, U. Morgner, Multi-μJ, CEP-stabilized, two-cycle pulses from an OPCPA system with up to 500 kHz repetition rate, Opt. Express 18 (2010) 27291.
[30] L. Bergé, S. Skupin, Few-cycle light bullets created by femtosecond filaments, Phys. Rev. Lett. 100 (2008) 113902.
[31] H. Leblond, D. Kremer, D. Mihalache, Ultrashort spatiotemporal optical solitons in quadratic nonlinear media: generation of line and lump solitons from few-cycle input pulses, Phys. Rev. A 80 (2009) 053812.
[32] H. Leblond, D. Kremer, D. Mihalache, Collapse of ultrashort spatiotemporal pulses described by the cubic generalized Kadomtsev–Petviashvili equation, Phys. Rev. A 81 (2010) 033824.
[33] H. Leblond, D. Mihalache, Ultrashort light bullets described by the two-dimensional sine–Gordon equation, Phys. Rev. A 81 (2010) 063815.
[34] Xiao-Tao Xie, M.A. Macovei, Single-cycle gap soliton in a subwavelength structure, Phys. Rev. Lett. 104 (2010) 073902.
[35] P. Dombi, S.E. Irvine, P. Rácz, M. Lenner, N. Kroó, G. Farkas, A. Mitrofanov, A. Baltuška, T. Fuji, F. Krausz, A.Y. Elezzabi, Observation of few-cycle, strong-field phenomena in surface plasmon fields, Opt. Express 18 (2010) 24206.
[36] N.N. Rosanov, V.V. Kozlov, S. Wabnitz, Maxwell–Drude–Bloch dissipative few-cycle optical solitons, Phys. Rev. A 81 (2010) 043815.
[37] V.V. Kozlov, N.N. Rosanov, S. Wabnitz, Obtaining single-cycle pulses from a mode-locked laser, Phys. Rev. A 84 (2011) 053810.
[38] H. Leblond, D. Mihalache, Few-optical-cycle dissipative solitons, J. Phys. A: Math. Theor. 43 (2010) 375205.
[39] E.D. Farnum, J. Nathan Kutz, Master mode-locking theory for few-femtosecond pulses, Opt. Lett. 35 (2010) 3033.
[40] A.V. Kim, S.A. Skobolev, Few-cycle vector solitons of light, Phys. Rev. A 83 (2011) 063832.
[41] Q. Lin, J. Zheng, J. Dai, I-Chen Ho, X.-C. Zhang, Intrinsic chirp of single-cycle pulses, Phys. Rev. A 81 (2010) 043821.
[42] X. Song, W. Yang, Z. Zeng, R. Li, Z. Xu, Unipolar half-cycle pulse generation in asymmetrical media with a periodic subwavelength structure, Phys. Rev. A 82 (2010) 053821.
[43] A.M. Heidt, J. Rothhardt, A. Hartung, H. Bartelt, E.G. Rohwer, J. Limpert, A. Tünnermann, High quality sub-two cycle pulses from compression of supercontinuum generated in all-normal dispersion photonic crystal fiber, Opt. Express 19 (2011) 13873.
[44] B. Piglosiewicz, D. Sadiq, M. Mascheck, S. Schmidt, M. Silies, P. Vasa, C. Lienau, Ultrasmall bullets of light focusing few-cycle light pulses to the diffraction limit, Opt. Express 19 (2011) 14451.
[45] V.V. Kozlov, N.N. Rosanov, C. De Angelis, S. Wabnitz, Generation of unipolar pulses from nonunipolar optical pulses in a nonlinear medium, Phys. Rev. A 84 (2011) 023818.
[46] A. Pusch, J.M. Hamm, O. Hess, Femtosecond nanometer-sized optical solitons, Phys. Rev. A 84 (2011) 023827.
[47] Peng-Cheng Li, I-Lin Liu, Shih-I Chu, Opt. Express 19 (2011) 23857.
[48] X. Tan, X. Fan, Y. Yang, D. Tong, Time evolution of few-cycle pulse in a dense V-type three-level medium, J. Modern Opt. 55 (2008) 2439.
[49] N.N. Rosanov, V.E. Semenov, N.V. Vyssotina, Collisions of few-cycle dissipative solitons in active nonlinear fibers, Laser Phys. 17 (2007) 1311.
[50] N.N. Rosanov, V.E. Semenov, N.V. Vysotina, Few-cycle dissipative solitons in active nonlinear optical fibres, Quantum Electron. 38 (2008) 137.
[51] A. Nazarkin, Nonlinear optics of intense attosecond light pulses, Phys. Rev. Lett. 97 (2006) 163904.
[52] A.I. Maimistov, Solitons in nonlinear optics, Quantum Electron. 40 (2010) 756.
[53] T. Brabec, F. Krausz, Nonlinear optical pulse propagation in the single-cycle regime, Phys. Rev. Lett. 78 (1997) 3282.
[54] M.V. Tognetti, H.M. Crespo, Sub-two-cycle soliton-effect pulse compression at 800 nm in photonic crystal fibers, J. Opt. Soc. Am. B 24 (2007) 1410.
[55] A.A. Voronin, A.M. Zheltikov, Soliton-number analysis of soliton-effect pulse compression to single-cycle pulse widths, Phys. Rev. A 78 (2008) 063834.
[56] A. Kumar, V. Mishra, Single-cycle pulse propagation in a cubic medium with delayed Raman response, Phys. Rev. A 79 (2009) 063807.
[57] P. Kinsler, G.H.C. New, Few-cycle pulse propagation, Phys. Rev. A 67 (2003) 023813.
[58] P. Kinsler, G.H.C. New, Few-cycle soliton propagation, Phys. Rev. A 69 (2004) 013805.
[59] A.A. Zozulya, S.A. Diddams, T.S. Clement, Investigations of nonlinear femtosecond pulse propagation with the inclusion of Raman, shock, and third-order phase effects, Phys. Rev. A 58 (1998) 3303.
[60] A.A. Zozulya, S.A. Diddams, A.G. Van Engen, T.S. Clement, Propagation dynamics of intense femtosecond pulses: multiple splittings, coalescence, and continuum generation, Phys. Rev. Lett. 82 (1999) 1430.
[61] N. Akozbek, M. Scalora, C.M. Bowden, S.L. Chin, White-light continuum generation and filamentation during the propagation of ultra-short laser pulses in air, Opt. Commun. 191 (2001) 353.
[62] J.E. Rothenberg, Space–time focusing-breakdown of the slowly varying envelope approximation in the self-focusing of femtosecond pulses, Opt. Lett. 17 (1992) 1340.
[63] J.K. Ranka, A.L. Gaeta, Breakdown of the slowly varying envelope approximation in the self-focusing of ultrashort pulses, Opt. Lett. 23 (1998) 534.
[64] E.M. Belenov, A.V. Nazarkin, Solutions of nonlinear-optics equations found outside the approximation of slowly varying amplitudes and phases, JETP Lett. 51 (1990) 288.
[65] A.I. Maimistov, S.O. Elytin, Ultrashort optical pulse propagation in nonlinear non-resonance medium, J. Modern Opt. 39 (1992) 2201.
[66] A.E. Kaplan, P.L. Shkolnikov, Electromagnetic bubbles and shock waves: unipolar, nonoscillating EM solitons, Phys. Rev. Lett. 75 (1995) 2316.
[67] M.A. Porras, Propagation of single-cycle pulsed light beams in dispersive media, Phys. Rev. A 60 (1999) 5069.
[68] S.V. Sazonov, Extremely short and quasi-monochromatic electromagnetic solitons in a two-component medium, JETP 92 (2001) 361.
[69] A.I. Maimistov, Propagation of ultrasort light pulses in a nonlinear medium, Optics Spectr. 76 (1994) 569 [Optika i Spektroskopiya 76 (1994) 636].
[70] I.V. Mel'nikov, D. Mihalache, F. Moldoveanu, N.-C. Panoiu, Quasiadiabatic following of femtosecond optical pulses in a weakly excited semiconductor, Phys. Rev. A 56 (1997) 1569.
[71] I.V. Mel'nikov, D. Mihalache, F. Moldoveanu, N.-C. Panoiu, Non-envelope formulation for femtosecond optical pulses in semiconductors, JETP Lett. 65 (1997) 393.
[72] I.V. Mel'nikov, D. Mihalache, N.-C. Panoiu, Localized multidimensional femtosecond optical pulses in an off-resonance two-level medium, Opt. Commun. 181 (2000) 345.
[73] H. Leblond, F. Sanchez, Models for optical solitons in the two-cycle regime, Phys. Rev. A 67 (2003) 013804.
[74] I.V. Mel'nikov, H. Leblond, F. Sanchez, D. Mihalache, Nonlinear optics of a few-cycle optical pulse: slow-envelope approximation revisited, IEEE J. Sel. Top. Quantum Electron. 10 (2004) 870.
[75] H. Leblond, F. Sanchez, I.V. Mel'nikov, D. Mihalache, Optical solitons in a few-cycle regime: breakdown of slow-envelope approximation, Math. Comput. Simul. 69 (2005) 378.
[76] H. Leblond, S.V. Sazonov, I.V. Mel'nikov, D. Mihalache, F. Sanchez, Few-cycle nonlinear optics of multicomponent media, Phys. Rev. A 74 (2006) 063815.
[77] H. Leblond, I.V. Mel'nikov, D. Mihalache, Interaction of few-optical-cycle solitons, Phys. Rev. A 78 (2008) 043802.
[78] H. Leblond, D. Mihalache, Few-optical-cycle solitons: modified Korteweg–de Vries–sine Gordon equation versus other non-slowly varying envelope approximation models, Phys. Rev. A 79 (2009) 063835.
[79] H. Leblond, D. Mihalache, Models for few-cycle optical solitons, J. Optoelectronics Adv. Materials 12 (2010) 1.
[80] H. Leblond, D. Mihalache, Optical solitons in the few-cycle regime: recent theoretical models, Rom. Rep. Phys. 63 (2011) 1254.
[81] S.A. Skobelev, D.V. Kartashov, A.V. Kim, Few-optical-cycle solitons and pulse self-compression in a Kerr medium, Phys. Rev. Lett. 99 (2007) 203902.
[82] Sh. Amiranashvili, A.G. Vladimirov, U. Bandelow, Solitary-wave solutions for few-cycle optical pulses, Phys. Rev. A 77 (2008) 063821.
[83] A.I. Maĭmistov, J.-G. Caputo, Extremely short electromagnetic pulses in a resonant medium with a permanent dipole moment, Optics Spectr. 94 (2003) 245–250 [Optika i Spektroskopiya 94 (2003) 275–280].
[84] E.V. Kazantseva, A.I. Maimistov, J.-G. Caputo, Reduced Maxwell–Duffing description of extremely short pulses in nonresonant media, Phys. Rev. E 71 (2005) 056622.

[85] R.K. Dodd, J.C. Eilbeck, J.D. Gibbon, H.C. Morris, Solitons and Nonlinear Wave Equations, Academic Press, London, 1982.
[86] M.J. Ablowitz, H. Segur, Solitons and the Inverse Scattering Transform, SIAM, Philadelphia, 1981.
[87] K. Konno, W. Kameyama, H. Sanuki, Effect of weak dislocation potential on nonlinear wave propagation in anharmonic crystal, J. Phys. Soc. Japan 37 (1974) 171.
[88] A.M. Kosevich, A.S. Kovalev, The supersonic motion of a crowdion. The one-dimensional model with nonlinear interaction between the nearest neighbours, Solid State Commun. 12 (1973) 763.
[89] G. Genty, P. Kinsler, B. Kibler, J.M. Dudley, Nonlinear envelope equation modeling of sub-cycle dynamics and harmonic generation in nonlinear waveguides, Opt. Expr. 15 (2007) 5382.
[90] M. Kolesik, J.V. Moloney, M. Mlejnek, Unidirectional optical pulse propagation equation, Phys. Rev. Lett. 89 (2002) 283902.
[91] M. Kolesik, J.V. Moloney, Nonlinear optical pulse propagation simulation: from Maxwell's to unidirectional equations, Phys. Rev. E 70 (2004) 036604.
[92] N.N. Akhmediev, I.V. Mel'nikov, A.V. Nazarkin, Propagation of the femtosecond optical pulse in the transparent region of a nonlinear medium, Sov. Phys. Lebedev. Inst. Rep. 2 (1989) 66 [Kratk. Soobshch. Fiz. FIAN 2 (1989) 49].
[93] H. Leblond, The reductive perturbation method and some of its applications, J. Phys. B: At. Mol. Opt. Phys. 41 (2008) 043001.
[94] H. Washimi, T. Taniuti, Propagation of ion acoustic solitary waves of small amplitude, Phys. Rev. Lett. 17 (1966) 996.
[95] T. Taniuti, C.-C. Wei, Reductive perturbation method in nonlinear wave propagation I, J. Phys. Soc. Japan 24 (1968) 941.
[96] C.H. Su, C.S. Gardner, Korteweg-of Vries equation and generalizations. III. Derivation of the Korteweg-of Vries equation and Burgers equation, J. Math. Phys. 10 (1969) 536–539.
[97] T. Taniuti, N. Yajima, Perturbation method for a nonlinear wave modulation I, J. Math. Phys. 10 (1969) 1369.
[98] T. Taniuti, N. Yajima, Perturbation method for a nonlinear wave modulation III, J. Math. Phys. 14 (1973) 1389.
[99] L.F. Mollenauer, R.H. Stolen, J.P. Gordon, Experimental observation of picosecond pulse narrowing and solitons in optical fibers, Phys. Rev. Lett. 45 (1980) 1095.
[100] J. Boussinesq, Théorie des ondes et des remous qui se propagent le long d'un canal rectangulaire horizontal, en communiquant au liquide contenu dans ce canal des vitesses sensiblement pareilles de la surface au fond, J. Math. Pures Appl. Sér. II 17 (1872) 55.
[101] H. Leblond, M. Manna, Coalescence of electromagnetic travelling waves in a saturated ferrite, J. Phys. A: Math. Gen. 26 (1993) 6451.
[102] H. Leblond, Interaction of two solitary waves in a ferromagnet, J. Phys. A: Math. Gen. 28 (1995) 3763.
[103] H. Leblond, Direct derivation of a macroscopic NLS equation from the quantum theory, J. Phys. A: Math. Gen. 34 (2001) 3109.
[104] R.W. Boyd, Nonlinear Optics, Third Edition, Academic Press, Amsterdam, 2008.
[105] G.I. Stegeman, R.A. Stegeman, Nonlinear Optics: Phenomena, Materials and Devices, Wiley, New York, 2012.
[106] A. Davey, K. Stewartson, On three-dimensional packets of surface waves, Proc. R. Soc. Lond. Ser. A 338 (1974) 101.
[107] S.M. Kurcbart, M.A. Manna, J.G. Pereira, A.N. Garazo, Shallow viscous fluid heated from below and the Kadomtsev–Petviashvili equation, Phys. Lett. A 148 (1990) 53.
[108] I. Nakata, Nonlinear electromagnetic waves in a ferromagnet, J. Phys. Soc. Japan 60 (1991) 77.
[109] H. Leblond, M. Manna, Benjamin–Feir type instability in a saturated ferrite. Transition between a focusing and defocusing regimen for polarized electromagnetic wave, Phys. Rev. E 50 (1994) 2275.
[110] H. Leblond, Electromagnetic waves in ferromagnets: a Davey–Stewartson type model, J. Phys. A: Math. Gen. 32 (1999) 7907.
[111] R. Ell, U. Morgner, F.X. Kärtner, J.G. Fujimoto, E.P. Ippen, V. Scheuer, G. Angelow, T. Tschudi, M.J. Lederer, A. Boiko, B. Luther-Davies, Generation of 5-fs pulses and octave-spanning spectra directly from a Ti: sapphire laser, Opt. Lett. 26 (2001) 373.
[112] H. Triki, H. Leblond, D. Mihalache, Derivation of a modified Korteweg–de Vries model for few-optical-cycles soliton propagation from a general Hamiltonian, Opt. Commun. 285 (2012) 3179;
H. Leblond, H. Triki, D. Mihalache, Derivation of a coupled system of Korteweg–de Vries equations describing ultrashort soliton propagation in quadratic media by using a general Hamiltonian for multilevel atoms, Phys. Rev. A 85 (2012) 053826.
[113] M. Wadati, The modified Korteweg–de Vries equation, J. Phys. Soc. Japan 34 (1973) 1289.
[114] R. Hirota, Direct method of finding exact solutions of nonlinear evolution equations, in: Bäcklund Transformations, the Inverse Scattering Method, Solitons, and their Applications, in: Lecture Notes in Math., vol. 515, Springer, Berlin, 1976, pp. 40–68.
[115] S.M. Cox, P.C. Matthews, Exponential time differencing for stiff systems, J. Comput. Phys. 176 (2002) 430.
[116] R.A. Kraenkel, M.A. Manna, V. Merle, Nonlinear short-wave propagation in ferrites, Phys. Rev. E 61 (2000) 976.
[117] M.A. Manna, Asymptotic dynamics of monochromatic short surface wind waves, Physica D 149 (2001) 231.
[118] R.K. Bullough, F. Ahmad, Exact solutions of the self-induced transparency equations, Phys. Rev. Lett. 27 (1971) 330.
[119] P.J. Caudrey, J.D. Gibbon, J.C. Eilbeck, R.K. Bullough, Exact multisoliton solutions of the self-induced transparency and sine–Gordon equations, Phys. Rev. Lett. 30 (1973) 237.
[120] H. Leblond, Half-cycle optical soliton in quadratic nonlinear media, Phys. Rev. A 78 (2008) 013807.
[121] E.V. Kazantseva, A.I. Maimistov, Propagation and interaction of extremely short electromagnetic pulses in quadratic nonlinear medium, Phys. Lett. A 263 (1999) 434.
[122] E.V. Kazantseva, A.I. Maimistov, Propagation of ultrashort pulses through a nonresonance quadratically nonlinear medium in the unidirectional wave approximation, Quantum Electron. 30 (2000) 623.
[123] E.V. Kazantseva, A.I. Maimistov, B.A. Malomed, Propagation and interaction of ultrashort electromagnetic pulses in nonlinear media with a quadratic-cubic nonlinearity, Opt. Commun. 188 (2001) 195.
[124] H. Mashiko, C.M. Nakamura, C. Li, E. Moon, H. Wang, J. Tackett, Z. Changa, Carrier-envelope phase stabilized 5.6 fs, 1.2 mJ pulses, Appl. Phys. Lett. 90 (2007) 161114.
[125] C.R. Menyuk, R. Schiek, L. Torner, Solitary waves due to $\chi^{(2)} : \chi^{(2)}$ cascading, J. Opt. Soc. Am. B 11 (1994) 2434.
[126] G.I. Stegeman, D.J. Hagan, L. Torner, $\chi^{(2)}$ cascading phenomena and their applications to all-optical signal processing, mode-locking, pulse compression and solitons, Opt. Quantum Electron. 28 (1996) 1691.
[127] A.V. Buryak, Yu.S. Kivshar, Solitons due to second harmonic generation, Phys. Lett. A 197 (1995) 407.
[128] R. Schiek, Y. Baek, G.I. Stegeman, One-dimensional spatial solitary waves due to cascaded second-order nonlinearities in planar waveguides, Phys. Rev. E 53 (1996) 1138.
[129] L. Torner, D. Mihalache, D. Mazilu, E.M. Wright, W.E. Torruellas, G.I. Stegeman, Stationary trapping of light beams in bulk second-order nonlinear media, Opt. Commun. 121 (1995) 149.
[130] B.A. Malomed, D. Mihalache, F. Wise, L. Torner, Spatiotemporal optical solitons, J. Opt. B: Quantum Semiclass. Opt. 7 (2005) R53.
[131] G.I. Stegeman, M. Sheik-Bahae, E. Van Stryland, G. Assanto, Large nonlinear phase-shifts in 2nd-order nonlinear optical processes, Opt. Lett. 18 (1993) 13.
[132] H. Leblond, Bidimensional optical solitons in a quadratic medium, J. Phys. A: Math. Gen. 31 (1998) 5129.
[133] L.-C. Crasovan, J.P. Torres, D. Mihalache, L. Torner, Arresting wave collapse by wave self-rectification, Phys. Rev. Lett. 91 (2003) 063904.
[134] H. Leblond, Spatiotemporal optical pulse control using microwaves, Phys. Rev. Lett. 95 (2005) 033902.
[135] R. Hirota, Direct method in soliton theory, in: R.K. Bulough, P.J. Caudrey (Eds.), Solitons, Springer, Berlin, 1980.
[136] R. Hirota, The direct Method in Soliton Theory, Cambridge University Press, Cambridge, 2004.
[137] R. Hirota, A new form of Bäcklund transformations and its relation to the inverse scattering problem, Progr. Theoret. Phys. 52 (1974) 1498.
[138] R. Hirota, Exact solutions of the Korteweg–de Vries equation for multiple collisions of solitons, Phys. Rev. Lett. 27 (1971) 1192.
[139] C.S. Gardner, J.M. Greene, M.D. Kruskal, R.M. Miura, Method for solving the Korteweg–de Vries equation, Phys. Rev. Lett. 19 (1967) 1095.
[140] D.-Y. Chen, D.-J. Zhang, S.-F. Deng, The novel multi-soliton solutions of the mKdV–sine Gordon equations, J. Phys. Soc. Japan 71 (2002) 658.
[141] S.A. Kozlov, S.V. Sazonov, Nonlinear propagation of optical pulses of a few oscillations duration in dielectric media, JETP 84 (1997) 221.

[142] V.G. Bespalov, S.A. Kozlov, Yu.A. Shpolyanskiy, I.A. Walmsley, Simplified field wave equations for the nonlinear propagation of extremely short light pulses, Phys. Rev. A 66 (2002) 013811.
[143] A.N. Berkovsky, S.A. Kozlov, Yu.A. Shpolyanskiy, Self-focusing of few-cycle light pulses in dielectric media, Phys. Rev. A 72 (2005) 043821.
[144] T. Schäfer, C.E. Wayne, Propagation of ultra-short optical pulses in cubic nonlinear media, Physica D 196 (2004) 90.
[145] A.N. Bugay, S.V. Sazonov, Faster-than-light propagation of electromagnetic solitons in nonequilibrium medium taking account of diffraction, J. Opt. B: Quantum Semiclass. Opt. 6 (2004) 328.
[146] S. Clarke, R. Grimshaw, P. Miller, E. Pelinovsky, T. Talipova, On the generation of solitons and breathers in the modified Korteweg–de Vries equation, Chaos 10 (2000) 383.
[147] Y. Chung, C.K.R.T. Jones, T. Schäfer, C.E. Wayne, Ultra-short pulses in linear and nonlinear media, Nonlinearity 18 (2005) 1351.
[148] A. Sakovich, S. Sakovich, The short pulse equation is integrable, J. Phys. Soc. Japan 74 (2005) 239.
[149] A. Sakovich, S. Sakovich, Solitary wave solutions of the short pulse equation, J. Phys. A: Math. Gen. 39 (2006) L361.
[150] Y. Chung, T. Schäfer, Stabilization of ultra-short pulses in cubic nonlinear media, Phys. Lett. A 361 (2007) 63.
[151] J.C. Brunelli, The short pulse hierarchy, J. Math. Phys. 46 (2005) 123507.
[152] M. Colin, D. Lannes, Short pulses approximations in dispersive media, SIAM J. Math. Anal. 41 (2009) 708.
[153] Y. Liu, D. Pelinovsky, A. Sakovich, Wave breaking in the short-pulse equation, Dyn. Par. Differ. Equ. 6 (2009) 291.
[154] Y. Matsuno, Multiloop soliton and multibreather solutions of the short pulse model equation, J. Phys. Soc. Japan 76 (2007) 084003.
[155] Y. Matsuno, Periodic solutions of the short pulse model equation, J. Math. Phys. 49 (2008) 073508.
[156] N.L. Tsitsas, T.R. Horikis, Y. Shen, P.G. Kevrekidis, N. Whitaker, D.J. Frantzeskakis, Short pulse equations and localized structures in frequency band gaps of nonlinear metamaterials, Phys. Lett. A 374 (2010) 1384.
[157] D. Pelinovsky, A. Sakovich, Global well-posedness of the short-pulse and sine–Gordon equations in energy space, Comm. Partial Differential Equations 35 (2010) 613.
[158] M. Pietrzyk, I. Kanattšikov, U. Bandelow, On the propagation of vector ultra-short pulses, J. Nonlinear Math. Phys. 15 (2008) 162.
[159] A.V. Kim, S.A. Skobelev, D. Anderson, T. Hansson, M. Lisak, Extreme nonlinear optics in a Kerr medium: exact soliton solutions for a few cycles, Phys. Rev. A 77 (2008) 043823.
[160] H. Leblond, H. Triki, F. Sanchez, D. Mihalache, Robust circularly polarized few-optical-cycle solitons in Kerr media, Phys. Rev. A 83 (2011) 063802.
[161] H. Leblond, H. Triki, F. Sanchez, D. Mihalache, Circularly polarized few-optical-cycle solitons in Kerr media: a complex modified Korteweg–de Vries model, Opt. Commun. 285 (2012) 356.
[162] H. Leblond, H. Triki, D. Mihalache, Circularly polarized few-optical-cycle solitons in the short-wave-approximation regime, Phys. Rev. A 84 (2011) 023833.
[163] H. Triki, M.S. Ismail, Solitary wave solutions for a coupled pair of mKdV equations, Appl. Math. Computation 217 (2010) 1540.
[164] G.M. Muslu, H.A. Erbay, A split-step Fourier method for the complex modified Korteweg–de Vries equation, Comput. Math. Appl. 45 (2003) 503.
[165] M.V. Foursov, Classification of certain integrable coupled potential KdV and modified KdV-type equations, J. Math. Phys. 41 (2000) 6173.
[166] A. Biswas, E. Zerrad, A. Ranasinghe, Dynamics of solitons in plasmas for the complex KdV equation with power law nonlinearity, Appl. Math. and Computation 217 (2010) 1491.
[167] Ö. Akin, E. Özuğurlu, Analytical and numerical methods for the CMKdV-II equation, Math. Probl. Eng. 2009 (2009) 935030.
[168] B.A. Malomed, J. Fujioka, A. Espinosa-Ceron, R.F. Rodriguez, S. González, Moving embedded lattice solitons, Chaos 16 (2006) 013112.
[169] A.A. Mohammad, M. Can, Exact solutions of the complex modified Korteweg–de Vries equation, J. Phys. A Math. Gen. 28 (1995) 3223.
[170] H. Zhang, New exact travelling wave solutions to the complex coupled KdV equations and modified KdV equation, Commun. in Nonl. Science and Numerical Simulation 13 (2008) 1776.
[171] D. Mihalache, Formation and stability of light bullets: recent theoretical studies, J. Optoelectronics Adv. Materials 12 (2010) 12.
[172] L. Allen, J.H. Eberly, Optical Resonance and Two-Level Atoms, Dover, New York, 1987.
[173] S.V. Branis, O. Martin, J.L. Birman, Discrete velocities for solitary-wave solutions selected by self-induced transparency, Phys. Rev. A 43 (1991) 1549.
[174] A.V. Andreev, Solitons of the untruncated Maxwell–Bloch equations, Sov. Phys. JETP 81 (1995) 434 [Zh. Éksp. Teor. Fiz. 108 (1995) 796].
[175] M.A. Manna, V. Merle, Asymptotic dynamics of short waves in nonlinear dispersive models, Phys. Rev. E 57 (1998) 6206.
[176] M.A. Manna, Nonlinear asymptotic short-wave models in fluid dynamics, J. Phys. A: Math. Gen. 34 (2001) 4475.
[177] H.A. Haus, J.G. Fujimoto, E.P. Ippen, Structures for additive pulse mode locking, J. Opt. Soc. Am. B 8 (1991) 2068.
[178] N. Akhmediev, A. Ankiewicz (Eds.), Dissipative Solitons: From Optics to Biology and Medicine, in: Lect. Notes Phys., vol. 751, Springer, Berlin, 2008.
[179] V. Skarka, N.B. Aleksić, Stability criterion for dissipative soliton solutions of the one-, two-, and three-dimensional complex cubic-quintic Ginzburg–Landau equations, Phys. Rev. Lett. 96 (2006) 013903.
[180] D. Mihalache, D. Mazilu, F. Lederer, Y.V. Kartashov, L.-C. Crasovan, L. Torner, B.A. Malomed, Stable vortex tori in the three-dimensional cubic-quintic Ginzburg–Landau equation, Phys. Rev. Lett. 97 (2006) 073904.
[181] N. Akhmediev, J.M. Soto-Crespo, P. Grelu, Spatiotemporal optical solitons in nonlinear dissipative media: from stationary light bullets to pulsating complexes, Chaos 17 (2007) 037112.
[182] I.S. Aranson, L. Kramer, The world of the complex Ginzburg–Landau equation, Rev. Modern Phys. 74 (2002) 99.
[183] N.N. Akhmediev, A. Ankiewicz, Solitons: Nonlinear Pulses and Beams, Chapman & Hall, London, 1997.
[184] H. Leblond, M. Salhi, A. Hideur, T. Chartier, M. Brunel, F. Sanchez, Experimental and theoretical study of the passively mode-locked Ytterbium-doped double-clad fiber laser, Phys. Rev. A 65 (2002) 063811.
[185] M. Salhi, A. Haboucha, H. Leblond, F. Sanchez, Theoretical study of figure-eight all fiber laser, Phys. Rev. A 77 (2008) 033828.
[186] A. Komarov, H. Leblond, F. Sanchez, Quintic complex Ginzburg–Landau model for ring fiber lasers, Phys. Rev. E 72 (2005) 025604(R).
[187] Ph. Grelu, J. Béal, J.M. Soto-Crespo, Soliton pairs in a fiber laser: from anomalous to normal average dispersion regime, Opt. Express 11 (2003) 2238.
[188] J. Lega, J.V. Moloney, A.C. Newell, Swift–Hohenberg equation for lasers, Phys. Rev. Lett. 73 (1994) 2978.
[189] H.A. Haus, Theory of mode locking with a slow saturable absorber, IEEE J. Quantum Electron. QE-11 (1975) 736.
[190] H.A. Haus, J.G. Fujimoto, E.P. Ippen, Analytic theory of additive pulse and Kerr lens mode locking, IEEE J. Quantum Electron. 28 (1992) 2086.
[191] T. Brabec, Ch. Spielmann, P.F. Curley, F. Krausz, Kerr lens mode locking, Opt. Lett. 17 (1992) 1292.
[192] D. Huang, M. Ulman, L.H. Acioli, H.A. Haus, J.G. Fujimoto, Self-focusing-induced saturable loss for laser mode locking, Opt. Lett. 17 (1992) 511.
[193] J. Herrmann, Theory of Kerr-lens mode locking: role of self-focusing and radially varying gain, J. Opt. Soc. Am. B 11 (1994) 498.
[194] C. Jirauschek, F.X. Kärtner, U. Morgner, Spatiotemporal Gaussian pulse dynamics in Kerr-lens mode-locked lasers, J. Opt. Soc. Am. B 20 (2003) 1356.
[195] E.N. Lorenz, Deterministic aperiodic flow, J. Atmospheric Sci. 20 (1963) 130.
[196] H. Haken, Analogy between higher instabilities in fluids and lasers, Phys. Lett. A 53 (1975) 77.
[197] D.E. Pelinovsky, A.V. Buryak, Yu.S. Kivshar, Instability of solitons governed by quadratic nonlinearities, Phys. Rev. Lett. 75 (1995) 591.
[198] L. Torner, D. Mihalache, D. Mazilu, N.N. Akhmediev, Stability of spatial solitary waves in quadratic media, Opt. Lett. 20 (1995) 2183.
[199] L. Torner, D. Mazilu, D. Mihalache, Walking solitons in quadratic nonlinear media, Phys. Rev. Lett. 77 (1996) 2455.
[200] D. Mihalache, F. Lederer, D. Mazilu, L.-C. Crasovan, Multiple-humped bright solitary waves in second-order nonlinear media, Opt. Eng. 35 (1996) 1616.
[201] B.A. Malomed, P. Drummond, H. He, A. Berntson, D. Anderson, M. Lisak, Spatiotemporal solitons in multidimensional optical media with a quadratic nonlinearity, Phys. Rev. E 56 (1997) 4725.
[202] D. Mihalache, D. Mazilu, L.-C. Crasovan, L. Torner, Stationary walking solitons in bulk quadratic nonlinear media, Opt. Commun. 137 (1997) 113.
[203] D.V. Skryabin, W.J. Firth, Generation and stability of optical bullets in quadratic nonlinear media, Opt. Commun. 148 (1998) 79.
[204] D. Mihalache, D. Mazilu, B.A. Malomed, L. Torner, Asymmetric spatio-temporal optical solitons in media with quadratic nonlinearity, Opt. Commun. 152 (1998) 365.

[205] X. Liu, L.J. Qian, F.W. Wise, Generation of optical spatiotemporal solitons, Phys. Rev. Lett. 82 (1999) 4631.
[206] D. Mihalache, D. Mazilu, L.-C. Crasovan, L. Torner, B.A. Malomed, F. Lederer, Three-dimensional walking spatiotemporal solitons in quadratic media, Phys. Rev. E 62 (2000) 7340.
[207] C. Etrich, F. Lederer, B.A. Malomed, T. Peschel, U. Peschel, Optical solitons in media with a quadratic nonlinearity, Prog. Opt. 41 (2000) 483.
[208] A.V. Buryak, P. Di Trapani, D. Skryabin, S. Trillo, Optical solitons due to quadratic nonlinearities: from basic physics to futuristic applications, Phys. Rep. 370 (2002) 63.
[209] J. Satsuma, M.J. Ablowitz, 2-dimensional lumps in non-linear dispersive systems, J. Math. Phys. 20 (1979) 1496.
[210] A. de Bouard, J.-C. Saut, Symmetries and decay of the generalized Kadomtsev–Petviashvili solitary waves, SIAM J. Math. Anal. 28 (1997) 1064.
[211] E. Infeld, A. Senatorski, A.A. Skorupski, Numerical simulations of Kadomtsev–Petviashvili soliton interactions, Phys. Rev. E 51 (1995) 3183.
[212] A. Senatorski, E. Infeld, Breakup of 2-dimensional into 3-dimensional Kadomtsev–Petviashvili solitons, Phys. Rev. E 57 (1998) 6050.
[213] A.-M. Wazwaz, Regular soliton solutions and singular soliton solutions for the modified Kadomtsev–Petviashvili equations, Appl. Math. Comput. 204 (2008) 227.
[214] L. Bergé, Wave collapse in physics: principles and applications to light and plasma waves, Phys. Rep. 303 (1998) 260.
[215] S.K. Turitsyn, G.E. Fal'kovitch, Stability of magnetoelastic solitons and self-focusing of sound in antiferromagnets, Sov. Phys. J.E.T.P. 62 (1985) 146.
[216] X.P. Wang, M.J. Ablowitz, H. Segur, Wave collapse and instability of solitary waves of a generalized Kadomtsev–Petviashvili equation, Physica D 78 (1994) 241.
[217] A. de Bouard, J.-C. Saut, Remarks on the stability of generalized KP solitary waves, Contemp. Math. 200 (1996) 75.
[218] Y. Liu, Blow up and instability of solitary-wave solutions to a generalized Kadomtsev–Petviashvili equation, Trans. Amer. Math. Soc. 353 (2000) 191.
[219] H. Leblond, M. Manna, Single-oscillation two-dimensional solitons of magnetic polaritons, Phys. Rev. Lett. 99 (2007) 064102.
[220] H. Leblond, M. Manna, Nonlinear dynamics of two-dimensional electromagnetic lumps in a ferromagnetic slab, Phys. Rev. B 77 (2008) 224416.
[221] H. Leblond, M. Manna, Two-dimensional electromagnetic solitons in a perpendicularly magnetized ferromagnetic slab, Phys. Rev. B 80 (2009) 064424.
[222] H. Leblond, M. Manna, Short waves in ferromagnetic media, Phys. Rev. E 80 (2009) 037602.
[223] J.X. Xin, Modelling light bullets with the two-dimensional sine–Gordon equation, Physica D 135 (2000) 345.
[224] T. Povitch, J. Xin, A numerical study of the light bullets interaction in the $(2+1)$ sine–Gordon equation, Nonlinear Sci. 15 (2005) 11.
[225] Y. Silberberg, Collapse of optical pulses, Opt. Lett. 15 (1990) 1282.
[226] H. Leblond, B.A. Malomed, D. Mihalache, Spatiotemporal vortex solitons in waveguide arrays, J. Optoelectronics Adv. Mat. 12 (2010) 6.
[227] D. Mihalache, Three-dimensional Ginzburg–Landau dissipative solitons supported by a two-dimensional transverse gratting, Proc. Romanian Acad. A 11 (2010) 142.
[228] D. Mihalache, Discrete light bullets in one- and two-dimensional photonic lattices: collision scenarios, Rom. Rep. Phys. 62 (2010) 99.
[229] D. Mihalache, Topological dissipative nonlinear modes in two- and three-dimensional Ginzburg–Landau models with trapping potentials, Rom. Rep. Phys. 63 (2011) 9.
[230] D. Mihalache, Recent trends in micro- and nanophotonics: a personal selection, J. Optoelectron. Adv. Mat. 13 (2011) 1055.
[231] D. Mihalache, Linear and nonlinear light bullets: recent theoretical and experimental studies, Rom. J. Phys. 57 (2012) 352.
[232] Bin Liu, Ying-Ji He, Zhi-Ren Qiu, He-Zhou Wang, Annularly and radially phase-modulated spatiotemporal necklace-ring patterns in the Ginzburg–Landau and Swift–Hohenberg equations, Opt. Express 17 (2009) 12203.
[233] F.W. Ye, Y.V. Kartashov, B. Hu, L. Torner, Light bullets in Bessel optical lattices with spatially modulated nonlinearity, Opt. Express 17 (2009) 11328.
[234] M. Peccianti, I.B. Burgess, G. Assanto, Roberto morandotti, space–time bullet trains via modulation instability and nonlocal solitons, Opt. Express 18 (2010) 5934.
[235] A. Chong, W.H. Renninger, D.N. Christodoulides, F.W. Wise, Airy-Bessel wave packets as versatile linear light bullets, Nat. Photonics 4 (2010) 103.
[236] V.E. Lobanov, Y.V. Kartashov, L. Torner, Light bullets by synthetic diffraction-dispersion matching, Phys. Rev. Lett. 105 (2010) 033901.
[237] D. Abdollahpour, S. Suntsov, D.G. Papazoglou, S. Tzortzakis, Spatiotemporal Airy light bullets in the linear and nonlinear regimes, Phys. Rev. Lett. 105 (2010) 253901.
[238] Wei-Ping Zhong, M. Belić, G. Assanto, B.A. Malomed, Tingwen Huang, Light bullets in the spatiotemporal nonlinear Schrödinger equation with a variable negative diffraction coefficient, Phys. Rev. A 84 (2011) 043801.
[239] Bin Liu, Xing-Dao He, Continuous generation of 'light bullets' in dissipative media by an annularly periodic potential, Opt. Express 19 (2011) 20009.
[240] Hui-jun Li, Yuan-po Wu, Guoxiang Huang, Stable weak-light ultraslow spatiotemporal solitons via atomic coherence, Phys. Rev. A 84 (2011) 033816.
[241] S. Minardi, F. Eilenberger, Y.V. Kartashov, A. Szameit, U. Ropke, J. Kobelke, K. Schuster, H. Bartelt, S. Nolte, L. Torner, F. Lederer, A. Tunnermann, T. Pertsch, Three-dimensional light bullets in arrays of waveguides, Phys. Rev. Lett. 105 (2010) 263901.
[242] F. Eilenberger, S. Minardi, A. Szameit, U. Ropke, J. Kobelke, K. Schuster, H. Bartelt, S. Nolte, L. Torner, F. Lederer, A. Tunnermann, T. Pertsch, Evolution dynamics of discrete-continuous light bullets, Phys. Rev. A 84 (2011) 013836.
[243] F. Eilenberger, S. Minardi, A. Szameit, U. Röpke, J. Kobelke, K. Schuster, H. Bartelt, S. Nolte, A. Tünnermann, T. Pertsch, Light bullets in waveguide arrays: spacetime-coupling, spectral symmetry breaking and superluminal decay, Opt. Express 19 (2011) 23171.